Evaluating Optimal Conditions for Composting Food Service Packaging and Techniques Used to Remediate *Per- and Polyfluoroalkyl Substances*

Publication Date: February 1, 2024

Produced Under Contract By: The University of California Davis

State of California

Gavin Newsom
Governor

California Environmental Protection Agency

Yana Garcia
Secretary

Department of Resources Recycling and Recovery

Rachel Machi Wagoner
Director

Public Affairs Office
1001 I Street (MS 22-B)
P.O. Box 4025
Sacramento, CA 95812-4025
www.calrecycle.ca.gov/Publications/
1-800-RECYCLE (California only) or (916) 341-6300

Publication # DRRR-2024-1730

Prepared as part of contract number DRR 18040.

The California Department of Resources Recycling and Recovery (CalRecycle) does not discriminate based on disability in access to its programs. CalRecycle publications are available in accessible formats upon request by calling the Public Affairs Office at (916) 341-6300. Persons with hearing impairments can reach CalRecycle through the California Relay Service, 1-800-735-2929.

Table of Contents

Acknowledgments

CalRecycle extends its appreciation to the California District Attorneys who invited the department to submit a compostable plastics research project for consideration. This contract was funded by several labeling violation settlements resulting from retailers misusing terms to market products, including “compostable” and “biodegradable.”

The University of California at Davis would like to thank and acknowledge Dr. Maureen Kinyua (Principal Investigator) and Dr. Jesús Velázquez (co-Principal Investigator) for directing the composting, food service packaging biodegradation and Per- and Polyfluoroakyl Substances (PFAS) research activities of this study performed at the University of California Davis. We especially want to thank their team of students: Gandhar Abhay Pandit (PhD candidate with the Civil and Environmental Engineering Department) and Fatima Hussain (PhD candidate with the Chemistry Department) for their role in study design, data collection, analysis, and reporting. We would not have done this work without them.

We also want to note our gratitude to our external collaborators that participated in actualizing this project. First, we would like to thank Dr. Ramin Yazdani, the Director of Integrated Waste Management at the County of Yolo for his assistance with sample collection and commercial-scale direction. We want to thank Will Kelly, Grey Kelly, and Chloe Kelly of the Napa Recycling and Composting Facility for helping with our commercial scale composting experiments. We would like to acknowledge Professor Graham Peaslee and his students; Molly DeLuca and Arthur Alvarez at the University of Notre-Dame, Indiana for their assistance with Particle Induced Gamma Ray Emission (PIGE) spectroscopy data processing.

We want to thank our internal UC Davis personnel and lab facilities for assisting with this research. A special thanks to Timothy Doane from the Plant and Science Department for helping us with the Carbon and Nitrogen Analysis, undergraduate students Myar Abou-Alfotouh and Konane Gurfield and Junior Specialist Jessica Hazard for their assistance with bench-scale experiments. We also extend our gratitude to Matthew Rolston from the Host Microbe Lab Core for microbial ecology analysis.

We acknowledge support from NSF-MRI grant DMR-1725618 for the use of the Thermofisher Quattro environmental scanning electron microscope (SEM) at the Advanced Materials Characterization and Testing Laboratory (AMCAT) at UC Davis. We would also like to acknowledge support from NSF 9808183 and NIH ES005707-13 (BACS 60) for the use of the 400 MHz Nuclear Magnetic Resonance Spectrometer.

Finally, we would like to thank CalRecycle’s environmental scientist Robert Contreras, for his work managing this contract and his contributions to the final report.

Glossary of Terms

The following terms are defined as used in this report. Some organizations may use alternate definitions, and some terms do not have universally accepted meanings.

Aerobic	Life or biological processes that can occur only in the presence of oxygen.
Acetonitrile	A solvent used in liquid chromatography.
Aliquot	A small portion of a larger sample taken for chemical analysis.
Aliphatic -aromatic copolymers	Aliphatic copolymer is a synthetic polymer made from a mixture of lactide and aliphatic polyester.
Anaerobic	Life or biological processes that can occur in the absence of oxygen.
ASTM	ASTM International, formerly known as American Society for Testing and Materials, is an international standards organization that develops and publishes voluntary consensus technical standards for a wide range of areas and materials such as metals, paints, plastics, textiles, petroleum, construction, energy, the environment, consumer products, medical services, devices and electronics, and advanced materials.
Bench – Scale	Testing of materials, methods, or chemical processes at small scale, such as in a laboratory.
Biodegradable	The ability of a substance to be broken down physically and/or chemically by microorganisms. Detailed scientific specifications have been developed to measure the disintegration and biodegradation performance of test samples within timeframes and under simulated environmental conditions.

Biodegradation	The process of being consumed by microorganisms and converted into carbon dioxide/methane, water, and biomass.
Bioplastic	A plastic made from biobased materials that is typically degradable.
Bulking Agents	A carbon-based material that adds structure to a composting matrix.
Byproduct	An incidental compound derived from a manufacturing process or chemical reaction that is not the primary compound being produced.
Carbon to Nitrogen Ratio	A ratio of the mass of carbon to the mass of nitrogen in a substance.
Compost	The product resulting from the controlled biological decomposition of organic material including but not limited to: landscape trimmings, agricultural crop residues, paper pulp, food scraps, wood chips, manure, and biosolids.
Composting	A biochemical process that converts organic waste in the presence of oxygen into carbon dioxide, heat, water, and a stable organic substance that can be recovered as a soil amendment or fertilizer.
Compostable plastic	As defined by ASTM, a plastic with a chemical structure that undergoes significant measurable change under specified environmental conditions.
Comonomers	A polymerizable precursor to a copolymer aside from the principal monomer.

Conductivity	The ability of an aqueous solution to carry an electric current. For the purposes of this report the units are expressed as µS/cm.
Degradation	The process of breaking down into a simpler form. In the context of composting, degradation refers to the combined process of disintegration and biodegradation. In the context of PFAS, degradation refers to the cleaving of PFAS molecules into smaller forms.
Deuterated water	Water where the hydrogen atoms are replaced with deuterium, an isotope of hydrogen that can be detected using spectroscopy.
Diffractometer	An instrument used to measure the structure of a crystal using X-rays.
Electrostatic	Attractions or repulsions of electric charges that are not dependent on their motion.
Extracellular Enzymatic Degradation	The degradation that occurs due to extracellular enzymes that help microbes to digest and utilize fractions of organic matter which can stimulate growth and enhance microbial activity.
Food Service Packaging and Products (FSP)	Products used to serve or transport food or beverages, such as, plates, cups, bowls, trays, hinged or lidded containers, and bags.
Fourier-transform Infrared Spectroscopy (FTIR)	Technique used to measure the infrared absorption and emission of infrared light from a sample.
Glass Transition Rate	Gradual transition in amorphous material from a brittle to viscous state as the temperature increases.

Greenhouse Gas	Any gas that absorbs infrared radiation in the atmosphere (leading to the "greenhouse effect"), including carbon dioxide, methane, nitrous oxide, ozone, and fluorocarbons.
Hydrolysis	Any chemical reaction in which a molecule of water breaks one or more chemical bonds.
Hydrophobic	A physical property of a compound that allows it to repel and not absorb water.
Inoculant	A substance containing microorganisms that is introduced into an environment to promote the growth of the contained microbial populations.
Landfill Sludge	The residual, semi-solid material that is produced as a by-product during sewage treatment of leachate (wastewater) generated in landfills.
Liquid Chromatography	A technique in analytical chemistry used to separate, identify, and quantify each component of a mixture.
Mass spectrometry	An analytical technique that is used to measure the mass-to-charge ratio of ions. The results are presented as a plot of intensity as a function of the mass-to-charge ratio. The spectra are used to determine the elemental or isotopic signatures of a sample.
Mesoporous hafnium oxide	A white metal oxide made of hafnium and oxygen containing macropores (pores with a diameter larger than 50 nm), and mesopores (pores that have a diameter in the range of 2-50 nm).
Microbes	An organism of microscopic size which may exist in its single-celled form or as a colony of cells. This includes but is not limited to bacteria and fungi.

Microcosms	An experimental setup regarded as encapsulating in miniature the characteristic qualities or features of something much larger.
Milli Q Water	Water that is purified using a Millipore Milli-Q lab water system.
Mixed Liquor	A combination of raw or unsettled wastewater or pre-settled wastewater and activated sludge within an aeration tank.
Nuclear magnetic resonance spectroscopy	A molecular identification technique used to determine the chemical structure of organic compounds by detecting specific nuclei in a molecule.
Organic	Materials or goods produced using an ecological management system that promotes and enhances biodiversity, biological cycles, and soil biological activity.
Overs	Large material that is screened out during the sorting of compost feedstocks.
Particle-induced gamma ray emission spectroscopy	A technique used to detect and quantify fluorine in a sample based on its wavelength. This technique measures total fluorine which includes fluorine's organic and inorganic forms.
Pathogens	A bacterium, virus, or other microorganism that may cause disease.
Plastic	A material that contains as an essential ingredient one or more organic polymeric substances of large molecular weight, is solid in its finished state, and, at some stage in its manufacture or processing into finished articles, can be shaped by flow.
Polyester	Polyester is a category of polymers that contain an ester functional group in every repeated unit of their main chain.

Polyethylene Terephthalate (PET)	A plastic polymer formed by combining the monomers ethylene glycol and terephthalic acid. PET is commonly used to make water bottles, soft drink bottles, and other food and drink packaging.
Per- and polyfluoroalkyl substances (PFAS)	A class of fluorinated organic chemicals containing at least one fully fluorinated carbon atom. This class includes more than 9,000 chemicals. PFAS vary in chain length from a chain of two carbons to large molecular-weight polymers.
Polyfluorinated compounds	Molecules consisting of a chain of carbon atoms bonded to each other where some carbons are bonded to hydrogen, and other carbons are bonded to fluorine atoms.
Polyhydroxyalkanoate (PHA)	A family of naturally occurring polymers synthesized by a biological process that involves conversion of carbon sources through microbial fermentation.
Perfluorobutanoic acid	A particular type of perfluoroalkyl substance that has four carbons.
Perfluorohexanoic acid	A particular type of perfluoroalkyl substance that has six carbons.
Perfluorooctanoic acid	A particular type of perfluoroalkyl substance that has eight carbons.
Piles	An industrial compost operation constructed of feedstock material mounded into a row with variable dimensions.
Polyhydroxybutyrate (PHB)	A member of the PHA family, used by microorganisms as a form of energy storage molecule, with properties like those of conventional polypropylene.

Polylactic acid (PLA)	A polyester derived from non-fossil resources such as corn or sugarcane, produced through fermentation and polymerization of lactic acid.
q_t	A variable denoting the quantity of PFAS in milligrams adsorbed per gram of mesoporous hafnium oxide at a specific time.
Rain-x	Synthetic hydrophobic liquid that causes water to run off a surface.
Respirometry Study	A study that measures the amount of oxygen consumed by microorganisms over time to measure biodegradation rates.
Standard	A document establishing consistent voluntary criteria for a material, product, system, or service; and developed by consensus using the principles, procedures, and approval regulations of the organization. ASTM Standard Specification D6400-12, which prescribes the requirements necessary for a plastic to be labeled compostable in industrial facilities, was used for this study.
Sol-gel	A method used to produce solid materials from monomers in solution. The process is used to fabricate metal oxides for testing purposes.
Synthetic Media	A synthetic environment used to cultivate microorganisms in laboratory settings.
Test Methods	A definitive procedure containing specific steps, instruments, and materials that produces a test result.
Wavenumber (cm^{-1})	The number of wavelengths in a specified distance.

Ultrapure water	Water that has been purified to remove all ions from solution.

Abbreviations and Acronyms

AD	Anaerobic Degradation
ASTM	American Society for Testing and Materials
BET	Brunauer-Emmet-Teller
BPI	Biodegradable Products Institute
C	Concentration after filtration
C_0	Initial concentration
C_t	Concentration at a time t
CalRecycle	California Department of Resources Recycling and Recovery
C/N	Carbon to Nitrogen Ratio
C13	Perfluoro tridecanoic acid
C14	Perfluoro tetradecanoic acid
D_2O	Deuteurium Oxide
DNA	Deoxyribonucleic acid
FSP	Food Service Packaging
FTIS	Fourier Transform Infrared Spectroscopy
GHG	Greenhouse Gas
GAC	Granular Activated Carbon
g COD/g VSS-L-hr	gram Chemical Oxygen Demand per gram Volatile Suspended Solids in liters in hour

ISO	International Organization for Standardization
IX	Ion Exchange
kDa	Kilo Dalton
kj/mol	Kilo Joules per mol
KeV	Electron Volt
LC-MS	Liquid Chromatography-Mass Spectrometry
MC	Moisture Content
MHO	Mesoporous Hafnium Oxide
mL	Milliliter
m^2/g	Meters Squared Per Grams
µS/cm	MicroSiemens per centimeter
Mt	Montmorillonite
NMR	Nuclear Magnetic Resonance
PCR	Polymerase Chain Reaction
PET	Polyethylene Terephthalate
PFAS	Per- and Polyfluoroalkyl Substances
PFAA	Perfluoroalkyl acids
PFSA	Perfluoroalkyl Sulfonic acids
PFCA	Perfluorocarboxylic acid
PFBA	Perfluorobutanoic acid
PFHxA	Perfluorohexanoic acid
PFOA	Perfluorooctanoic acid
PHA	Polyhydroxyalkanoate
PHB	Polyhydroxybutyrate
PHBV	Polyhydroxybutyrate-valerate
PIGE	Particle-induced gamma ray emission
PLA	Polylactic acid
PPM	Parts per million (One out of a million)
PZC	Point of Zero Charge
RPM	Revolution Per Minute
SEM	Scanning Electron Microscopy
Tg	Glass Transition Temperature
TFA	Trifluoroacetic acid
µm	Micron (One millionth of meter)
µL	Microliter (One millionth of liter)
XRD	X-ray Diffraction

Executive Summary

California residents annually produce approximately seven million tons of organic municipal solid waste, which consists of organic debris and inorganic food service products such as cups, bowls, lids, plates, and containers that are sold and labeled as compostable (CalRecycle, 2021). These types of food service packaging and products (FSP) are designed to biodegrade and become usable compost.

Although FSP has the potential to facilitate collection and diversion of food materials from landfills, there are a limited number of industrial composting facilities in California that currently accept them. These products can pose significant contamination issues for compost operators and can jeopardize certification of their finished compost. Others do not accept FSP because compostable products do not always disintegrate and biodegrade at the rate required to process compostable material feedstocks into a finished product. Leftover fragmented plastics must be screened out of compost which requires further processing.

Additionally, some types of compostable FSP contain per- and polyfluoroalkyl substances (PFAS), which can transfer from products into finished compost as they degrade (CalRecycle, 2021). PFAS are a large group of over 9000 synthetic industrial chemicals that are used in the production of consumer goods. PFAS are used for their hydrophobic and lipophobic properties, which helps to release FSP from production molds and makes them resistant to water and grease. Long-term exposure to PFAS is a public health concern due to their association with kidney cancer, thyroid disease, and immune toxicity in children (Schaider et al., 2017).

This research study was developed to assess the optimal conditions that facilitate disintegration and biodegradation of compostable FSP and to evaluate inoculants that could potentially improve composting. It included testing of four types of FSP labeled as “compostable” and sold in California.

The research also examined the concentration of PFAS contained in the FSP test specimens. This included chemical sampling to detect the presence of fluorinated compounds (a proxy for PFAS) in FSP and samples of finished compost. The removal of short and long chain PFAS molecules from water as a simulation of compost leachate was also assessed using porous materials via adsorption and filtration.

Limitations of this Research Project

This research study included a limited number of test samples and was not intended to evaluate all types and brands of compostable FSP offered for sale in CA. Additionally, the FSP samples varied in thickness, shape, size, and material. These samples were chosen to generally represent commonly used types of compostable FSP; however, the limited number of samples is not representative of the wide range of FSP available and marketed as “compostable.”

The bench-scale testing was limited to a single inoculant (cow manure) and commercial-scale testing did not evaluate inoculants. An evaluation of different types of inoculants at commercial-scale is necessary to understand their effectiveness in aiding the biodegradation of FSP. Further in-depth research could reveal that a wider variety of inoculants are available to facilitate improvements in composting processes.

Moisture content and oxygen availability were the only variables modified during the bench-scale experiments. Variables such as temperature, pH, and conductivity were measured, but not scientifically modified. Therefore, a more thorough evaluation of these parameters is necessary to fully understand their boundary limits as mentioned in the study objectives.

While a compost remediation technique would be most informed by evaluating compost leachate, the PFAS remediation testing was conducted in water. The test solution (water) is significantly less complex than compost leachate. It is unclear if mesoporous hafnium oxide (MHO) monoliths would behave similarly in compost leachate due to factors such as competition for PFAS binding sites by other molecules and potential impacts on flow rate. A more thorough evaluation of MHO in compost leachate is essential to determine the feasibility of this remediation technique at commercial-scale.

Throughout the bench-scale and commercial-scale composting experiments, PFAS did not migrate from the FSP into the solid compost. During the 24-day commercial-scale composting experiment there was a relatively low change in total fluorine concentration in the FSP. The absence of PFAS detected in compost extractions suggest PFAS is retained in the FSP rather than released into the compost. Although PFAS were not detected in solid compost samples, leachate from commercial-scale piles was not assessed as part of this study and may have contained measurable amounts of PFAS. Further research evaluating PFAS concentration in liquid leachate is necessary to better understand the fate and migration of PFAS from FSP.

Biodegradation was estimated in both bench and commercial-scale testing by measuring the FSP sample's weight change. Weight change is a cost-effective method used to assess biodegradability of a material. However, weight change estimates in this report may be inaccurate due to insufficient collection of the whole sample as it disintegrated. A more accurate method for determining biodegradation is measuring the amount of organic carbon converted to CO_2. A more comprehensive study utilizing both carbon conversion and weight loss methods would further inform this research area.

Research Findings

Evaluation of the Optimal Conditions that Facilitate Biodegradation

Bench-scale experiments:

1. The degree of biodegradation shown in FSP samples exposed to the cow manure inoculant was 25 percent higher in reactors with 60 percent moisture content when compared to reactors with 45 percent moisture content.

2. The rate of biodegradation in the tested FSP products was highest in the positive control (62.3 ± 32.3 percent) followed by synthetic/starch blended bag (57.4 ± 34.2 percent), and the fiber plate (39.5 ± 34.3 percent). The negative control (low-density polyethylene plastic film) displayed no signs (0 percent) of biodegradation.
3. The bench scale study determined the 60 percent moisture content with the cow manure inoculant produced the highest rate of biodegradation for all tested products.

In general, the rate of biodegradation was higher at 60 percent moisture content than at 45 percent moisture content across all types of FSP with cow manure used as the inoculant.

Commercial-scale experiments:

1. The rate of biodegradation in the tested products was highest in synthetic/starch blended bag (94 ± 5.17 percent), followed by positive control (68 ± 20.5 percent) and then fiber plate (24 ± 7.4 percent). The PLA lined bagasse clamshell showed 12 ± 11.1 percent biodegradation. Overall, the commercial-scale pile containing food waste feedstock had higher rates of biodegradation than the commercial-scale pile containing no food waste.
2. The negative control and the PLA lined bagasse clamshell showed no signs (0 percent) biodegradation.
3. The FSP samples tested in the commercial-scale pile containing food waste showed higher rates of FSP degradation when compared to the FSP samples tested in the pile containing old compost. The commercial-scale experiments also displayed similar results to the bench-scale experiments where the synthetic/starch blended bags had the highest rate of degradation.

In general, the pile containing food waste feedstock had higher degradation rates for all FSP when compared to the pile with old compost.

PFAS Experiments during Composting and Remediation of PFAS from Water

1. The fiber plate and PLA lined bagasse clamshell contained high PFAS concentrations (883 ± 52 ppm and 854 ± 50 ppm, respectively).
2. There were no PFAS detected in any of the compost extracts from bench-scale or commercial-scale experiments.
3. Mesoporous hafnium oxide (MHO) successfully adsorbed PFAS from fabricated water samples demonstrating that MHO has potential usefulness in remediation of PFAS present in contaminated liquids, such as compost leachate.
4. MHO has higher adsorption capacity for longer chain PFAS than shorter chain PFAS.

During both bench-scale and commercial-scale composting, weight loss was observed in the FSP. However, no PFAS were detected in the compost. The FSP weight loss is mostly related to biodegradation of plant fibers such as bamboo, and sugarcane bagasse. The data suggests that adsorption is an effective technique to remediate PFAS-contaminated water. MHO successfully adsorbed PFAS from fabricated water samples demonstrating that MHO could have potential utility in remediation of PFAS present in contaminated liquids, such as compost leachate. MHO has the potential to remove a wide variety of PFAS molecules due to the pores present in the adsorbent material.

Overview of the Research Project

Project Objectives

1. Identify the optimal conditions that facilitate disintegration and biodegradation of FSP by determining the boundary limits for moisture, temperature, and oxygen availability in a composting environment.
2. Examine the effects of different microbial inoculants on the mineralization of FSP in the composting environment.
3. Conduct chemical sampling of the FSP to detect the presence of PFAS.
4. Examine nanomaterial remediation techniques for removal of PFAS from the composting environment.

Compostable Food Service Packaging Biodegradation

Test Specimens

Bench-scale and commercial-scale composting experiments were performed to determine the optimal composting conditions of four types of compostable FSP. A positive and negative control were additionally tested for quantitative comparison to test samples. The products tested are listed below:

a. Chlorine free unbleached coffee filter made from cellulose (positive control)
b. Low-density polyethylene (LDPE) plastic film (negative control)
c. Bamboo and unbleached plant fiber plate (fiber plate)
d. Synthetic plastic and starch blended plastic (synthetic/starch blended bag)
e. Clear polylactic acid (PLA) clamshell derived from corn
f. PLA lined bagasse clamshell derived from sugar cane

Test Protocols

Bench-Scale Conditions: To begin the bench-scale experiment, an exploratory respirometry study was conducted to examine the effect of different inoculants (i.e., cow

manure, mixed liquor, landfill sludge and finished compost) on the rate of oxygen uptake during composting. Cow manure was determined to be the most biologically active inoculant. The relatively high biological activity suggests this inoculant is the most likely to facilitate disintegration and biodegradation of compostable FSP and therefore was utilized as the inoculant in all subsequent bench-scale experiments.

Eleven bench-scale composting reactors, with moisture contents of 45, 50, and 60 percent were operated with food waste feedstock and a cow manure inoculant. The bench-scale composting reactors were designed to simulate industrial composting conditions by following the ASTM Standard Specification D6400-12. Biodegradation rates were determined based on the weight change of the FSP test samples throughout a 24-day testing timeframe. Commercial compost facilities typically operate a total of 45–60 days to compost materials. The first 24–25 days are considered to be the active phase, while the remaining days are considered to be the maturing phase. Previous studies have demonstrated that the microorganisms are active during the first 24-25 days. Thus, a period of 24 days was selected for bench scale composting experiments.

Commercial Scale Conditions: This study quantified the biodegradation of FSP in industrial-scale composting conditions. Eight 94 x 30 x 10 feet composting piles were constructed with grasses, food scraps, and dry leaves as feedstock and either food waste or old compost were added to each pile. FSP biodegradation rates were determined based on the weight change of samples throughout a 24-day testing timeframe. Synthetic starch bags demonstrated more than 80 percent biodegradation after 24 days of composting in all experiments. Commercial-scale piles containing additional old compost supported higher rates of FSP biodegradation for the positive control and synthetic starch bags (0.028-0.039g FSP degraded/g FSP initial). The fiber plate and PLA lined bagasse clamshell displayed low rates of biodegradation (i.e., less than 0.01 g FSP degraded/g FSP initial) regardless of the additional feedstock.

PFAS Sampling and Remediation

PFAS detection methods were developed for solid compost and products marketed as compostable using Fourier-transform infrared spectroscopy (FTIR) and particle-induced gamma ray emission spectroscopy (PIGE) in collaboration with the Peaslee group at the University of Notre Dame. Both methods measure the total fluorine contained in a sample in parts per million (ppm). The fiber plate, and PLA lined bagasse clamshell had high concentrations of PFAS, measured at 883 ± 52 ppm and 854 ± 50 ppm, respectively. However, during the 24 days of bench-scale composting higher concentrations of PFAS were observed on products marketed as compostable and composted at 60 percent moisture content when compared to 45 percent moisture content.

At the conclusion of the 24-day commercial-scale experiments, the fiber plate displayed the highest change in total fluorine concentration (883 ± 52 ppm to 831 ± 519 ppm). The high margin of error observed at the end of the experiment is due to the buildup of compost on the surface of the FSP, increasing its thickness. Thicker samples inhibit the PIGE beam and decrease fluorine detection accuracy. The relatively low change in total

fluorine concentration and lack of PFAS in compost extractions suggest PFAS is retained on or contained in, the FSP rather than released into the compost.

The nanomaterial mesoporous hafnium oxide (MHO) was synthesized using the sol-gel method to examine remediation of PFAS from water. Methods were developed using liquid chromatography-mass spectrometry and ^{19}F nuclear magnetic resonance (NMR) spectroscopy to quantify PFAS in liquid. The data suggests the effectiveness of MHO as a PFAS remediation agent increases with PFAS chain length. The adsorption capacity of perfluorooctanoic acid (PFOA), 8 carbon chain length, on MHO was determined to be 20.9 ± 0.4 mg of PFOA per gram of MHO. The adsorption capacity of the shorter perfluorobutanoic acid (PFBA), 4 carbon chain length, on MHO was determined to be 1.08 $\pm$ 0.2 mg of PFBA per gram of MHO.

Part I. Introduction

1.1 Food Waste Composting

1.1.1 Introduction

There is a growing interest and effort by the waste management industry and consumers to divert food waste from landfills to be composted. Composting is a biochemical process that converts organic waste in the presence of oxygen into a stable organic substance that can be used as a soil amendment or fertilizer (Bewick, 1980; Li et al., 2013). Industrial composting involves breaking down fresh feedstock materials by mechanical means then utilizing microorganisms, such as bacteria and fungi, to chemically convert the remaining organic matter into finished compost (Bewick, 1980). The resulting compost can enhance soil properties, provide essential nutrients for plants, stimulate biological activity, and improve soil structure (CalRecycle, 2018).

FSP has been a barrier to the composting process in California because it is not typically compatible with commercial compost operations. Historically, FSP has not been easily sorted from the food waste stream, and compostable FSP often does not degrade in commercial compost facility processing time frames. Thus, FSP and its contents are usually landfilled.

Compostable FSP was developed to help solve this issue and divert any remaining food waste on, or contained in, the FSP to industrial compost facilities. The materials used to make compostable FSP, including compostable plastics, have come under scrutiny due to the required processing timeframe to fully disintegrate and biodegrade the product. The most common processing timeframes associated with industrial composting in California is between 45 and 60 days. The feedstock material passes through the entire operation and is available for sale as finished compost within that timeframe. The compostable product standard specifications ASTM D6400 and D6868 utilize a 180-day timeframe to measure biodegradability. The disconnect in specification and facility timeframes has limited industrial compost facilities' willingness to accept compostable plastic products. Additionally, the lack of standardized labeling and resemblance to traditional non-degradable plastics prevents industrial composting facilities from differentiating between plastics that may be compostable and ones that are contaminants.

1.1.2 Composting Operating Conditions

Composting relies on optimal microbial activity. Industrial composting facilities control parameters such as moisture, aeration, pH, temperature, and carbon to nitrogen ratio (C/N) to ensure microbial communities can thrive in these systems. (Juárez et al., 2015; Li et al., 2013; Onwosi et al., 2017). Additional material, such as bulking agents and inoculants, are sometimes added to alter the inherent characteristics of food waste, to optimize composting performance.

Moisture Content

Moisture content is a composting parameter that directly affects the biodegradation rate of compost feedstocks by modifying microbial population and activity. Moisture content is generally affected by the feedstock's inherent properties. Feedstocks that are loose and compressible, such as food waste, generally have higher moisture contents. Bulky feedstocks with rigid and absorptive structure, like straw and woodchips, generally have lower moisture content. The optimal moisture content of an industrial compost pile is between 45 and 60 percent by weight. Moisture content below 45 percent inhibits microbial activity and decreases biodegradation rates. Moisture content above 60 percent decreases the aeration rate and requires excessive energy to reach composting temperatures (Herbert, 2010). Data suggest that even forced aeration is not sufficient for compost feedstocks with moisture content above 60 percent (Das and Keener 1994). The lack of oxygen from decreased aeration leads to anaerobic conditions and microbial communities which, decreases the overall microbial activity (Cooperband, 2002; Herbert, 2010).

pH

The overall pH of composting material affects microbial growth rates. The optimal pH range for most industrial composting operations is 6.5 to 8.0. Biodegradation byproducts vary throughout the composting process and alter pH. Volatile fatty acids accumulate as microbes degrade the fresh compost feedstocks increasing the overall acidity. The initial pH of fresh feedstocks is likely between 5.0 and 7.0. Composting material typically drops in pH over the first two to three days of the composting process in aerobic composting systems and rises overtime if kept aerobic. Poorly aerated compost piles that become anaerobic, further acidify conditions because anaerobic microorganisms produce acids as byproducts (CalRecycle 2021). A study by Gajalakshmi and Abbasi (2008) demonstrated that acidity during the initial composting phase, specifically for food waste, significantly lowered microbial activity. Since food waste has a high concentration of organic matter, adding additional buffer solutions to maintain pH may enhance composting efficiency. Sundberg et al. (2013) also observed slow biodegradation rates during the initial phase of food waste composting. Data suggest that a combination of high initial aeration rates and bulking agents, such as wood waste or finished compost, aid in maintaining consistent pH (Li et al. 2013; Gajalakshmi and Abbasi 2008).

Temperature

Temperature affects microbial growth rates and consequently impacts the compost feedstock biodegradation rate. Higher temperatures result in a faster breakdown of organic materials, but temperatures higher than 71°C, inhibit microbial activity. Temperatures between 55°C and 65°C are optimal for supporting beneficial microbes and inactivating pathogens (Herbert, 2010; Stentiford, 1996). Industrial composting operations in California are required to reduce pathogens by maintaining a temperature above 55°C for a specified number of days specific to the composting system. Windrow composting systems are required to maintain 55°C for 15 days. Enclosed, within-vessel,

and aerated static pile composting systems are required to maintain 55°C for 3 days. Temperatures typically rise during the composting process, peak at the height of microbial activity, and then fall as the compost matures (CalRecycle 2021).

Carbon to Nitrogen Ratio

The carbon and nitrogen ratio (C/N) of the compost is a key indicator of its suitability to support microbial populations (CalRecycle, 2018). Carbon content is utilized by microbes as an energy source, while nitrogen is a crucial component of nucleic acids, amino acids, enzymes, and co-enzymes necessary for cell growth and function. The optimal composting C/N is between 25-30:1 depending on the bioavailability of the carbon and nitrogen (Kumar et al., 2010). Low nitrogen levels (excessively high C/N) prevent compost from becoming microbially active and reaching optimal temperatures. High nitrogen levels (excessively low C/N) increase compost temperatures beyond the ideal threshold and may become anaerobic. The C/N gradually decreases throughout the composting process from approximately 30:1 to approximately 10:1 as the microbes consume organic waste and release carbon dioxide. Green vegetation and food waste tend to have higher nitrogen levels (lower C/N) than brown vegetation such as wood waste and dried garden waste. Therefore, feedstocks are intentionally mixed to attain the optimal C/N.

Aeration

Oxygen is necessary for aerobic respiration. Compost piles are aerated either passively or actively to keep aerobic microbes active and to prevent the development of anaerobic conditions (Finstein and Morris, 1975; Herbert, 2010). Passive aeration relies on introducing oxygen through the initial mechanical mixing and allowing any additional oxygen to diffuse into the materials as the process continues. Active aeration, utilizing pumps and tubing underneath the composting material, forces air throughout the pile during the entire composting process. Aerobic microbes can survive at oxygen concentrations between 5 and 10 percent; however, concentrations greater than 10 percent are ideal (Finstein and Morris, 1975). Guo et al. (2012) determined that the aeration rate for forced aeration, greatly influences the stability of the resulting compost. Uniform air distribution throughout the composting material is necessary to maintain aerobic conditions that promote microbial activity and prevent isolated anaerobic spots throughout the pile (Guo et al. 2012). Both forced aeration and pile turning sufficiently aerate compost piles containing food waste (Rasapoor et al. 2016).

Bulking Agents

Bulking agents are carbon-based materials that add structure to compost piles and improve porosity (Herbert, 2010). The porosity of a compost pile affects the rate that air and liquid can diffuse through the pile. Porosity is increased when using common bulking agents which remove excess moisture from their immediate environment (Chang and Chen 2010). Common bulking agents include, wood chips, wheat straw, sawdust, rice husk, rice bran, chopped hay, wood shavings, and peanut shells. Bulking agents typically contain high levels of carbon and low levels of nitrogen. Industrial composting operations

can utilize the properties of bulking agents to adjust the overall C/N and moisture content of the compost pile (Adhikari et al., 2009; Gea et al., 2007; Iqbal et al., 2010; Kim et al., 2008). Food waste is typically high in nitrogen and moisture content so the addition of bulking agents may significantly aid in composting of this set of substrates.

Inoculants

Inoculation, as it relates to composting, is the practice of introducing microorganisms or enzymes into the compost system. Microbes contained in fresh compost feedstocks require several days to reach population thresholds that initiate composting. This delay is usually referred to as the lag phase. The purpose of inoculants is to increase the initial concentration of microbes and enzymes and therefore decrease the lag phase. Data suggest that the addition of inoculants also aid in achieving higher composting temperatures, reducing odors, and improving the final compost quality (Cerda et al., 2018). Typical inoculants include material screened from previously processed compost (overs), old compost, or commercial products containing microbial communities and enzymes. Inoculants are typically mixed with fresh feedstocks before compost pile formation. The purchase and incorporation of inoculants incurs an additional cost that may dissuade some industrial composting facility operators from utilizing them. Incorporation of inoculants into windrow composting systems may incur a cost savings due to reduced windrow turning. However, an aerated static pile composting system may not gain significant lag phase decreases because the system already benefits from forced air. The use of inoculants to reduce lag phase is therefore operation specific and not as crucial as the other operating conditions mentioned previously.

1.2 Food Service Packaging and Products

1.2.1 Introduction

Food Service Packaging and Products (FSP) refers to products used for serving or transporting food or beverages, including, but not limited to, plates, cups, bowls, trays, hinged or lidded containers, and bags. FSP can be made from a variety of materials such as petroleum-based plastics, compostable plastics, lignocellulosic fiber materials, or combinations of these materials. Recycling of FSP has historically been difficult even for traditionally recycled materials such as PET because products are often contaminated with food waste. In addition to aiding in the diversion of food waste from landfill, compostable FSP is intended to counteract recycling difficulty by providing a product that can be composted along with any residual food waste. Some cities in California allow certain compostable FSP (e.g., food soiled paper and compostable plastic-coated food soiled paper) to be discarded with food waste as part of their organic waste collection programs. However, most industrial composting facilities in California are unable to accept and process compostable plastic FSP. This study focuses on the industrial composting of products marketed as compostable and available for sale in California. This includes compostable plastics and lignocellulosic fiber with compostable plastic incorporated on or into its substrate.

1.2.2 Compostable Food Service Packaging

Degradable FSP sold with the intent of being industrially composted is typically marketed as compostable. These products are made of compostable plastic materials, lignocellulosic fiber materials, or a combination of the two material types. A compostable plastic is defined by ASTM as a plastic that is degraded biologically during composting to produce carbon dioxide, water, inorganic compounds, and biomass at a similar rate to other known compostable materials and does not leave any visually distinguishable or toxic residues (ASTM D6400, 2012). Lignocellulosic fibers are derived from plant matter such as wood fiber, cotton fiber, starch, and paper pulp. These products in California require certification to either the ASTM D6400-19 for compostable plastic materials or ASTM D6868-19 for lignocellulosic materials incorporating compostable plastics in the material matrix. These certifications require products to pass disintegration, biodegradation, and ecotoxicity testing protocols.

1.2.3 Compostable Food Service Packaging Material Types

Lignocellulosic Fiber

Lignocellulosic polymers include but are not limited to wood fiber, cotton fiber, starch, bagasse, bamboo, and wheat straw. FSP made from this material type are typically called molded fiber products. Lignocellulosic polymers are blended with water to create a pulp which is shaped by a mold to produce the final form. All FSP variations can be made as molded fiber products and products can be waterproofed with spray or dip coatings of wax. This material type contains no compostable plastic materials and is not the focus of this study.

Industrially Compostable Plastics

These plastic materials are marketed to disintegrate and biodegrade in industrial composting settings in timeframes like other common compostable feedstocks. Compostable plastics and non-degradable petroleum-based plastics have similar mechanical properties and uses. Manufacturing practices for compostable plastic materials includes all blow molding, injection molding, and thermoforming techniques that are typical of non-degradable petroleum-based plastics. Compostable plastic materials are marked with the Resin Identification Code 7 indicating the “other” category.

Compostable plastics must be certified to ASTM D6400-21 to be labeled as compostable in California pursuant to California Public Resources Code Sections 42355 – 42358.5. Although many FSP products of this type hold the ASTM D6400-21 certification and are available for sale in California, many industrial composting facilities do not accept these types of materials as feedstocks. The ASTM D6400-21 certification utilizes a disintegration testing timeframe 84 days and a biodegradation timeframe of 180 days. California industrial composting operations fully process their compost between 45 and 60 days after receiving it. Compostable plastics typically do not disintegrate or biodegrade in California-based industrial composting systems because common processing times do

not allow the materials sufficient exposure to the composting environment. Many certified industrially compostable plastic materials are not compostable in California for this reason.

Compostable Plastic-Coated Lignocellulosic Fiber

This category includes all lignocellulosic fiber materials that incorporate compostable plastics as coating or additives. Typical manufacturing practices include laminating and extruding of compostable plastic materials on the food contact surface of lignocellulosic substrates. Some common FSP of this type includes coffee cups, soup bowls, and clam shells. This type of packaging utilizes the water and grease repellant characteristics of plastics.

1.2.3 Factors Affecting the Rate of Compostable FSP Biodegradation

The rate of biopolymer biodegradation depends on microbial activity, the material's chemical characteristics (molecular weight, size, crystallinity, and copolymer composition), and environmental conditions (temperature, moisture content, pH, and enzyme specificity) (Siracusa et al., 2008; Ahmed et al., 2018). In general, industrial composting parameters that increase microbial activity additionally increase the biodegradation rate of compostable plastics.

1.2.4 Environmental Characteristics

Temperature

Both microbial activity and compostable FSP biodegradation rates increase as temperature increases. Plastic materials, including compostable plastic materials, transition from a hard and brittle state into a viscous and rubbery state as temperature increases. The range of temperatures at which this occurs is specific to each plastic material and is commonly referred to as the glass transition temperature (Tg). The Tg affects the rate of biodegradation (ISO, 2013). Compostable plastics with lower Tg soften, which enhances enzymatic activity on the polymer chain. Compostable plastics with higher Tg are more difficult to biodegrade than ones with lower Tg (Ahmed et al., 2018).

pH

Changes in pH affect the rate of hydrolysis and microbial growth. Prior studies have shown that alkaline solutions promote surface erosion as hydroxyl ions on the surface of the plastics react during base-catalyzed hydrolysis (Tsuji and Ikada, 1998). PLA films had the same durability in both acidic and neutral solution and hydrolysis mainly occurred through bulk erosion (Tsuji et al., 2001; Auras et al., 2004). Makino et al. (1985) evaluated the effect of various pH values on PLA hydrolysis. They found that hydrolysis rates were higher in strong acidic (pH 1.6) and strong alkaline (pH 9.6) solutions, with the greatest reduction in molecular weight at pH 9.6.

Enzyme Specificity

The rate of biodegradation depends on enzyme specificity for various compostable materials. The material's polymer chain must fit into the enzyme's active site for biodegradation to occur.

1.2.5 Characteristics of the FSP

Molecular Weight

The maximum molecular weight that microbes can degrade differs by polymer. Generally, enzymatic activity increases as molecular weights decrease. High molecular weight polymers have a high Tg and long chain lengths that must be cleaved for microbial activity to proceed (Göpferich, 1996). Microbes can only internally degrade molecules with low molecular weight. For natural polymers such as cellulose and starch, extracellular enzymatic activity directly reduces the molecular weight for further intracellular biodegradation. For synthetic polymers, physical (photodegradation) and/or chemical (hydrolysis) degradation is necessary to reduce the molecular weight before biodegradation can occur (Kale et al., 2007).

Form

The form of compostable FSP refers to the product's general shape, size, and thickness. These properties directly affect disintegration and biodegradation rates because they affect the available surface area of the FSP. Materials with high surface area have more exposed surface for microbes and environmental factors to directly contact. Generally, high surface areas result in higher disintegration and biodegradation rates (Kale et al., 2007). However, FSP with high surface area may be in a form that prevents surfaces from encountering the composting environment. As an example, compostable plastic films may crumple or be bunched in a way that inhibits contact with interior surfaces. Product forms that potentially prevent exposure may degrade at similar rates to lower surface area forms because the majority of their surface area is not immediately in contact with the surrounding environment.

Crystallinity

Polymers consist of small crystallite material linked by amorphous regions. The degree of crystallinity affects biodegradation rates because the crystalline regions restrict the diffusion of water. Auras et al. (2004) investigated the effect of crystallinity on PLA biodegradation rates. They found that L-lactide and D-lactide content had an impact on the rate of hydrolysis. An increase in D-lactide content reduces crystallinity and increases biodegradation rates (Kale et al., 2007).

Copolymer Composition

Addition of comonomers with hydrolysable groups into the polymer structure reduces the polymer's crystallinity and Tg and increases its rate of biodegradation. In contrast, the addition of non-hydrolysable comonomers lowers a polymer's biodegradability. The level

of change in the biodegradation rates depends on the comonomer and the type of bond. For example, Chiellini and Corti (2003) noted that the addition of lignin to PCL increased biodegradability by 60 percent in old compost.

1.3 Per- and Polyfluoroalkyl Substances

1.3.1 Introduction to PFAS

Per- and Polyfluoroalkyl substances (PFAS) contained in compostable food service packaging may contaminate finished compost due to the persistence of the chemical class. PFAS are a large group of over 9,000 synthetic industrial chemicals which have been found in a variety of environments including groundwater, soils, and the ocean. PFAS have a wide variety of applications in industries such as textiles, firefighting foams, and compostable FSP. PFAS have different uses for different FSP material types. The main use for plastic FSP is as a mold release agent. Molds are sprayed with PFAS compounds to ensure final products do not stick to the molds. PFAS are used in fiber FSP to repel water and grease. Typically, the surfaces are sprayed with PFAS chemicals to prevent the fiber FSP from absorbing liquids which would weaken the structural integrity of the product. In some cases, residual PFAS on plastic FSP and added PFAS in fiber FSP can migrate to food contained in the packaging. Direct and indirect exposure to PFAS contaminated food items has led to serious health issues such as cardiovascular disease, kidney disease, and in some cases cancer.

Polyfluorinated compounds are not fully fluorinated, whereas per fluorinated compounds are fully fluorinated as shown in the table below Polyfluoroalkyl substances comprise a far more diverse group than the perfluoroalkyl substances because they contain carbon-hydrogen bonds as well as carbon-fluorine bonds in their carbon chain which increases the potential molecular configurations. Table 1.2 provides examples of perfluoroalkyl substances and polyfluoroalkyl substances and their chemical structure. There are also various functional groups that can be anionic, cationic, neutral, or zwitterionic. Polyfluorinated compounds include fluorotelomer alcohols, fluorotelomer sulfonic acids, polyfluorinated alkyl phosphates, and many others (De Silva et al., 2012).

Table 1.1: Examples of Chemical Structure of Perfluoroalkyl and Polyfluoroalkyl Substances

Perfluoroalkyl Substances	Polyfluoroalkyl Substances
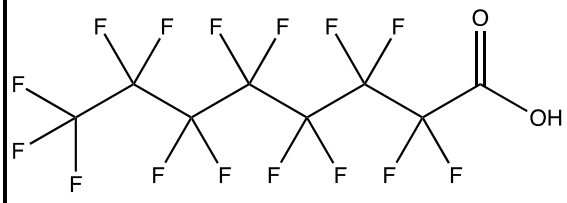	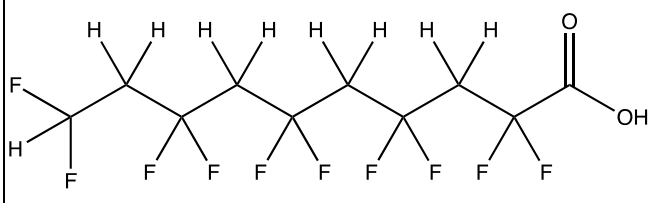
Perfluorooctanoic acid (PFOA)	Polyfluorinated carboxylic acid

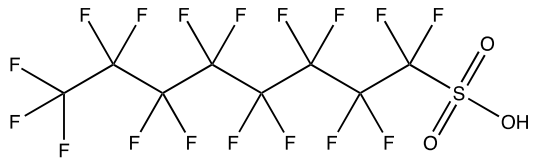	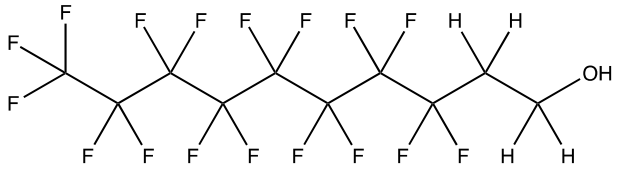
Perfluorooctanesulfonic acid (PFOS)	8:2 Fluorotelomer alcohol (FTOH)
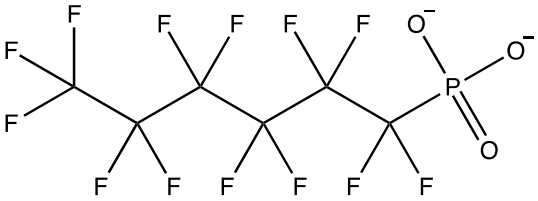	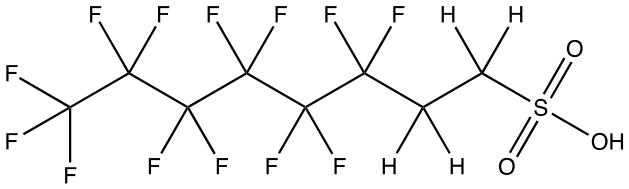
C6 Perfluorophosphonate	6:2 Fluorotelomer sulfonic acid

All PFAS contain extremely stable carbon-fluorine bonds with a bond energy of 485 kJ/mol. The bond energy refers to the bonds relative strength and is significantly higher thancarbon-carbon bonds (346 kJ/mol), carbon-nitrogen bonds (305 kJ/mol), and carbon-oxygen bonds (358 kJ/mol) (Lindstrom, 2017). Polyfluorinated substances are often the precursors for perfluoroalkyl acids (PFAAs). Including perfluoroalkyl sulfonic acids (PFSAs), perfluorocarboxylic acids (PFCAs), polyfluoroalkyl phosphoric acid diesters, perfluorophosphinates, and perfluorophosphonates. PFAAs usually contain between 2 to 18 carbons. The PFAAs are amphiphilic: both hydrophobic and hydrophilic, as they contain a perfluoroalkyl group which is hydrophobic and an anionic carboxylate or sulfonate group which is hydrophilic. Such amphiphilic properties make PFAAs useful for coatings and surfactants. The perfluorinated carbon chain is also lipophobic, which makes it resist oil, grease, and other non-polar components (Ross et al., 2018).

1.3.2 Physicochemical Properties

Properties of PFAS depend on chain length and functional groups on the molecule. Short-chain PFAS have a carbon chain length of seven carbons or less for carboxylic acids and five carbons or less for sulfonic acids. Long-chain PFAS have a carbon chain of eight carbons or more for carboxylic acids and six carbons or more for sulfonic acids. Short-chain PFAS tend to be less persistent and have shorter half-lives in human blood. Their size however allows them to be more mobile in the environment and difficult to remove from water. Long-chain PFAS are the opposite with increased half-lives and less environmental mobility. For example, perfluorohexanoic acid (PFHxA) a short chain PFAS has a human half-life of 32 days whereas the long chain perfluorooctanoic acid (PFOA) has a half-life of 3.8 years (Lindstrom, 2017).

1.3.3 Major Sources of PFAS in the Environment

Primary facilities manufacture PFAS from precursor chemicals for sale to secondary manufacturers. Secondary manufacturers then use PFAS in their products to take advantage of their chemical and physical properties. PFAS may be released into the environment from spills and disposal of manufacturing waste and wastewater from both primary and secondary manufacturers. Table 1.3 summarizes several types of manufacturing facilities that use PFAS, with examples of how they are used.

Table 1.2: Sources of PFAS from Various Industries with Examples

Industry	Example Uses	Reference
Textiles	Coating to repel oil and water. Applied to umbrellas, tents, sails, carpets, upholstery, outerwear, and protective clothing	Rao and Baker, 1994
Wire Manufacturing	Coating and insulation	Kissa, 2001
Food Service Packaging (FSP)	Plastic FSP: Mold release agent. Fiber FSP: Surface coatings to repel grease and moisture. This includes food containers like pizza boxes, popcorn bags, and fast-food packaging	Rao and Baker, 1994
Industrial Surfactants, Resins, Molds, and Plastics	Manufacturing plastics. Fluoropolymers, rubber, plumbing agents, composite resins, and flame retardant for polycarbonate	Kissa, 2001

PFAS are used to coat surfaces of compostable FSP to repel grease and moisture. Upon testing each of the FSP studied in this project, it was determined that some contained high concentrations of PFAS which could enter the human body if transferred to food.

Water from facilities that produce PFAS often makes its way to wastewater treatment plants. Sewage treatment at these facilities cannot remove PFAAs from water but they can change the concentration of PFAS as they degrade to form PFAAs (Schultz et al., 2006). The two most common PFAS found in wastewater are PFOA and PFOS. The ambient air around these facilities is also affected by the amount PFAS in the water. Studies have shown that the amount of PFAS in the air surrounding wastewater treatment plants is 1.5 to 15 times greater than reference sites (Hamid and Li, 2016).

1.3.4 Public Health Concerns

People can be exposed to PFAS by eating food or drinking water that is contaminated. Breathing air that is contaminated with PFAS is also a possible pathway. Data suggests that PFAS can transfer from FSP to food which leads to ingestion by humans (Xu et al. 2013). PFAS can also transfer from FSP to compost as the FSP degrades. When PFAS contaminated compost is applied to agricultural land, leaching of PFAS into the soil can occur. The leachate then contaminates crops, livestock that consume the crops, and the meat and milk that is consumed by humans (Kowalzyck et al.,2012). One of the most common PFAS found in FSP as well as drinking water is PFOA. Studies show that exposure to PFOA can lead to various health issues such as testicular and kidney cancer, increased cholesterol levels, thyroid problems, and decreased fertility in adults (C8 Science Panel, 2012). PFOA also adversely effects child development and immune response in infants who were exposed to PFAS by breast milk especially during the first six months of life (Grandjean et al., 2017).

1.3.5 Regulations Restricting PFAS

In 2006, the EPA implemented the 2010/2015 PFOA Stewardship Program. The main goal involved companies voluntarily reducing all PFOA materials including chemical precursors that can breakdown to form PFOA by 2010. By 2015, the goal was to have eliminated these chemicals from emissions and products. The eight major companies that participated were Arkema, Asahi, BASF Corporation, Clariant, Daikin, 3M, DuPont, and Solvay Solexis. Most companies met these goals by completely stopping the manufacturing and importing of long-chain PFAS and transitioned to other chemicals. There are additional Chemical Data Reporting requirements, which requires manufacturers and importers of PFOS to report if they meet certain production volume thresholds (usually 25,000 pounds) at a single site. The last time the manufacturing of PFOS was reported to EPA as part of this collection effort was 2002. In addition to these programs, the EPA has issued regulations known as Significant New Use Rules (SNURs) that require manufacturers to notify the EPA of new uses of such chemicals before they are on the market. The regulation also specifies that the company needs to notify the EPA at least 90 days before beginning any such activity, which would allow the EPA time to review the plan and make any necessary changes to the products and chemicals used (EPA, 2018). The EPA drinking water health advisory states that levels of PFOA and PFOS alone or in combination should not exceed 70 parts per trillion (EPA, 2016). However, the California EPA submitted a draft report in July 2021 proposing even lower

concentrations of PFOA in drinking water to 0.007 parts per trillion and 1 parts per trillion for PFOS (OEHHA, 2021).

Beginning January 1, 2023, California will ban any person from distributing, selling, or offering for sale in the state any plant-based food packaging that contains PFAS (AB 1200, Ting, Chapter 503, Statutes of 2021). Since PFAS are used in a variety of compostable FSP it is important to note another California law, AB 1201 (Ting, Chapter 504, Statues of 2021), which prohibits products containing PFAS (as measured by total organic fluorine concentration) from being labeled as “compostable.”

Finally, the regulations implementing the Sustainable Packaging for the State of California Act of 2018 SB 1335 (Allen, Chapter 610, Statues of 2021) prohibit “compostable” and “recyclable” food service packaging made from plastic or fiber from containing more than 100 parts per million total fluorine (a proxy for determining the presence of PFAS), as determined by combustion ion chromatography, particle-induced gamma-ray emission spectroscopy, instrumental neutron activation analysis, or other technique utilized by an ISO/IEC 17025:2017 accredited laboratory.

1.4 PFAS Mitigation Methods

1.4.1 Treatment of Solid Waste

Commercial incineration at high temperatures is often the easiest way to dispose of PFAS in soil. The estimated temperature needed for an incinerator to destroy PFAS differs widely in the range of 300°C to sometimes even larger than 1000°C (Vecitis et al., 2008).

1.4.1.1 Sorption

Sorption does not destroy PFAS as sorption is the removal of a liquid contaminant by a solid. Organoclays are useful sorbents because of their high adsorption capacity and because they are not toxic to the environment. Organoclays can be modified to increase their adsorption capacity with mesopores (2–50 nanometers in diameter) and by changing the cation on the surface. For instance, the montmorillonite (Mt) clay often has a hydrophilic surface and is therefore not very useful in adsorbing long-chain PFAS. However, some cationic modifications to the Mt clay surface can change the adsorption capacity. Adding a sodium cation (making the surface Na-Mt) makes the clay more lipophilic, which increases the adsorption capacity for PFAS (Zhu et al., 2016).

1.4.1.2 Ball Milling

Ball milling is a form of mechanochemical destruction, which means that chemicals at the surface are destroyed by mechanical force. Ball milling uses small stainless-steel balls with a diameter between 5–10 nanometers in a standard planetary ball mill. The steel balls are mixed with the soil and rotated at hundreds of revolutions per minute with changes in direction during the process. The non-deformable steel balls collide with the deformable solid waste. The deformation of the solid waste leads to an increase in temperature which is needed for the destruction of PFAS. In some settings, co-milling agents are added to the ball mill mixture. Some examples of co-milling agents that have

been used include potassium hydroxide (KOH), sodium hydroxide (NaOH), lime (CaO), and silicon dioxide (SiO_2). One study was able to show greater than 90 percent removal of PFOA and PFOS after six hours of ball milling using KOH as the co-milling agent (Zhang et al., 2013). Ball milling has been tested in bench-scale laboratory experiments, so the scale-up of this process needs significantly more research.

1.4.2 Treatment of Liquid Waste

The methods used to remove PFAS from liquids are applied to drinking water supplies, groundwater, industrial wastewater, surface water, and other runoff water. Water contaminated with toxic chemicals from sewage or runoff are two forms of liquid waste. Liquid waste can be treated using granular media as an adsorbent. This review will discuss granular activated carbon, biochar, and ion exchange.

1.4.2.1 Granular Activated Carbon

Granular activated carbon (GAC) is made from organic matter such as coal and coconut. These are effective for adsorption because of their high porosity, which provides a large surface area for the contaminants to adhere. GAC removes PFAS from water by a physical adsorption process which means that the contaminants in the water bind to the surface of the adsorbent without penetrating the material. This is not a destructive process and the PFAS are not transformed or degraded. Studies have shown GAC to remove almost 100 percent of PFAS from liquid waste samples. GAC tends to retain longer-chain PFAS, six carbons or more, better than short-chain PFAS. Short-chain PFAS breakthrough the GAC about 5 times faster than the long-chain PFAS (McNamara et al., 2017). Furthermore, studies have found that GAC retain non-branched isomer chains better than branched chain PFAS (Östlund, 2015).

1.4.2.2 Biochar

Biochar is a hybrid porous adsorbent made from charcoal and biomass from wood or manure, through a high temperature and low oxygen process known as pyrolysis (Ahmad et al., 2014). The properties of the resulting biochar, such as pore size, hydrophobicity, and chemical composition depend on the type of biomass used and pyrolysis conditions. A study was done to compare GAC to biochar for treating liquid waste with PFAS. They concluded that high surface area biochar could be an alternative to GAC; however, biochar has its limitations (Xiao et al., 2017). When treating river water, biochar was ineffective and had slower adsorption kinetics in comparison to GAC. Biochar is an effective adsorbent in ultrapure water (Rahman, 2014).

1.4.2.3 Ion Exchange

Ion exchange (IX) resins are organic polymers or plastics and are made as reusable and single use IX media. The reusable resins must be flushed with brine or a highly acidic or highly basic solution to regenerate the resin. For the removal of PFAS from water, an anionic positively charged IX medium is used to remove the negatively charged PFAS. This exchange of counter ions leads to an electrostatic interaction in the IX medium. The collection of PFAS on the IX medium allows for a hydrophobic interaction to occur as well

which aids in the PFA removal. Researchers observed nearly 100 percent removal of PFOA and PFOS using IX (Contea et al., 2015).

1.4.2.4 Membrane Filtration

Membrane filtration is a separation technique that is based on the pore size of the membrane used. Low pressure membranes like ultrafiltration and microfiltration are not effective in the removals of PFAS since their pore size is larger than the effective diameter of PFA molecules (about 1 nanometer). Therefore, only nanofiltration and reverse osmosis membranes will be discussed.

1.4.2.5 Nanofiltration

Nanofiltration (NF) technology has been used since the 1980's in several industries including drinking water preparation and food production processes. In drinking water treatment plants, NF can remove toxic contaminants that come from pesticides and other contaminants that are endocrine disrupters, as well as reducing the hardness of water without removing wanted salts (Mänttäri et al., 2013). NF membranes can be made from a variety of materials, such as organic polymers, ceramics, or highly crosslinked polymers. The highly crosslinked polymeric membranes are advantageous since they function at high temperatures, pressures, and pH (Van der Bruggen and Geens, 2008). Sometimes materials with different properties are layered to form a composite membrane.

Membranes are classified by the molecular weight using Daltons, which is in the range of 90–1000 Daltons (g/mol) for NF membranes. This is equivalent to a 90 percent removal of substances of that molecular weight. A molecule that has a larger molecular weight would be retained to a larger extent. Three different NF membranes were tested using wastewater that contains PFOS. The results show that NF membranes had a removal efficiency of between 90 to 99 percent (Tang et al., 2007). The removal efficiency is usually greater than 95 percent for PFAS that have a molecular weight in the range of 214 g/mol to 713 g/mol. Lower separation efficiencies were observed for perfluoropentanoate (PFPeA) and perfluorooctane sulfonamide which was about 70 percent and 90 percent respectively (Steinle-Darling and Reinhard, 2008).

1.4.2.6 Reverse Osmosis

Reverse osmosis (RO) membranes separate compounds by pressurizing water. The water that passes through the membrane (permeate) and the rejected water (concentrate) are collected separately to be disposed of or discharged accordingly. The main difference between RO and NF is that RO will reject all salts from the liquid, whereas NF will reject most hard salts to a higher degree but will allow sodium chloride to pass. This means that NF can remove unwanted particles and retain minerals, but RO will remove all particles and minerals from liquid waste. Five different RO membranes were evaluated for the removal efficiency of PFOS from wastewater. The removal efficiency was found to be higher than 99 percent (Tang et al., 2007). Both the NF and RO membrane filtration technologies are very energy-intensive since they require high pressures to function properly. Disposal of the concentrate in this membrane is a design factor that needs

improvement. The other issue with membranes is their degradation over time. More studies need to be done to understand membrane fouling and how to combat it.

1.4.2.7 Redox Manipulation

Redox chemistry involves manipulation of the charged species in water to change its oxidation or reduction potential. Redox processes involve the transfer of electrons between reactants. Oxidation is the loss of electrons and reduction is the gain of electrons. In PFAS the carbon chain is not easily oxidized or reduced as the carbon-carbon bonds are shielded by the tightly bound fluorine atoms. The carboxylic or sulfonic group attached to the molecule is more susceptible to change when compared to the carbon chain. This results in a partial transformation of the molecule and incomplete removal. Scientists evaluated the performance of two photocatalyst semiconductors for the degradation of PFOA in water. The first is the relatively well-known monoclinic BiPO4 and the second is $Bi_3O(OH)(PO_4)_2$, also known as BOHP. A stronger photocatalytic degradation was observed with BOHP (Sahu et al., 2018).

Part II. Composting and Food Service Packaging Biodegradation Experiments

2.1 Composting Experiment Approach

2.1.1 Inoculant

The objective of this study was to investigate the microbial structure of different inoculants such as cow manure, mixed liquor, i.e., wastewater from the activated sludge process, aged compost, and landfill sludge. A respirometry study was performed to understand how various inoculants impacted the oxygen consumption rate and microbial community structure of the composted materials. The respirometry experiment provided insight into the metabolic activity of the microbial populations. Oxygen consumption is also a good indicator for polymer biodegradation (Rastogi et al., 2009). Section 2.1.2 and 2.1.3 below provide further information on these experiments.

2.1.2 Respirometer Experiment

Synthetic compost was made from a mixture of food waste, dried leaves, woodchips, and inoculants at a ratio of 12:6:1:1 by weight. The target carbon-to-nitrogen ratio was 30:1, and the target moisture content was 60 percent. Four different inoculants were tested: cow manure, mixed liquor (wastewater from the activated sludge process), aged compost, and landfill sludge. Cow manure and mixed liquor samples were freshly collected while the old compost sample was three months old, and the landfill sludge sample was excavated from the 20 – 28 years old landfill cell. An RSA PF–8000 Pulse Flow Respirometer was used to conduct the experiment. All the experiments were performed as per the ASTM D6400-12 standard specification. Microbial samples were analyzed as per Section 2.1.4

2.1.3 Initial Food Service Packaging Biodegradation Experiment

Results from the respirometry study were utilized to inform initial FSP biodegradation experiments. Cow manure was determined to be the most microbially active inoculant due to a relatively high oxygen consumption rate and was used as the sole inoculant for all subsequent bench-scale tests. The effect of oxygen availability on the rate of FSP biodegradation was investigated using a microcosm study. Two microcosms (i.e., microaerobic and fully anaerobic conditions) were set up in duplicate in one liter glass serum bottles with a 500 mL working volume to mimic oxygen conditions in a compost pile. Each bottle contained 50 g of cow manure and 0.5 L of synthetic media. Two FSP samples were analyzed: The fiber plate and PLA lined bagasse clamshell (See table 2.1). The samples were cut into two x two cm sheets, then the initial weight of at least ten FSP samples was collected to determine the average initial weight. Microcosms were incubated at 35°C in a shaker incubator for 32 days. Samples were collected every four to five days and analyzed for change in FSP weight. The rate of FSP biodegradation (k;

g FSP degraded/g FSP initial) was determined using first order kinetics with the following (equation 1):

$C = C_o e^{-kt}$ ..... (1)

Where C = weight of FSP at time t (g FSP degraded),
C_o = FSP weight at time t = 0 (g FSP added) and t = time (day)

Table 2.1: Types of FSP Used in Initial Biodegradation Experiments

Type of Food Service Packaging	Manufacturing Material	Manufacturer & Item Name	Product Photo
Fiber Plate	Bamboo + Unbleached Plant Fiber	World Centric (7 inches Fiber Square Plate) UPC - SQ-SC-7-P	
PLA Lined Bagasse Clamshell	Sugar Cane Bagasse + PLA Lined	Eco Products (8 x 8 x 3 inches - Hinged Sugarcane Clamshell) UPC – EP-HC81	

2.1.4 Microbial Gene Analysis

Biomass samples were taken on day zero and 30 of the respirometry experiment and sent to UC Davis Genome Center for DNA extraction, PCR amplification, and amplicon sequencing. Specifically, DNA was extracted using PowerSoil® DNA Isolation Kit. The V3-V4 region of bacterial 16S rRNA gene was amplified. The Internal Transcribed Spacer region of the fungal community was also amplified. Raw sequences were analyzed on QIIME 2 platform (Bolyen et al., 2019). Paired-end sequences were merged and quality filtered using denoising algorithm DADA2, which generated exact amplicon sequence variants equivalent to 100 percent similarity in operational taxonomic unit (Callahan, McMurdie, & Holmes, 2017; Callahan et al., 2016). Bacteria taxonomy was assigned using a built-in Naïve Bayesian classifier with MiDAS database v3.6 (McIlroy et al., 2015), while the fungi taxonomy was assigned using UNITE database v7 (Kõljalg et al., 2020).

2.2 Results and Discussion for Composting

2.2.1 Respirometry Assessment: Specific Oxygen Uptake Rate

A key objective of this research was to quantify the effect of different inoculants on oxygen uptake rate during food waste composting. The Specific Oxygen Uptake Rate provides information on a sample's microbial activity where higher rates indicate higher microbial activity and therefore likely indicate an increased rate of FSP biodegradation. A specific oxygen uptake rate curve produced during the respirometry test is shown in Figure 2.1. The average specific oxygen uptake rate for the compost, cow manure, mixed liquor, and landfill sludge inoculants were: 0.33 ± 0.03, 0.37 ± 0.06, 0.27 ± 0.14, and 0.27 ± 0.07 g COD/g VSS-L-hr., respectively. The data suggest that the aged compost initially had the highest specific oxygen uptake. However, the cow manure was consistently higher after day four. Higher oxygen uptake rates indicate higher biological activity and likely correlate to higher rates of FSP biodegradation. The study concluded that the cow manure had the highest average oxygen uptake rate over the entire duration of the experiment even though the peak rate was lower than 2 other inoculants.

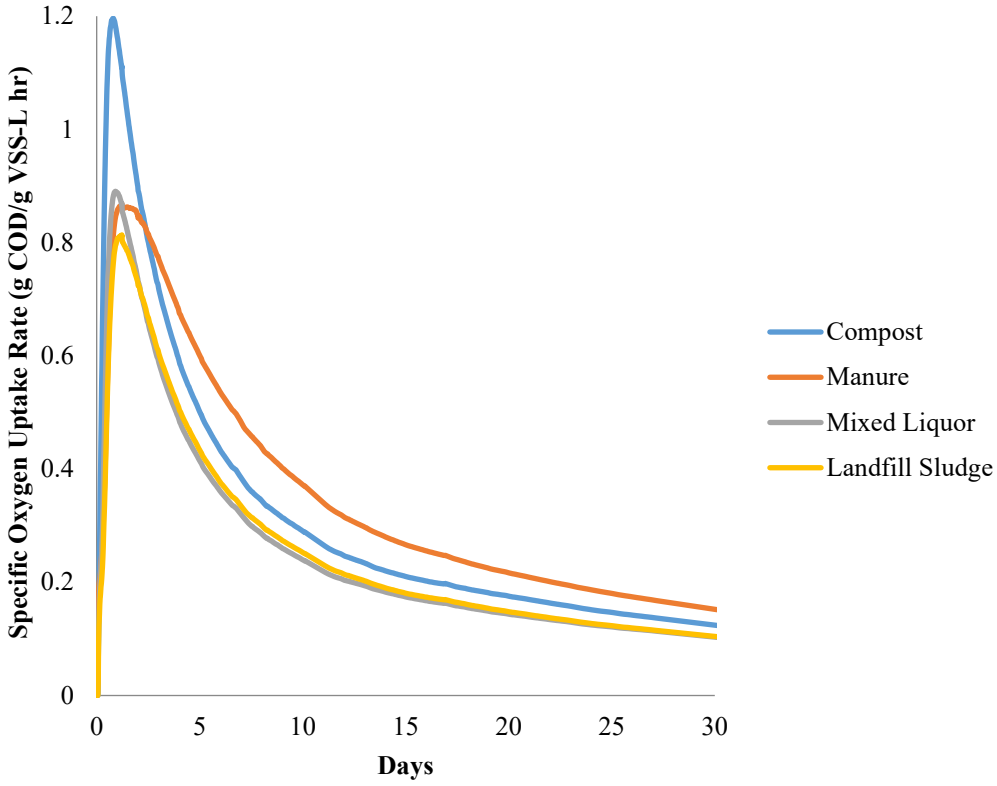

Figure 2.1: Specific Oxygen Uptake Rate for Different Inoculants

2.2.2 Food Service Packaging Biodegradation Microcosm

Results of the microcosm tests are shown in Figure 2.2. The rate of FSP biodegradation under microaerobic conditions (i.e., oxygen concentrations > 2.0 g/L) was 0.05 and 0.097 g FSP degraded/g FSP initial for the bamboo fiber plate and PLA lined bagasse clamshell, respectively. For fully anaerobic conditions (i.e., no oxygen conditions), the biodegradation rate was 0.037 and 0.034 g FSP degraded/g FSP initial for the fiber plate and PLA lined bagasse clamshell, respectively. The introduction of oxygen concentrations in the microcosm reactors resulted in a higher rate of degradation for both types of compostable FSP. Statistical analysis (t-test) was run to determine a statistical difference between the means of FSP biodegradation rate under two oxygen conditions and FSP type. P values less than 0.05 were considered statistically significant, and values less than 0.0001 were considered extremely significant. The difference in biodegradation rate was not statistically different between the oxygen conditions for the brown plate ($p = 0.07$). However, oxygen conditions had a statistically significant impact on the rate of biodegradation for the white plate ($p = 0.0001$). This difference in results may be attributed to the type of FSP components (i.e., bamboo and unbleached plant fiber vs. sugarcane bagasse lined with PLA) in the plate, as discussed in the literature review section of this report. However, additional experiments are required to elucidate this observation further.

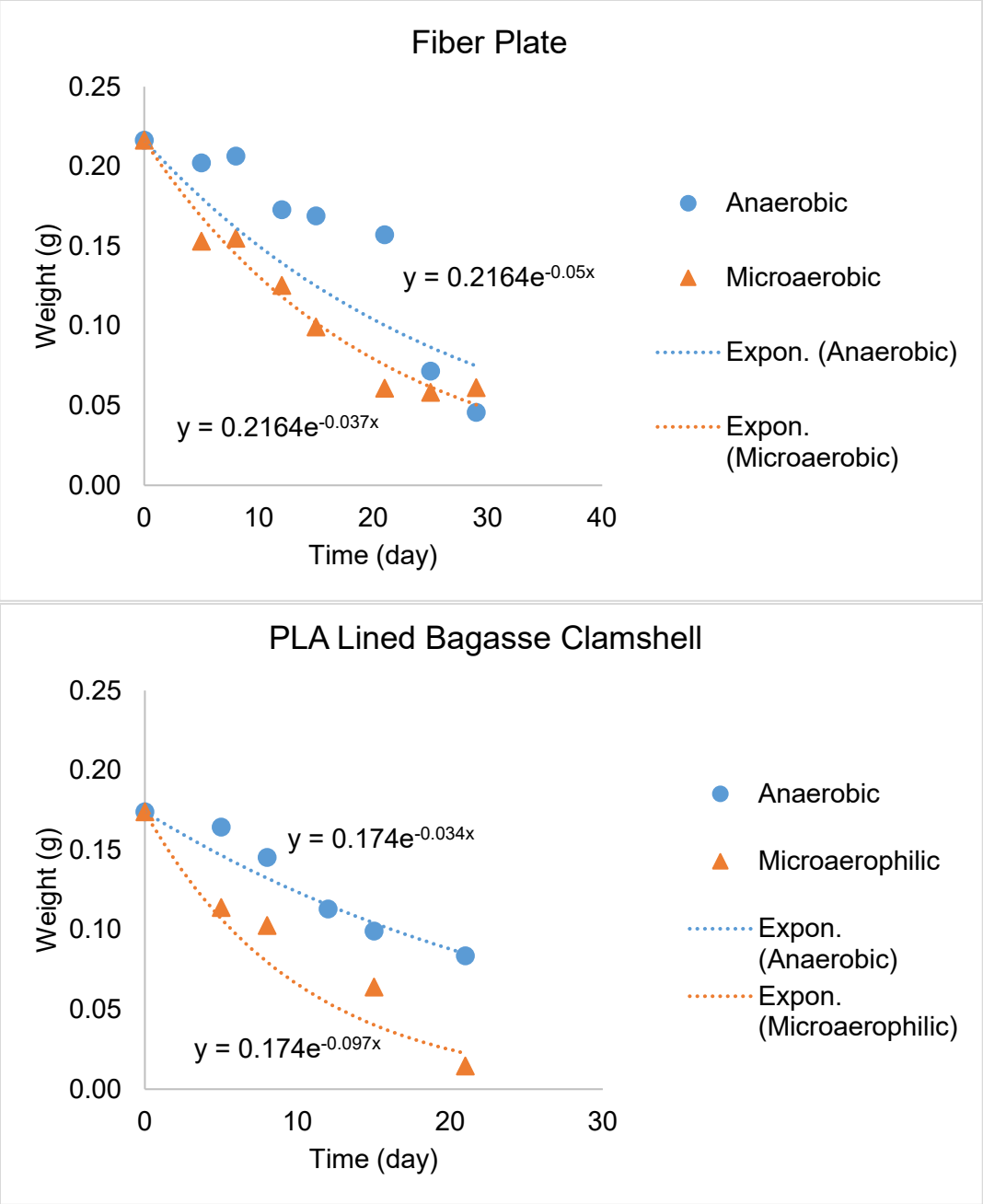

Figure 2.2: FSP Biodegradation Profiles Using Cow Manure as an Inoculant - Fiber Plate; PLA Lined Bagasse Clamshell

2.2.3 Microbial Structure and Ecology

Figure 2.3 shows the top 15 most abundant bacterial genera across the inoculants. In the figure, each bar represents a different inoculant. The subsections in the bar represent different bacterial genera. The main bacterial genus in the final compost after 30 days of composting were: *Bacillaceae Bacillus, S. Streptomyces, P. Paenibacillus, and P.*

Brevibacillus. Figure 2.4 shows the relative frequency of fungi with respect to the family for different inoculants during composting. DNA sequencing data showed that the most abundant fungal species was *Aspergillaceae* in all four inoculant types (Figure 2.4). From these results, two main conclusions can be drawn. First, the age of the inoculant at the time of collection seemed to have an impact on the bacterial structure during composting. Specifically, inoculant samples collected from active systems (i.e., dairy cattle and an operational wastewater treatment plant) showed a different trend in changes to the bacteria structure compared to the 30-day old compost and 23-year-old landfill sludge (Figure 2.3). Second, the fungal community regarding family was different between the bulk compost and those attached to FSP using landfill sludge (Figure 2.4). Besides *Aspergillaceae*, the second most abundant fungal family on the FSP was Microascales, a low oxygen fungi (Gallardo-Altamirano et al., 2021). While *Streptomyces* was the most abundant bacterial genus in the bulk compost and FSP, the general bacterial community proliferating on the FSP differed. Mainly anaerobic or obligate aerobes were found on the FSP, indicating a natural stratification between the bulk compost, where oxygen concentrations were likely to be higher, and the FSP samples. Bacterial genera found on the FSP samples likely produce enzymes that aid in biodegradation of FSP.

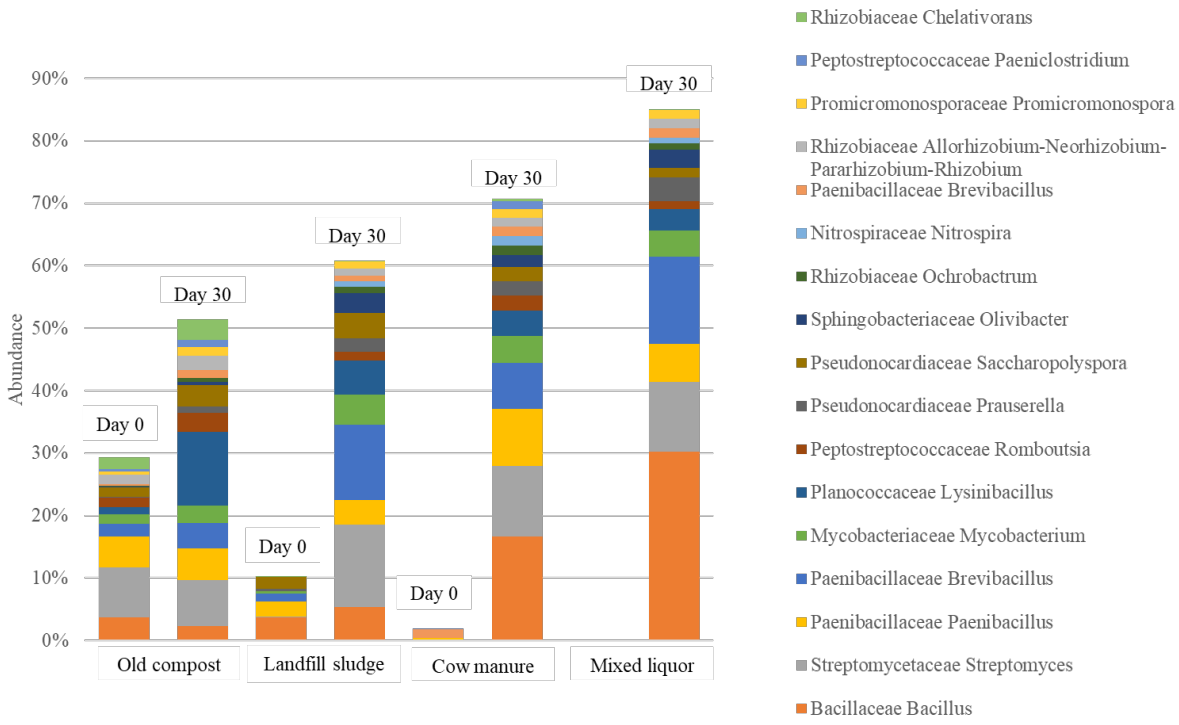

Figure 2.3: Abundance of the Top 15 Bacterial Genera Across Different Inoculants

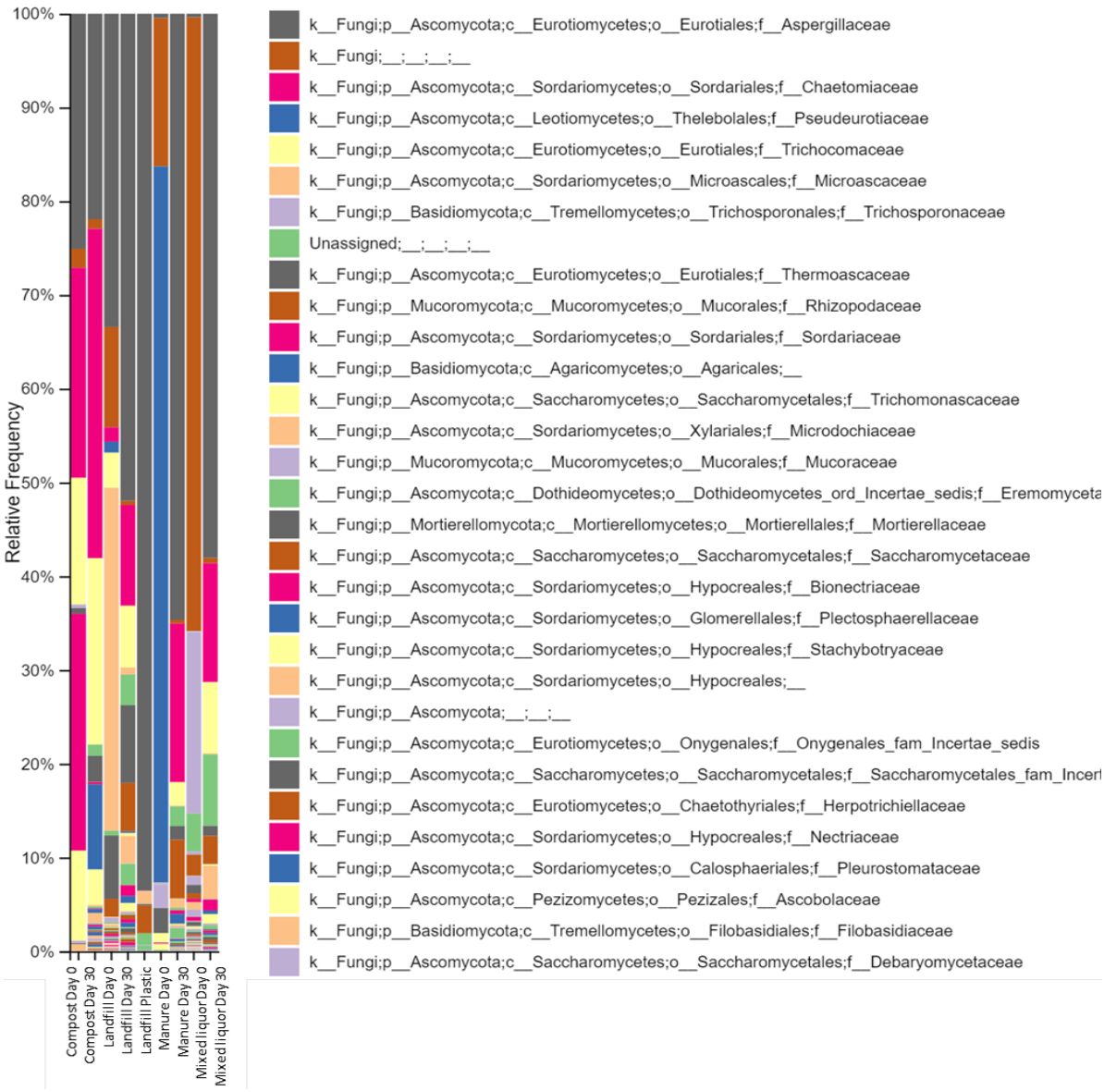

Figure 2.4: Relative Frequency of Fungi with Respect to the Family for Different Inoculants During Composting.

Part III. Bench-Scale and Commercial-Scale Composting Experiments

3.1 Composting Reactors

A bench-scale experiment was conducted in the Wastewater Laboratory of Dr. Maureen Kinyua in the Department of Civil and Environmental Engineering at the University of California, Davis. Gandhar Abhay Pandit performed the bench and commercial-scale experiments as part of his Ph.D. research. A total of eleven reactors were constructed to carry out the experiment. Figure 3.1 provides a schematic of the reactors. Each reactor was built with cast acrylic non-reactive tubing with an inner diameter of 7.5 inches and a height of 11 inches. Two ports were added at the bottom of the reactor for the inlet of air and leachate sampling. Similarly, one port was fitted at the top of the reactor for the air outlet for condensation. Aeration was provided through the perforated (opening diameter of 0.25) plate that was placed in the lower bottom part (3.5 inches from bottom) of the reactor.

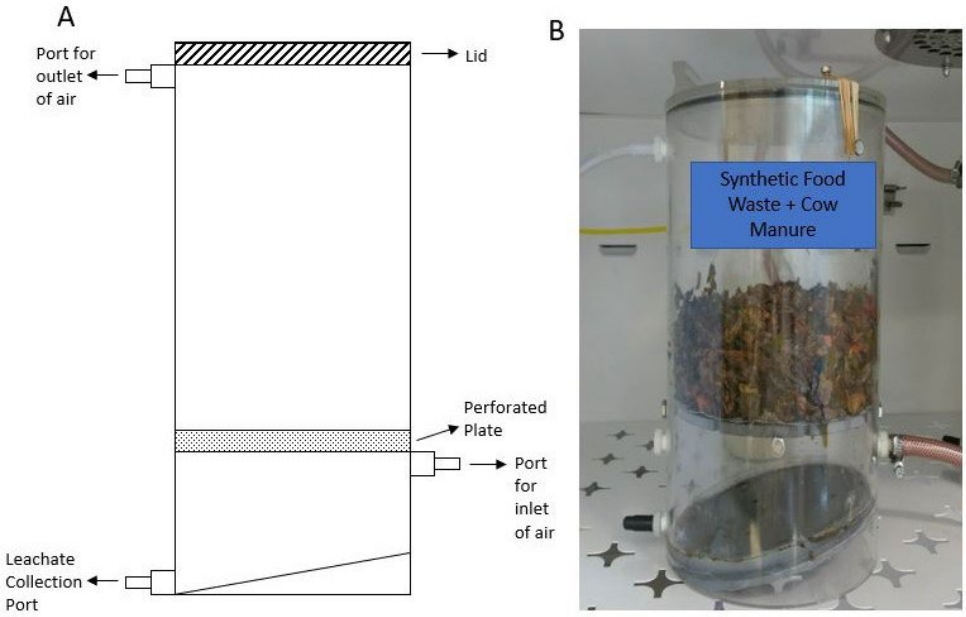

Figure 3.1: Schematic of the Reactor (A) and Reactor with Synthetic Food Waste (B)

Figure 3.1 shows the bench-scale setup of the reactors. Out of eleven reactors, five were operated at 45 percent moisture content, five were performed at 60 percent moisture content, and one reactor was operated at 50 percent moisture content (control). The total duration of the experiment was 24 days. Sampling was conducted on day 0, 3, 5, 7, 10, 14, 18, 20, and 24. The reactors were placed in an incubator at a constant temperature of 56.0℃, and constant airflow of 0.3 liters of air per minute, supplied through a commercial air pump.

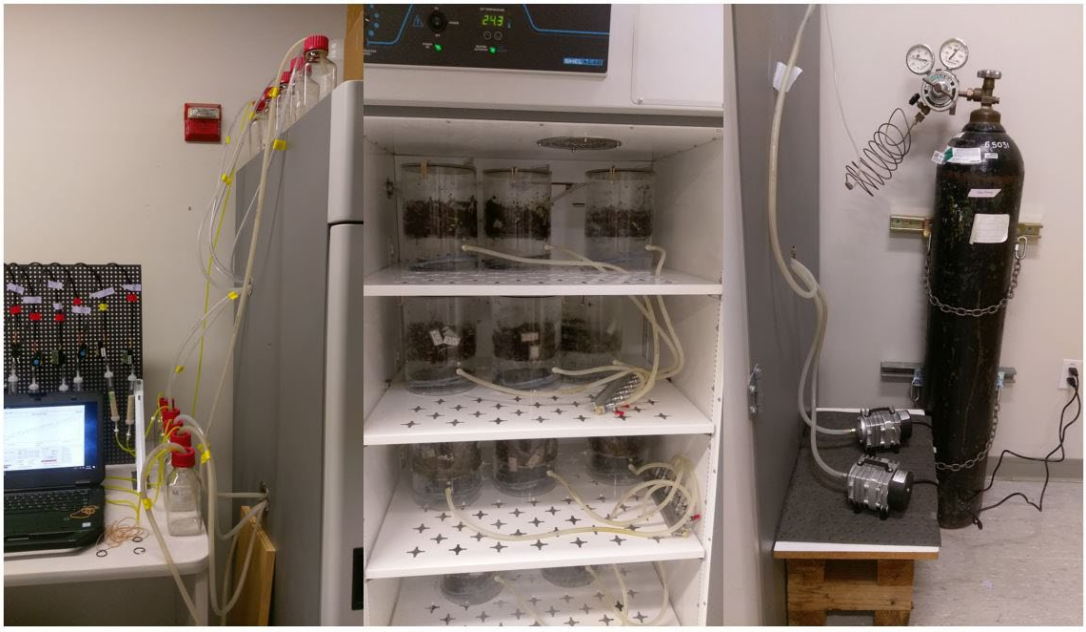

Figure 3.2: Bench-Scale Set Up for 11 Composting Reactors During Bench-Scale Experiments

See Table 3.2 for the FSP contents and moisture content of each bench-scale reactor. All of the FSP samples were cut into two-by-two centimeter squares and sealed in mesh plastic bags to avoid loss in the reactor. Synthetic food waste was created using a mixture of tomatoes, carrots, and lettuce at a ratio of 1:1:1 by weight. Dried leaves and wood chips (which acted as bulking agents) were added in a ratio of 1:2 by weight. Finally, 175 grams of cow manure (pH 7.2 ± 0.2) was added to 400 mL of Mili Q water, and the slurry of Mili Q water and cow manure was added to reactors. The fresh cow manure was obtained from the UC Davis Dairy Teaching and Research Facility.

Table 3.1: Bench-Scale Experimental Setup

Reactor Name	Moisture Content by Weight (%)	Types of Food Service Packaging (FSP) Added
$R_{Control\_50}$	50	No FSP
$R_{Positive\_45}$	45	Unbleached Coffee Filter
$R_{Positive\_60}$	60	Unbleached Coffee Filter
$R_{Negative\_45}$	45	LDPE Sheet
$R_{Negative\_60}$	60	LDPE Sheet
R_{45} (triplicates)	45	Fiber plate + Synthetic/Starch Blended Bag + PLA Clamshell
R_{60} (triplicates)	60	Fiber plate + Synthetic/Starch Blended Bag + PLA Clamshell

Table 3.2: Types of FSPs used in the bench scale experiments

Type of Food Service Packaging	Manufacturing Material	Manufacturer & Item Name	Product Photo
Unbleached Coffee Filter (Positive Control)	Chlorine-Free Paper	If you care (Unbleached Coffee Filter #6) UPC - 770009001161	
LDPE Sheet (Negative Control)	Low-Density Polyethylene Plastic	Uline (4 x 4 inches 1.5 Mil Autobags on roll) UPC – S-11111	
Fiber Plate	Bamboo + Unbleached Plant Fiber	World Centric (7 inches Fiber Square Plate) UPC - SQ-SC-7-P	
Synthetic/Starch Blended Bag	Starch (Hemp + Corn + Wheat Straw + Silver grass + Sugarcane + Bamboo + Agave + Wood Pulp) + Synthetic Material	World Centric (17x18 inches - 3 Gallon Waste Bag) UPC – BG-CS-3	
PLA Clamshell	Renewable PLA made from Corn	Eco Products (9.5 x 5 x 3.5 inches PLA clamshell) UPC – EP-LC96	

3.2 Aerated Static Pile Composting

This study aimed to determine the impact of feedstock on FSP biodegradation at commercial-scale conditions. Three aerated static compost piles were set at the Napa Recycling and Waste Services in American Canyon, California. For the aerated static composting process, organic waste was mixed in a large pile, and the piles were placed over the network of pipes that deliver air into the piles (See Figure 3.3). To aerate the piles, layers of loosely piled bulking agents like garden trimmings and wood waste were added to the piles so that the air could pass from bottom to top. Air blowers were used to blow the air from the bottom to the top through the perforated openings in the floor. All air blowers were active throughout the process. Three experiments were conducted at the facility from October 2020 to April 2021. Two different piles were constructed on-site using either food waste or old compost. Each pile (94 feet (L) x 30 feet (W) x 10 feet (H)) consisted of inoculant, feedstock (grasses, food scraps, and dry leaves), and bulking agents (garden trimmings and wood waste).

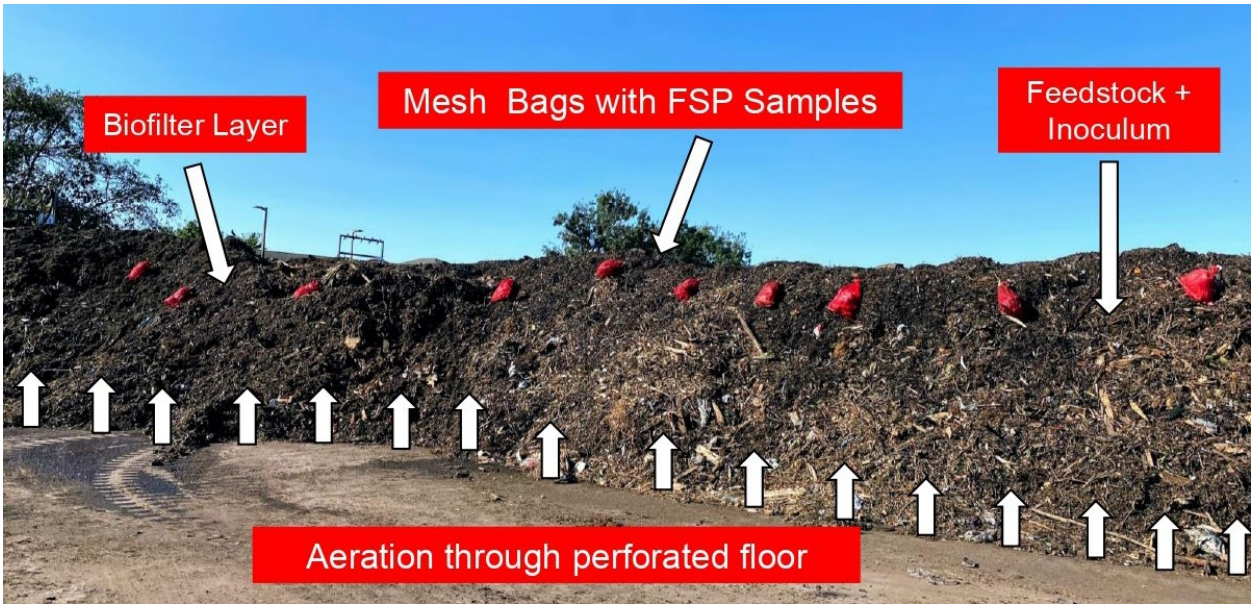

Figure 3.3: Aerated Composting Pile at Napa Recycling Facility

Compost piles either contained food waste or old compost at a ratio of 15:85 (by volume) to other feedstocks. None of the inoculants tested at bench-scale were able to be tested at commercial scale due to the limitations set by the testing site. Piles were constructed from bottom to top, and the top layer was covered with a biofilter layer. The biolayer was a simple top covering layer of soil that protects the piles from heat loss and helps to reduce the escape of foul odors. For the 2nd and 3rd experiments, three piles were constructed on-site. While the first two piles were like the 1st experiment, the third pile consisted of typical feedstocks commonly accepted by the Napa Recycling Facility. For the purposes of this report, the third pile is referred to as the business as usual pile or the BAU pile. No food waste or old compost was added in excess of what is commonly contained in the business as usual (BAU) pile. The pile consisted of a mixture of grasses,

food waste dry leaves, food waste, and bulking agents (garden trimmings and wood waste). No FSP were placed in the BAU pile. The purpose of the BAU pile was to act as a control pile for collecting physical and chemical data like pH, conductivity, temperature, and moisture content of the compost. The pile acted as a control pile. Each pile had five temperature sensors engineered by Engineered Compost Services for continuous monitoring of temperature. Sprinklers watered the piles four to six times a day (from seven am to seven pm) depending on the pile's temperature. The piles were constantly aerated at a rate of 4.5 cubic feet per minute. Four FSP samples and a positive and negative control (seen in Table 3.3) were placed in different mesh plastic bags and placed in the piles for 24 days. Compost and samples of each type of FSP were collected from the piles on days 3, 5, 7, 10, 14, 18, 20, and 24.

3.2.1 Food Service Packaging Biodegradation Kinetics

To determine the rate of FSP biodegradation, samples were removed from the mesh bags and cleaned to remove organic matter. Later they were dried at room temperature for one hour, and the final weight was noted. The resulting weight measurements were compared to the initial weights of each type of sample, and the percent weight decrease was calculated. The rate of FSP biodegradation (k; g FSP degraded) was determined using the slope-intercept form of the linear equation (2):

(2) $y = mx + b$

Where m = slope of line = k (g FSP degraded).

The specific rate of FSP biodegradation (Q; g FSP degraded/g FSP added) was calculated using equation (3):

(3) $Q = \frac{k}{Co}$

Where Co = weight of FSP (g FSP added) at t = 0.

3.2.2 Microbial Analysis

For microbial analysis, 2.5 grams of compost samples were shaken with Phosphate Buffered Saline solution for 15 minutes. Afterward, the samples were centrifuged at 12,000 rpm for 12 minutes using a microcentrifuge. The centrifuged samples were saved in a microcentrifuge tube at -80 ℃ temperature. Genomic DNA was extracted using the Qiagen's DNeasy® PowerSoil Pro Kit. Samples were sent to UC Davis Host Microbe Core Lab for PCR amplification and amplicon sequencing as discussed in section 2.1.4 above.

3.2.3 Analytical Methods

Laboratory measurements included moisture content, pH, conductivity, and C/N. Five grams of compost samples were collected and dried in an oven at 105 ℃ for 24 hours for moisture content measurement. The dried samples were ground using a Krups Coffee

Table 3.3: Types of FSPs used in the commercial scale experiments

Type of Food Service Packaging	Manufacturing Material	Manufacturer & Item Name	Product Photo
Unbleached Coffee Filter (Positive Control)	Chlorine-Free Paper	If you care (Unbleached Coffee Filter #6) UPC - 770009001161	
LDPE Sheet (Negative Control)	Low-Density Polyethylene Plastic	Uline (4 x 4 inches 1.5 Mil Autobags on roll) UPC – S-11111	
Fiber Plate	Bamboo + Unbleached Plant Fiber	World Centric (7 inches Fiber Square Plate) UPC - SQ-SC-7-P	
Synthetic/Starch Blended Bag	Starch (Hemp + Corn + Wheat Straw + Silver grass + Sugarcane + Bamboo + Agave + Wood Pulp) + Synthetic Material	World Centric (17x18 inches - 3 Gallon Waste Bag) UPC – BG-CS-3	
PLA Clamshell	Renewable PLA made from Corn	Eco Products (9.5 x 5 x 3.5 inches PLA clamshell) UPC – EP-LC96	
PLA Lined Bagasse Clamshell	Sugar Cane Bagasse + PLA Lined	Eco Products (8 x 8 x 3 inches - Hinged Sugarcane Clamshell) UPC – EP-HC81	

Grinder before C/N analysis by the Department of Plant Sciences - University of California, Davis. For measuring compost's pH and conductivity, 2.5 grams of compost

sample was mixed with 25 mL Mili Q water, and the mixture was shaken for 30 minutes and then allowed to settle. The pH and conductivity of the clear supernatant were measured with a pH meter and a conductometer. Standard Methods (APHA, 2018) were used to measure pH (4500-H^+), conductivity (2510), and C/N (5310). Standard method (ASTM D2216) was used to measure moisture content.

3.2.4 Data Analysis

All results are reported in triplicates. The average and the standard deviation as the error bars. Statistical analysis was performed using Wilcoxon Test using R studio. The test's purpose was to compare the two paired groups by calculating the difference between the sets of pairs and analyzing these differences to determine if the results are statistically significantly different from one another. The p values less than 0.05 were considered statistically significant.

3.3 Results and Discussion for Bench-Scale Experiments

3.3.1 Physicochemical Parameters

One of the objectives of this study was to determine the impact of moisture content on FSP biodegradation using a bench-scale approach. Table 3.4 shows the average characteristics of the different physicochemical parameters of the different reactors that were operated during bench-scale composting. Moisture content is an essential factor in the composting process as it influences the oxygen uptake rate, free air space, microbial activity, and temperature (Cerda et al., 2018). High moisture content may result in waterlogs resulting in anaerobic conditions. Similarly, low moisture content can cause early dehydration, hindering the biological process (Guo et al., 2012). Studies have suggested that the optimal moisture content should be in the range of 50-60 percent, whereas some have recommended it to be 40-70 percent (Bernal, Alburquerque, & Moral, 2009; R. Zhang et al., 2007). Thus, to determine the impact of moisture content on FSP biodegradation, we utilized two experimental moisture contents of 45 percent and 60 percent and a control moisture content of 50 percent. Conventional trends were observed with respect to MC, high MC (70-90 percent) at t=0 with stabilization and desired content of 40–60 percent by day three. Zhang et al., (2007) have reported similar results where the initial moisture content of the food waste containing piles was between 70-90 percent. These values represent the moisture content before the addition of water during sampling.

Initially, the pH was acidic (4.0) and by the end of the investigation, it was in the range of 7.0–8.5. Wilcoxon Test showed no statistical difference ($p=0.726$). All the reactors followed a similar steady rise in the pH from acidic to neutral range. Chan, Selvam, & Wong, (2016) has demonstrated that pH affects the microbial activities in the composting process. Initially, pH decreases due to the volatilization of ammonium (NH_4^+-N) releasing protons (H^+). However, in this study, a pH increase was observed, and this may have been due to the accumulation of ammonia (NH_3). Studies have shown a delayed increase in pH and attributed it to the decomposition of the organic acids (Jolanun & Towprayoon,

(2010); Chan, Selvam, and Wong (2016)) showed a delayed increase in pH and attributed it to the decomposition of the organic acids.

Table 3.4: Average Characteristics of the Physicochemical Parameters of the Different Reactors Operated During Bench-Scale Composting

Parameters	Moisture Content (%)	pH	Conductivity (mS/cm)	C/N
$R_{Control\_50}$	50.8 ± 11.8	7.49 ± 0.54	2.29 ± 0.39	18.33 ± 2.64
$R_{Positive\_45}$	47.4 ± 10.9	7.20 ± 0.84	2.69 ± 0.91	19.75 ± 3.75
$R_{Positive\_60}$	55.0 ± 10.0	7.29 ± 0.64	2.46 ± 0.90	19.71 ± 2.88
$R_{Negative\_45}$	47.7 ± 10.9	7.39 ± 0.70	2.42 ± 0.70	20.22 ± 3.40
$R_{Negative\_60}$	59.2 ± 8.21	7.58 ± 0.54	1.35 ± 0.23	21.91 ± 6.89
R_{45}	53.4 ± 11.8	6.71 ± 0.23	2.12 ± 0.36	22.08 ± 1.31
R_{60}	60.3 ± 9.04	6.86 ± 0.28	2.10 ± 0.43	21.33 ± 2.00

Reactors at each moisture content level showed a similar pattern of increase and decrease in the values of electrical conductivity. Initial conductivity was around 1.74 ± 0.39 mS/cm for all the reactors. Eventually, it increased to about 2.03 ± 0.91 mS/cm to 2.64 ± 0.70 mS/cm, except for the positive control reactors with 60 percent moisture content, which had a conductivity of 5.29 ± 0.90 mS/cm. The Wilcoxon Test showed a statistical difference ($p=0.014$) between the reactors of different moisture content. Availability of more moisture might have resulted in accelerated microbial activity, resulting in a high rate of biotransformation of complex materials. Huang, Wong, Wu, and Nagar (2004) showed that an increase in the conductivity can be due to the formation of mineral salts from ammonium and phosphate ions produced during the biotransformation of the organic matter. This might be the reason for the increase in conductivity during the experiment. Similarly, the volatilization of ammonia and the precipitation of mineral salts can also decrease electrical conductivity (Awasthi et al., 2014). This might be a reason for the decrease in the conductivity during the experiment's later phase ($t=18$).

The C/N started at approximately 21.30 for all reactors. The negative controls decreased to 15.60 ± 2.64 for 45 percent MC. For 60 percent MC, C/N increased to 21.91 ± 6.89= by the end of the experiment. For the positive control, the values decreased to 19.80 ± 3.75 and 19.0 ± 2.88 for 45 percent and 60 percent moisture content, respectively. Our results were similar to a study conducted by Yang, Li, Shi, and Wang, (2015), which showed that the C/N ratio decreases during composting. Iqbal, Shafiq, and Ahmed, (2010) concluded that C/N between 20 and 25 is optimum. Similar results were found by Huang et al., (2004); Kumar, Ou, & Lin, (2010); Zhu, (2007). According to Palaniveloo et al., (2020), C/N affects the decomposition rate in the composting process. As the

microbial community uses carbon as a source of energy and nitrogen to build proteins, lower C/N nitrogen ratios (less than ten) reflect more nitrogen loss. In contrast, a higher C/N ratio (greater than 30) indicates a slower rate of decomposition. Bulking agents can be used to adjust the C/N ratios (L. Zhang & Sun, 2016). In our study, wood chips were used as bulking agents.

3.3.2 Biodegradation of FSP During Bench-Scale Composting

The FSP biodegradation time plots, and biodegradation rates are shown in Table 3.5. The overall degree of biodegradation was higher by 25 percent in 60 percent moisture content than 45 percent moisture content. Although the rate of biodegradation for the positive control at 60 percent moisture content was higher compared to 45 percent moisture content, the difference was not statistically significant (p=0.624). However, the Wilcoxon Test showed a statistical difference between the two moisture contents for the fiber plate (p=0.042) and bioplastic bag (p=0.020). Negative controls and the PLA clamshell showed no biodegradation.

Table 3.5: Rate of FSP Biodegradation and Specific Rate of Biodegradation during Bench-Scale Composting

FSP Type	FSP Content	Rate of FSP Biodegradation	Rate of FSP Biodegradation	Specific Rate of FSP Biodegradation	Specific Rate of FSP Biodegradation
		k; g FSP degraded	k; g FSP degraded	Q; g FSP degraded/g FSP added	Q; g FSP degraded/g FSP added
		R 45	R 60	R 45	R 60
Positive control	Chlorine Free Paper	9.00×10^{-4}	1.40×10^{-3}	0.014	0.021
Negative control	LDPE Film	-	-	-	-
Synthetic/Starch Blended Bag	Synthetic + Starch-Based Plastics	7.00×10^{-5}	3.00×10^{-4}	0.004	0.018
Fiber Plate	Bamboo + Unbleached Plant Fiber	1.30×10^{-3}	4.10×10^{-3}	0.003	0.010
PLA Clamshell	Renewable Poly Lactic acid (PLA) from Corn	-	-	-	-

3.4 Results and Discussion for Commercial-Scale Experiment

3.4.1 Physicochemical Results

To determine the impact of feedstock on composting at commercial-scale, experiments were conducted from October 2020 to April 2021 at Napa Recycling and Waste Services in American Canyon, California. The physicochemical parameters (i.e., moisture content, C/N, pH, and conductivity) for three pile mixtures (i.e., food waste, old compost and BAU) are shown in Table 3.6.

Table 3.6: Average Physicochemical Characteristics during a 24-day Commercial-Scale Experiment for Three Pile Conditions

Parameter	Units	Food Waste	Old Compost	Business as Usual (BAU)
Moisture Content	%	60.9 ± 6.82	58.4 ± 5.16	57.2 ± 6.13
Temperature	℃	56.4 ± 8.16	54.7 ± 4.61	55.0 ± 3.14
pH	-	7.20 ± 0.36	7.41 ± 0.23	7.27 ± 0.18
Conductivity	mS/cm	1.03 ± 0.26	0.82 ± 0.19	0.97 ± 0.29
C/N	-	16.0 ± 1.63	15.3 ± 1.55	14.5 ± 0.41

Generally, all piles had a similar physicochemical performance typical of the composting system. Food waste piles had slightly higher moisture content than the other piles, likely because the food itself has and holds moisture at higher levels (Zhang et al., 2007). In addition, the increase in pH at the start of the experiment may have been due to the mineralization of proteins, amino acids, and peptides to ammonia, as described in the study by Hachicha et al., (2009); Sánchez-Monedero, Roig, Paredes, & Bernal, (2001). Generally, the pH remained neutral throughout the experiment, and the differences between the pile conditions were not statistically significant ($p=0.203$). Like the bench-scale experiments, the electrical conductivity of the commercial-scale compost samples followed a similar increase and decrease trend as discussed in Section 2.4.1. Lastly. However, food waste piles had the highest C/N content followed by old compost and BAU; the differences were not significantly different ($p=0.496$).

Lastly, the conventional composting temperature stages; mesophilic, thermophilic, and maturation (Emadian, Onay, & Demirel, 2017) were noted. In fact, for this study, there were significant differences in temperature ($p=0.039$) between the three piles for the

different stages of the composting - thermophilic (0–5 days), mesophilic (5–10 days), and the curing stages (10–5 days) can be depicted from Figure 3.4.

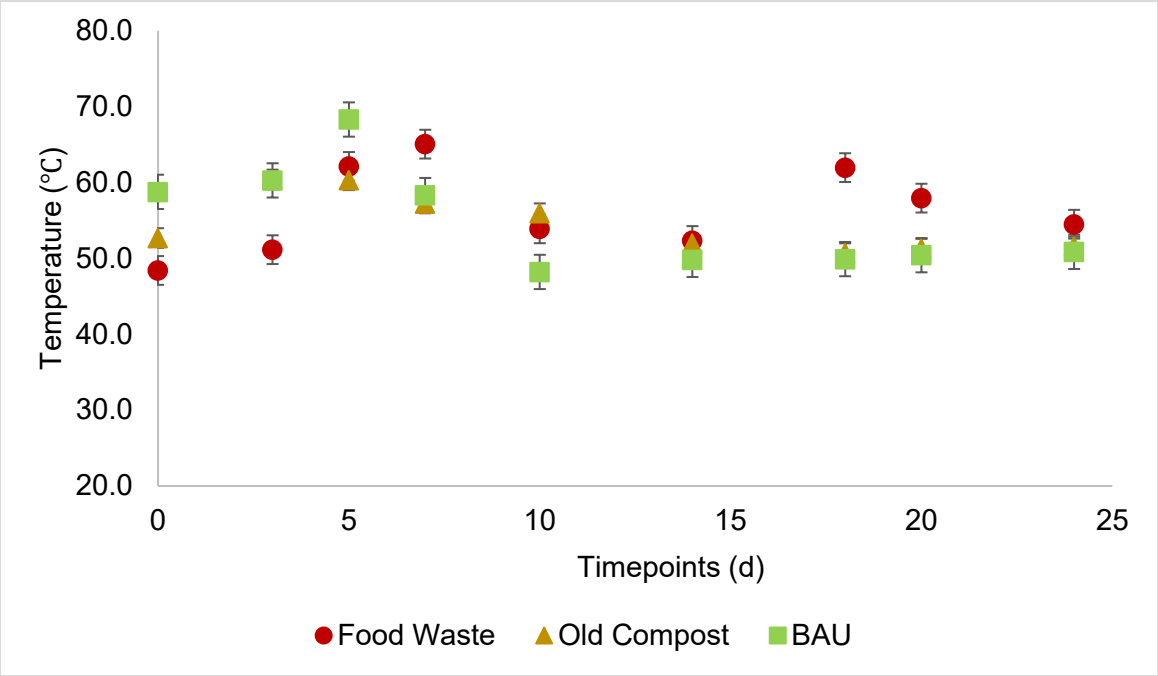

Figure 3.4: Changes in the Temperature in the Different Piles during the Commercial-Scale Composting Experiments

3.4.2 Biodegradation of FSP in Composting Environments for Commercial-Scale Experiments

The aim of this study was to determine the impacts of different feedstocks on FSP biodegradation at commercial scale. The commercial-scale piles either contained food waste or old compost.

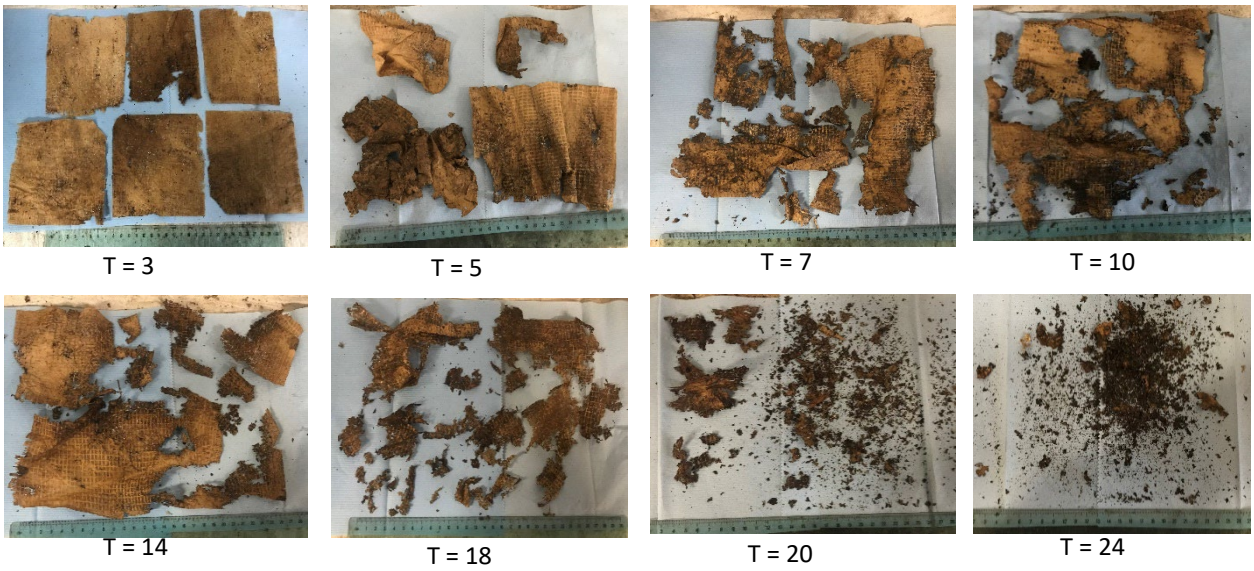

Figure 3.5: Changes in the positive control (unbleached coffee filter made from cellulose) placed in the commercial-scale food waste pile

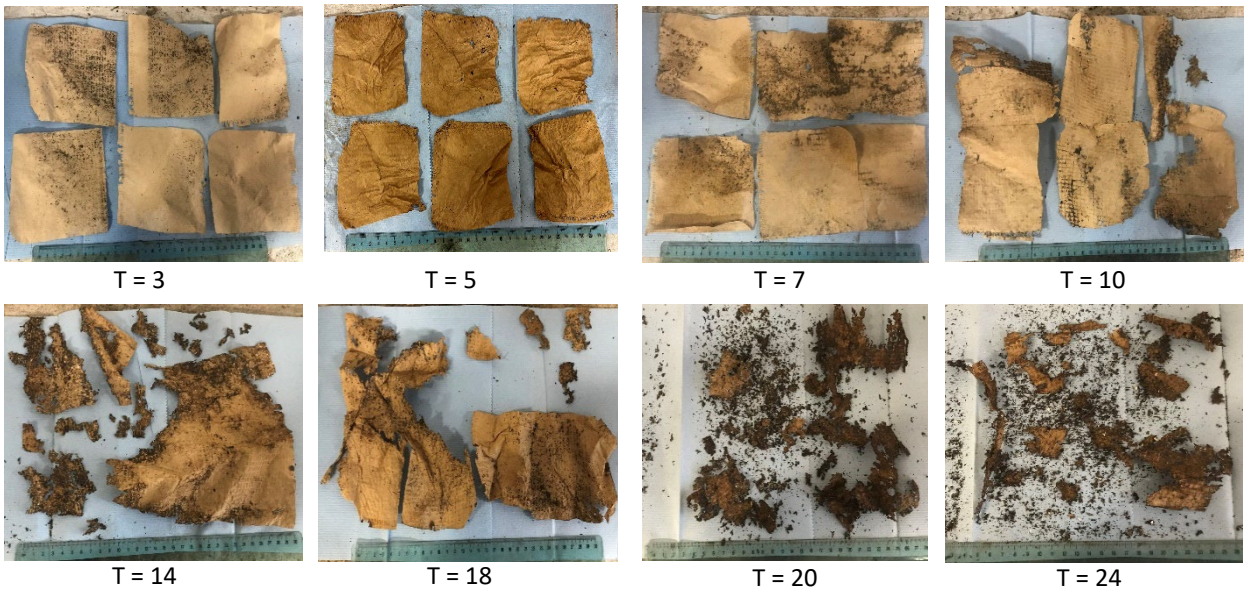

Figure 3.6: Changes in the positive control (unbleached coffee filter made from cellulose) placed in the commercial-scale old compost pile

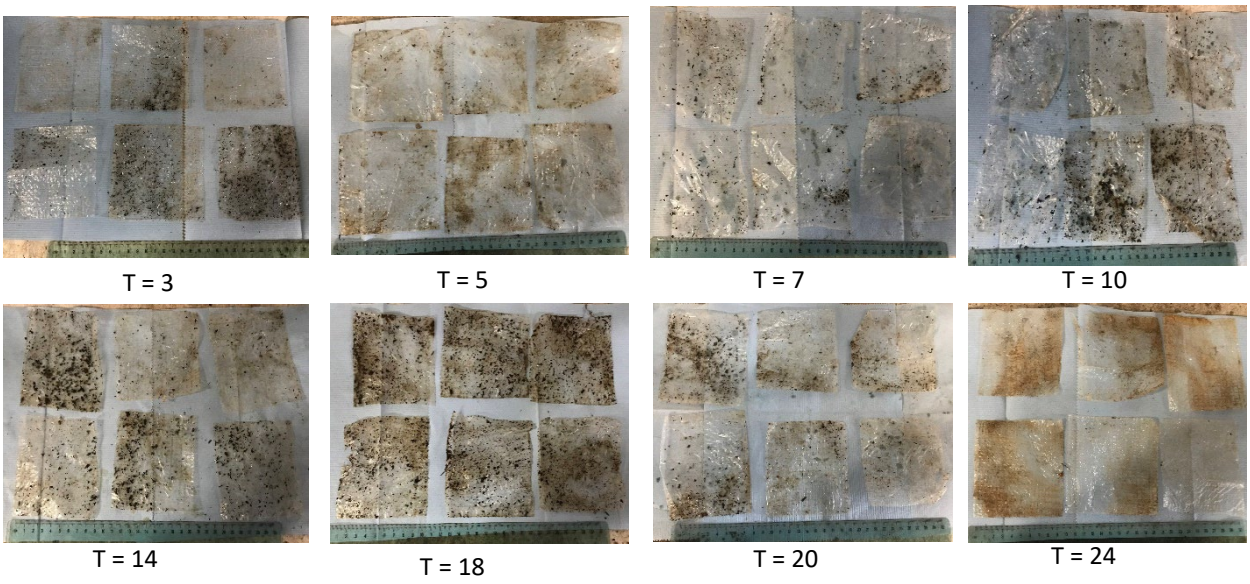

Figure 3.7: Changes in the negative control (LDPE film) placed in the commercial-scale food waste pile

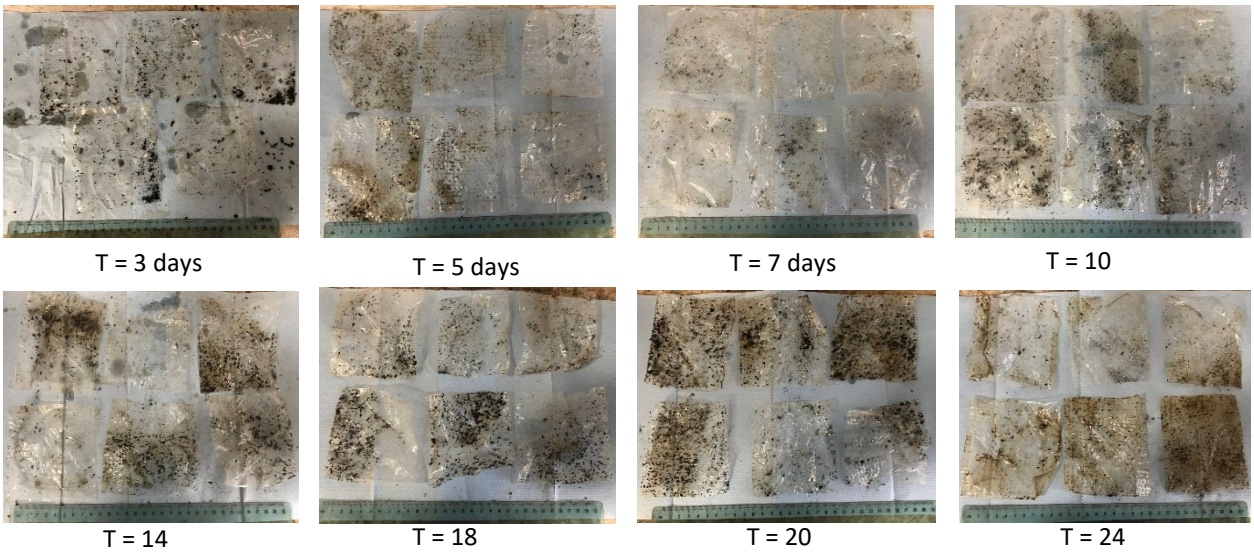

Figure 3.8: Changes in the negative control (LDPE film) placed in the commercial-scale old compost pile

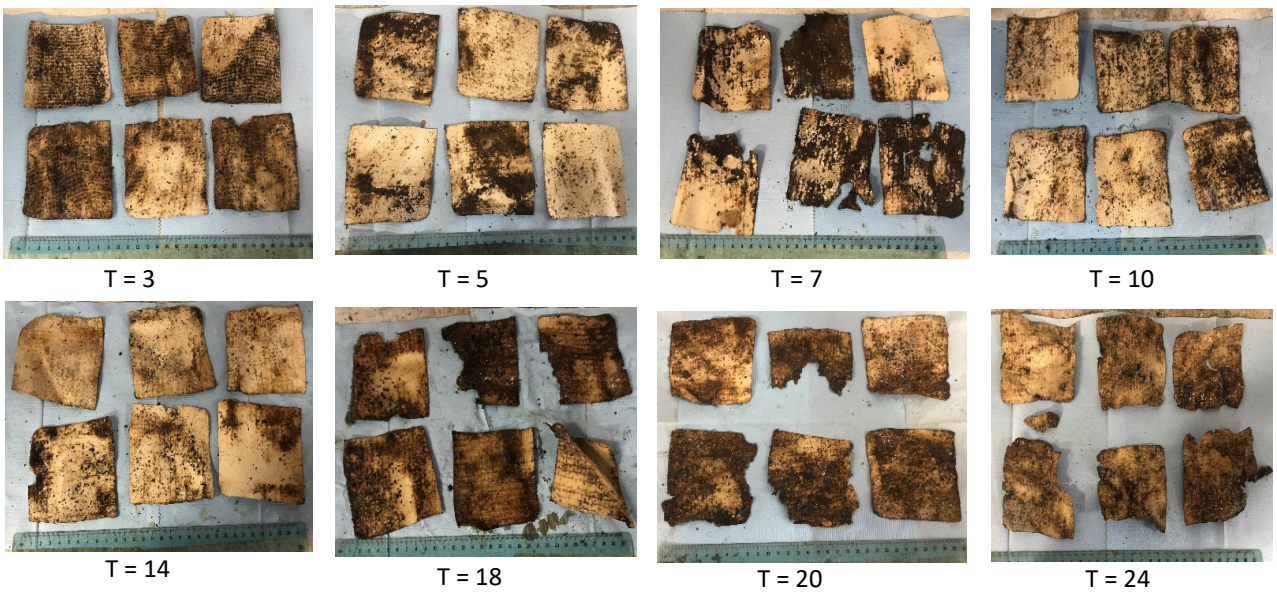

Figure 3.9: Changes in the fiber plate test samples placed in the commercial-scale food waste pile

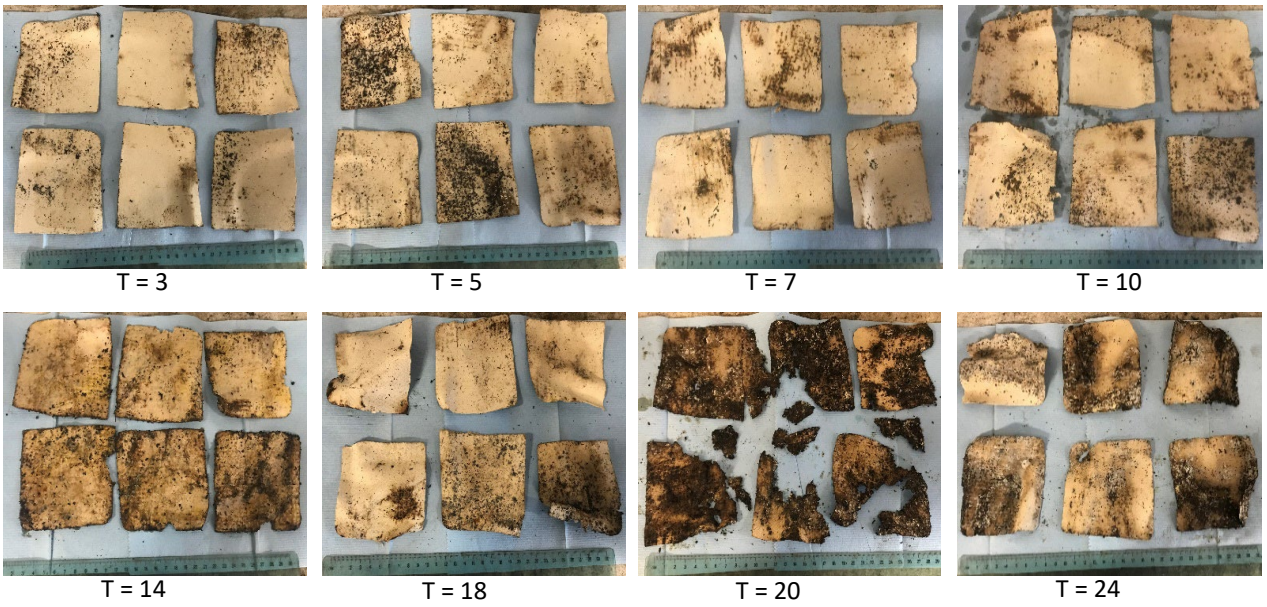

Figure 3.10: Changes in the fiber plate test samples placed in the commercial-scale old compost pile

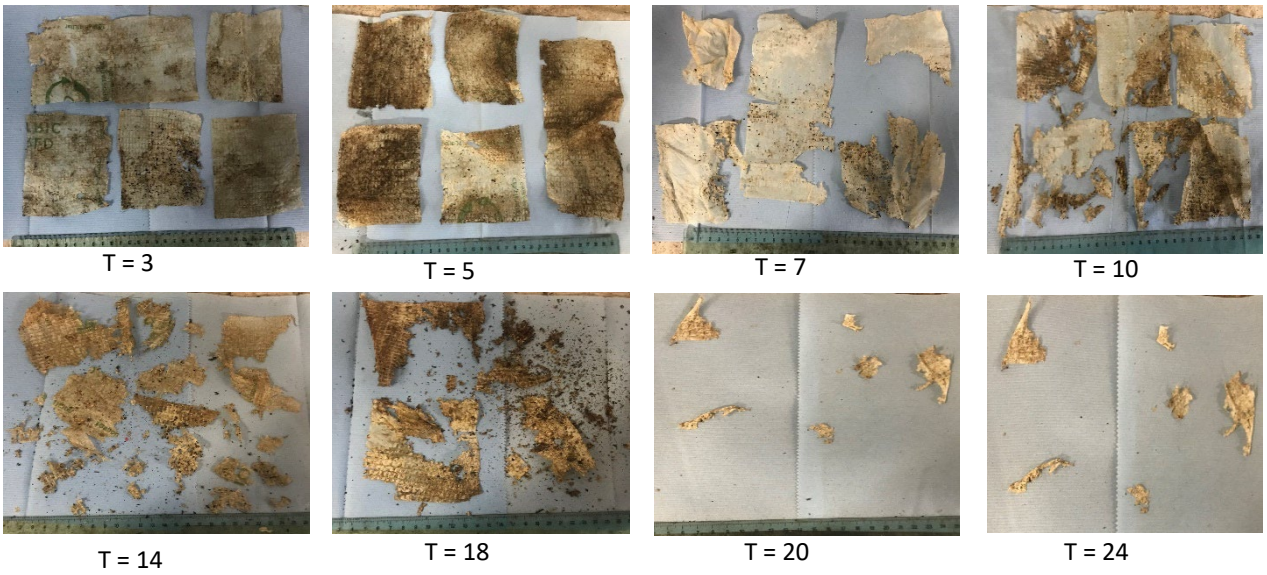

Figure 3.11: Changes in the synthetic/starch blended bag test samples placed in the commercial-scale food waste pile

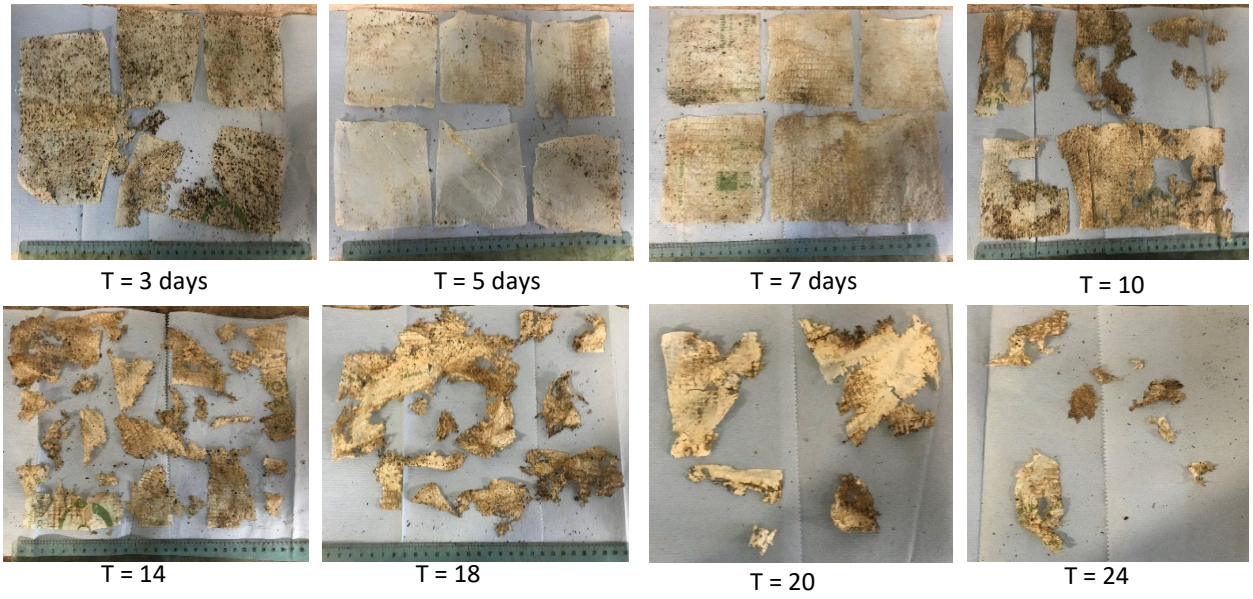

Figure 3.12: Changes in the synthetic/starch blended bag test samples placed in the commercial-scale old compost pile

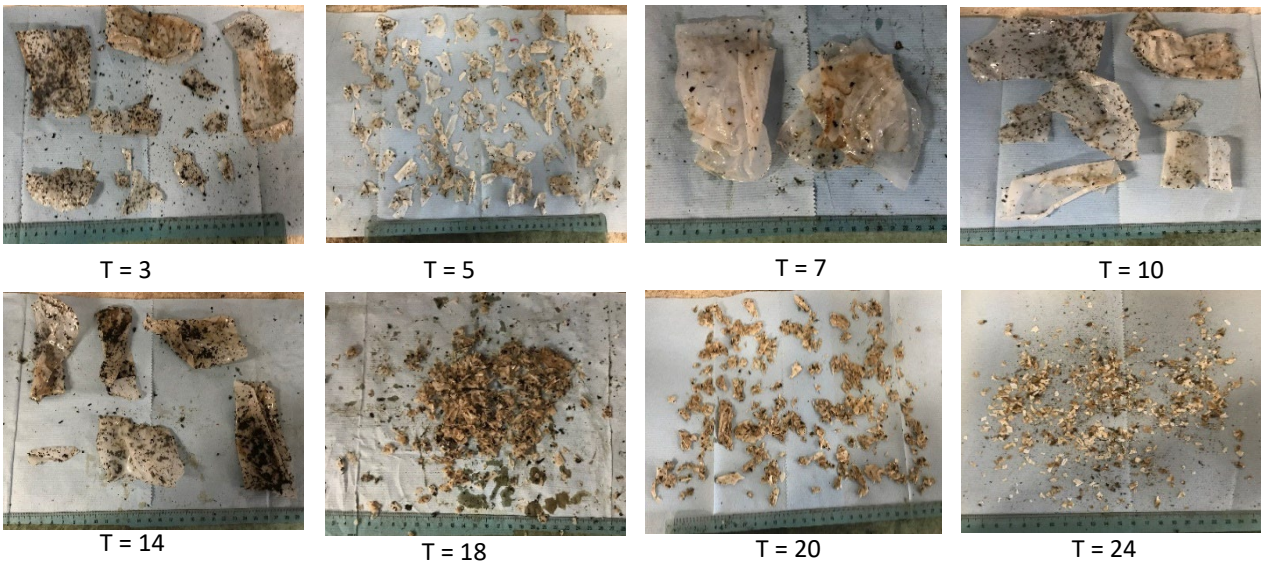

Figure 3.13: Changes in the PLA clamshell test samples placed in the commercial-scale food waste pile

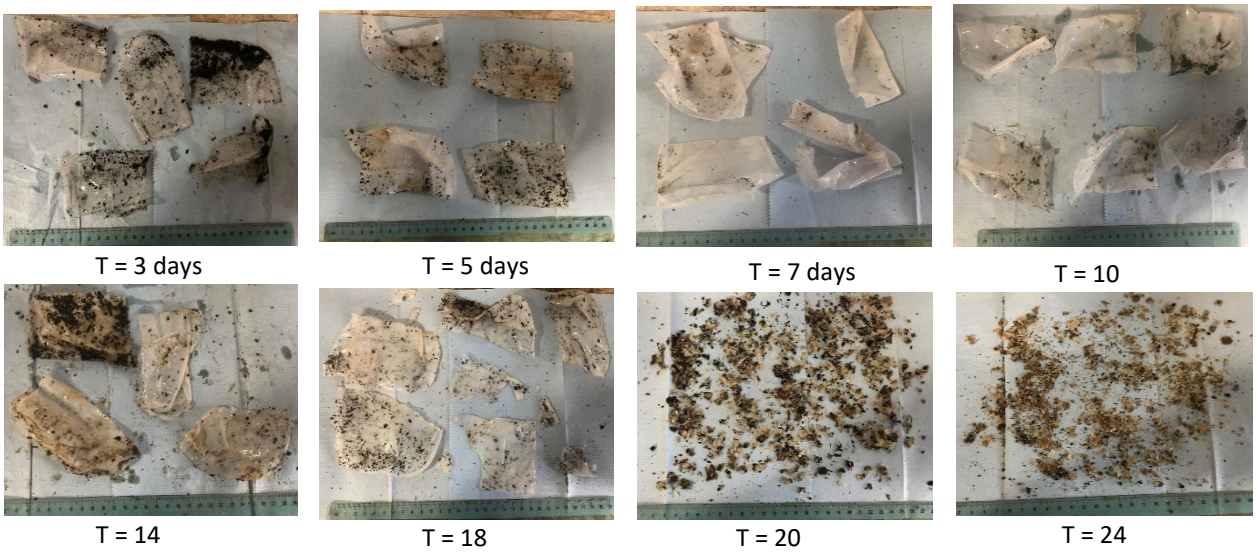

Figure 3.14: Changes in the PLA clamshell placed in the commercial-scale old compost pile

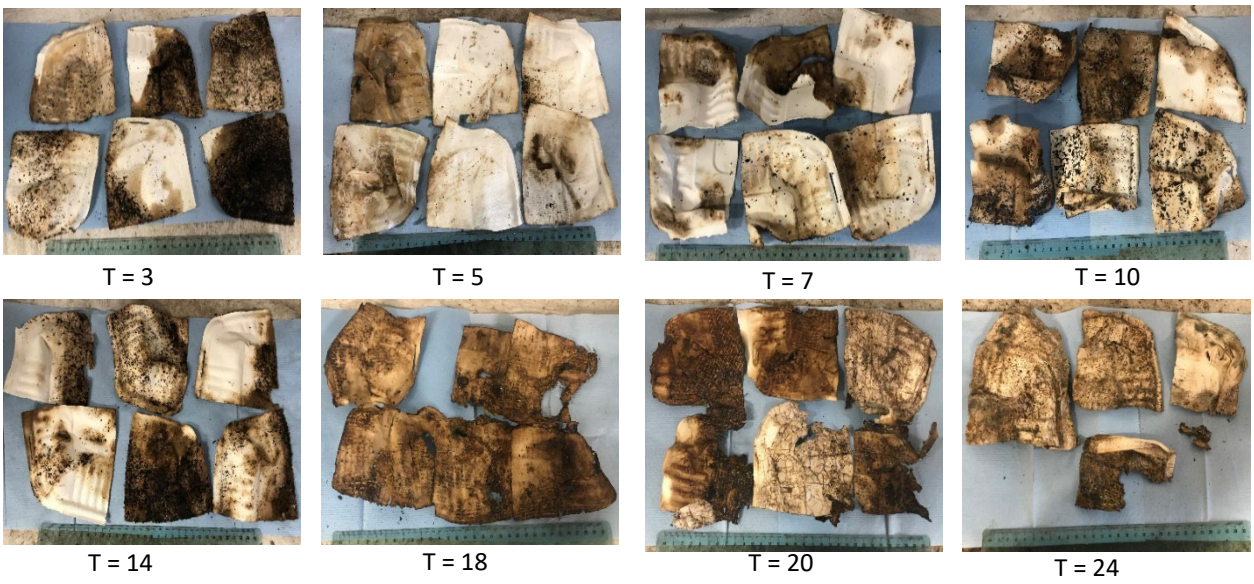

Figure 3.15: Changes in the PLA lined bagasse clamshell placed in the commercial-scale food waste pile

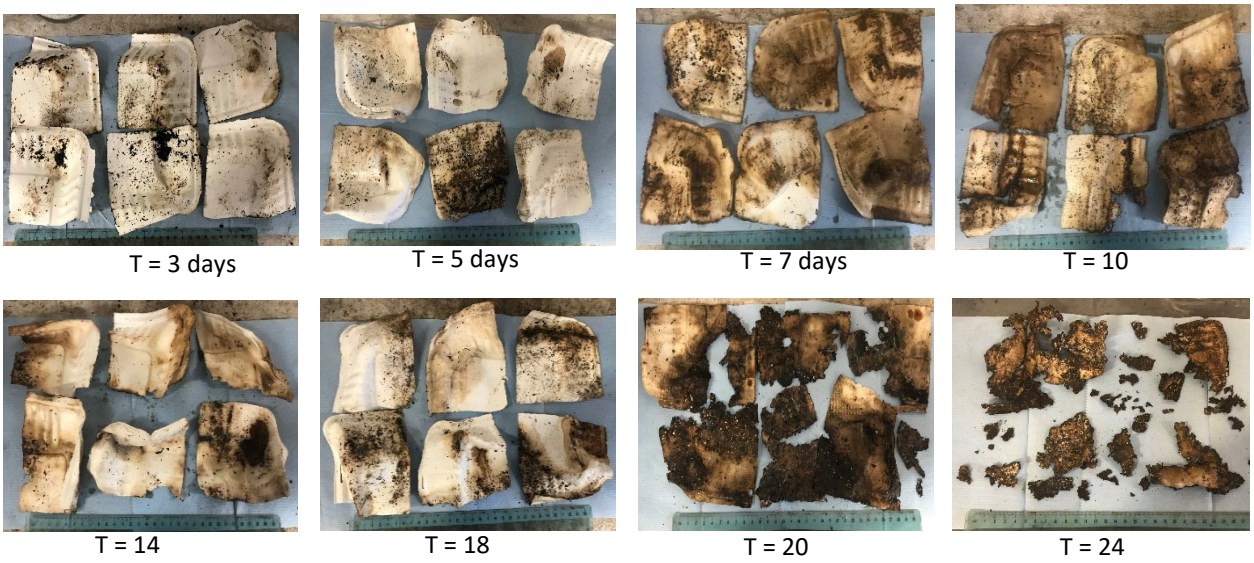

Figure 3.16: Changes in the PLA lined bagasse clamshell placed in the commercial-scale food waste pile

Table 3.7 shows the biodegradation of the FSP at t-3 and t-24 days. The synthetic/starch blended bag degraded at a higher rate than other FSP. The PLA clamshell disintegrated into smaller pieces however no biodegradation (weight loss) was observed. The biodegradation of the PLA lined bagasse clamshell did not follow a similar pattern as the other FSP sampled. These FSP pieces broke down into smaller fragments that were difficult to determine the weight loss. Instead, a sieving analysis was done by sieving the

PLA clamshell samples through 10mm, 4mm, 2mm, and 1mm sieves, and the weights of the FSP retained on each sieve size were noted. Figure 3.5 represents the weight of FSP retained in each of the sieves for both the inoculant conditions. The disintegration of the FSP placed in the inoculant began after 10 days. However, the breakdown of the FSP was much slower in the case of food waste inoculant compared to old compost. The breakdown of the FSP began around 14 days in both experimental piles. However, the size of the disintegrated particles was larger in the old compost pile than in food waste. The rise in the total retained weights of the samples from 10 days to 20 days was due to mixing of compost (fine soil particles) with the FSP which were difficult to separate.

Table 3.7: Rate of FSP Biodegradation and Specific Rate of Biodegradation for FSP during the Commercial-Scale Composting Experiment

FSP Type	FSP Content	Rate of FSP Biodegradation	Rate of FSP Biodegradation	Specific Rate of FSP Biodegradation	Specific Rate of FSP Biodegradation
		k; g FSP degraded	k; g FSP degraded	Q; g FSP degraded/g FSP added	Q; g FSP degraded/g FSP added
		Food Waste	Old Compost	Food Waste	Old Compost
Positive control	Chlorine Free Paper	0.190	0.201	0.026	0.028
Negative control	LDPE Film	-	-	-	-
Synthetic/Starch Blended Bag	Synthetic + Starch-Based Plastics	0.042	0.047	0.035	0.039
Fiber Plate	Bamboo + Unbleached Plant Fiber	0.062	0.055	0.006	0.005
PLA Lined Bagasse Clamshell	Sugar Cane Bagasse + PLA Lined	0.086	0.033	0.006	0.002

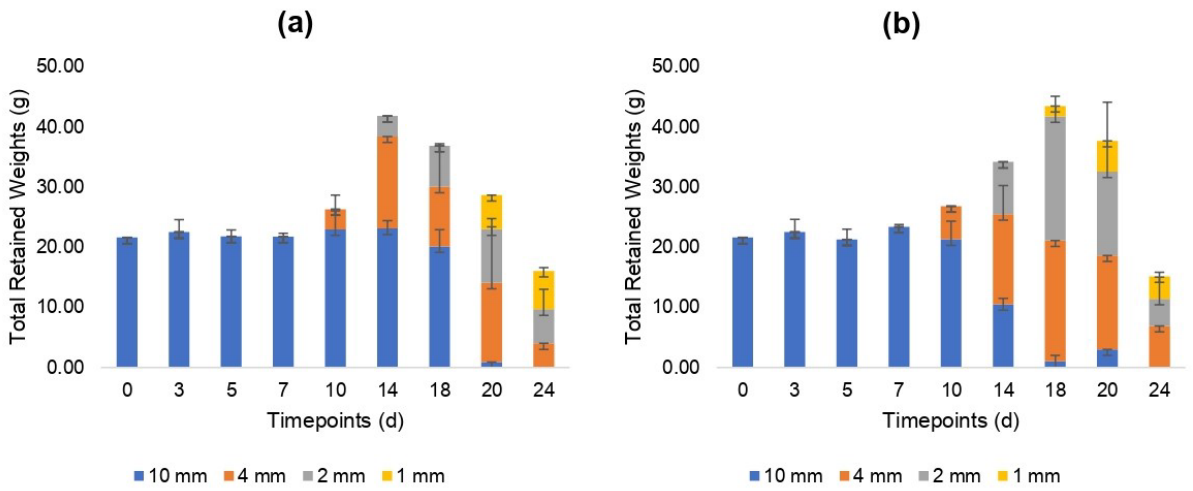

Figure 3.17 (a): Retained Weights of Clear PLA Clamshell for Pile containing Food Waste and (b) Retained Weights of Clear PLA Clamshell for Pile containing Old Compost

Conclusion

This research project investigated the impacts of moisture content and inoculant on the microbial community and FSP biodegradation at bench-scale, and the effect of differing feedstock on FSP biodegradation at commercial-scale. Cow manure was determined to have the highest oxygen uptake rate and therefore was determined to be the most biologically active inoculant. For this reason, cow manure was utilized for all subsequent bench-scale experiments. Bench-scale studies demonstrated that the overall degree of biodegradation was higher by 25 percent in reactors with 60 percent moisture content as compared to reactors with 45 percent moisture content. The rate of biodegradation in the tested products was highest in the synthetic/starch blended bag (57.4 ± 34.2 percent), followed by the fiber plate (39.5 ± 34.3 percent), and then by the positive control (62.3 ± 32.3 percent). The negative control showed no signs (0 percent) of biodegradation.

The commercial-scale experiments produced similar results. The negative control and the PLA lined bagasse clamshell that were tested showed no signs (0 percent) of biodegradation in both food waste and old compost containing piles. The rate of biodegradation was highest in the synthetic/starch blended bag (94 ± 5.17 percent), followed by the fiber plates (24 ± 7.4 percent), and then by the positive control (68 ± 20.5 percent). The PLA lined bagasse clamshell showed 12 ± 11.1 percent biodegradation. In general, the pile containing food waste had higher biodegradation rates when compared to pile with old compost containing pile. The study concluded that cow manure was the most microbially active out of the 4 tested inoculants, 60 percent moisture content has higher FSP biodegradation rates than 45 percent moisture content at bench-scale, microaerobic conditions favor increased rates of FSP biodegradation over anaerobic conditions, and food waste containing commercial-scale piles have higher rates of FSP biodegradation when compared to old compost containing piles.

Part IV. Evaluating Fate of PFAS During Bench-Scale and Commercial-Scale Experiments

4.1 Description of Method Development for Analysis

4.1.1 Approach

For the analysis of solid PFAS, Attenuated Total Reflectance Fourier Transform Infrared (FTIR) Spectroscopy was used to observe the characteristic bonds in the PFAS molecule (Figure 4.1). A 5-10 mg aliquot of sample was placed on the FTIR sample holder and scans were performed from 600-4000 wavenumbers (centimeter $^{-1}$). To detect PFAS in water, standards for each PFAS studied (C4-C14) were created by dissolving known standards in water at a concentration of 1000 parts per million (ppm) for analysis using ^{19}F Nuclear Magnetic Resonance (^{19}F NMR) spectroscopy. 200 µL of this solution matrix was placed in an NMR tube with 400 µL of D_2O (deuterated water) spiked with an internal standard of trifluoroacetic acid (TFA) for calibration. A 400 MHz NMR instrument was used for these measurements, and each sample was analyzed with 128 scans. Liquid samples were also analyzed using liquid chromatography coupled with mass spectrometry (LC-MS). The liquid samples were diluted in Acetonitrile with 0.1 percent formic acid in a 50:50 ratio.

Particle-induced gamma ray emission spectroscopy (PIGE) was used to determine presence of fluorine on FSP. The FSP samples were trimmed to fit in 1mm-by-1mm plastic bags; for samples where the FSP was broken into pieces, the bags were filled such that the thickness approximated that of the intact samples. Each bag was manually adhered with masking tape to separate stainless steel target frames with a hole of 1 cm in diameter. The portion of the sample exposed through the target's hole was irradiated with protons for 180 seconds. PIGE exploits the isotope-specific wavelengths of the electromagnetic radiation emitted in the nuclear reactions. Fluorine content is calculated by numerically integrating the 110 and 197 electronvolts (KeV) gamma-ray peaks; because fluorine is mono-isotopic, these signals are indicative of all elemental fluorine present in the samples. PIGE is a comparative measurement; levels of detected fluorine vary daily with the intensity, energy, and tune of the beam. Therefore, each set of samples is preceded with a set of standards treated with stock solutions of sodium fluorine in cellulose. The number of counts detected at these characteristic wavelengths is proportional to fluorine content on the sample's surface. A linear regression applied to the graph of standards' measured fluorine counts vs. known concentration in ppm was used to accurately convert measured fluorine counts to ppm fluorine content in the samples (Ritter et al., 2017). Because of its natural abundance in the atmosphere and lack of interference with fluorine peaks, argon was employed as a normalizing element (Wilkinson, McGuinness, & Peaslee, 2020).

4.1.2 Results and Discussion:

Figure 4.1 demonstrates the different bonds of perfluoro butanoic acid (PFBA) in the FTIR spectrum. The peaks in between 1000-1300 wavenumbers (centimeter^{-1}) correspond to the C-F bonds in PFBA. The peak at 1800 cm^{-1} corresponds to the C=O stretch in the carboxylate group. The broad peak at 3300 cm^{-1} corresponds to the OH stretch in the carboxylate group as seen in literature (Gao & Chorover, 2012). Figure 4.2 shows one example of a ^{19}F NMR spectrum of PFBA. The peak at -75 ppm is TFA, the internal standard. The area of the TFA peak is normalized to 1 and is compared to the area of peak 1 corresponding to CF_3 at -81 ppm and is used to determine the concentration of PFAS in the sample. Figure 4.3 shows the PIGE analysis of each of the six FSP items used in the commercial-scale and bench-scale experiments. The fiber plate and PLA lined bagasse clamshell were the two FSP items that showed high PFAS concentration at 883 $\pm$ 52 ppm and 854 $\pm$ 50 ppm, respectively.

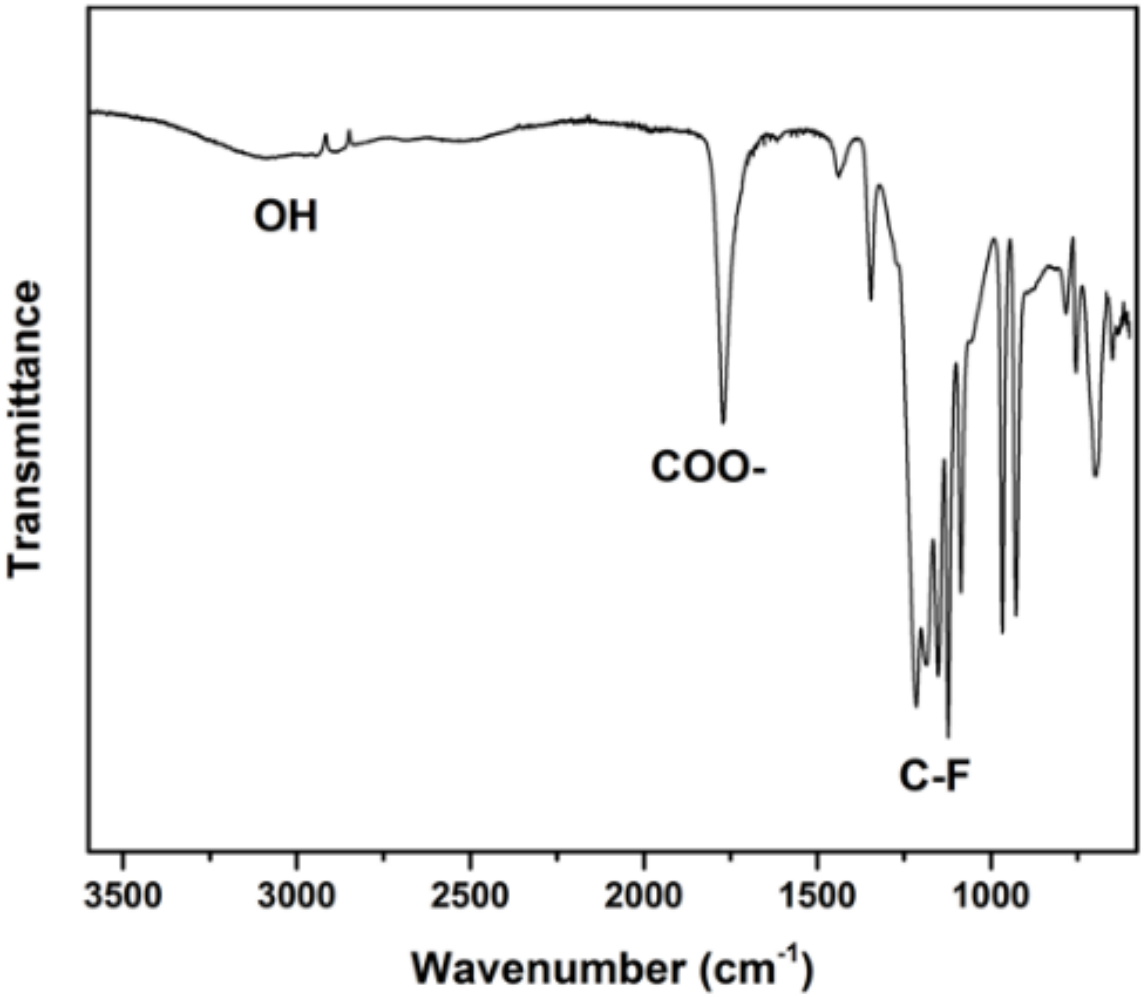

Figure 4.1: Sample FTIR Spectrum of Perfluorobutanoic acid (PFBA)

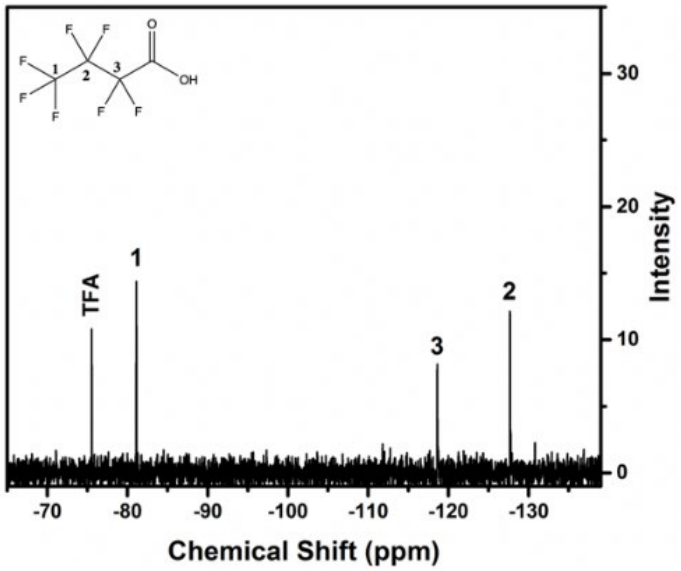

Figure 4.2: Sample ^{19}F NMR Spectrum of Perfluorobutanoic acid (PFBA)

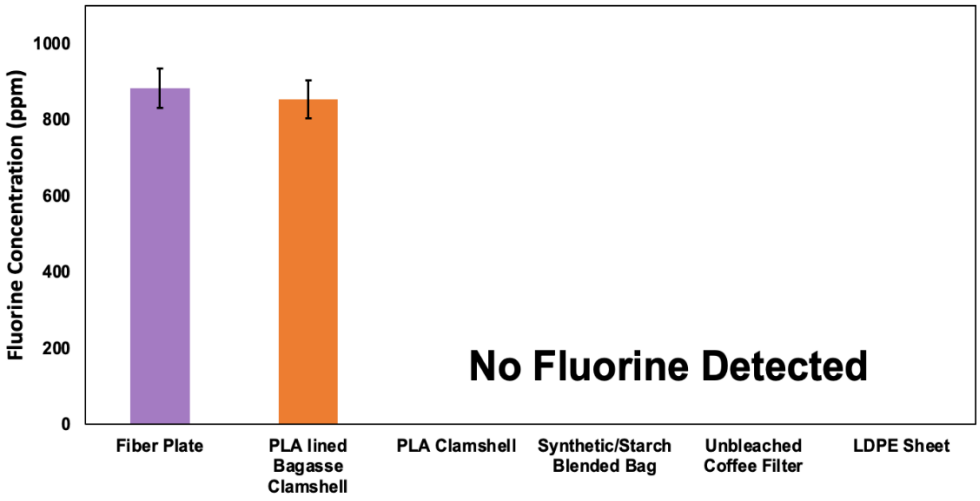

Figure 4.3: Results of PIGE Analysis on all Six FSP Used in the Commercial and Bench-Scale Composting Experiments

4.2 A Database of Possible PFAS in the Leachate Produced During Composting

4.2.1 Approach:

A database of PFAS that can be detected using FTIR, LC-MS, and ^{19}F NMR was created based on the methods described in section 4.1.1 The summary is shown in Table 4.1 below.

4.2.2 Results and Discussion:

All specifically measured PFAS chemicals were detectable by FTIR; however, since the ^{19}F NMR required liquid samples for detection, Perfluoro tridecanoic acid (C13) and Perfluorotetradecanoic acid (C14) could not be detected in water. This is due to the fact that the molecule becomes more hydrophobic as its chain length increases therefore the solubility in water decreases. (Zhao et al., 2016) Since LC-MS has a lower detection limit, it could detect all 10 PFAS in the liquid state. If samples are not soluble in water, they can be dissolved in other solvents, but this study was concerned with detecting PFAS in leachate, which is mostly water.

Table 4.1: Database of PFAS Detected Through FTIR, LC-MS, and ^{19}F NMR

PFAS Name	Molecular Weight (g/mol)	Solubility in Water (g/L)	Detected in FTIR? (Y/N)	Detected in ^{19}F NMR? (Y/N)	Detected in LC-MS? (Y/N)
Perfluorobutanoic acid (C4)	214.04	214	Y	Y	Y
Perfluoropentanoic acid (C5)	254.05	112.6	Y	Y	Y
Perfluorohexanoic acid (C6)	314.05	21.7	Y	Y	Y
Perfluoroheptanoic acid (C7)	364.06	4.2	Y	Y	Y
Perfluorooctanoic acid (C8)	414.07	3.4-9.5	Y	Y	Y
Perfluorononanoic acid (C9)	464.08	9.5	Y	Y	Y
Perfluoroundecanoic acid (C11)	564.09	0.004	Y	Y	Y
Perfluorododecanoic acid (C12)	614.1	0.0007	Y	Y	Y
Perfluorotridecanoic acid (C13)	664.1	0.0002	Y	N	Y
Perfluorotetradecanoic acid (C14)	714.1	0.00003	Y	N	Y

4.3: Evaluation of PFAS During Bench-Scale Composting

4.3.1 Approach:

PFAS were extracted from the solid contained in bench-scale reactors at day 0,3,5,7,10,14,18,20, and 24. Two extractions were done on each sample of the reactor solids in a 50 mL centrifuge tube to ensure efficiency. In the first extraction, 13 mL of acidified methanol was added to 5 grams of the reactor solids and vortexed for 30 seconds and sonicated for one hour in warm water. Then the tube was placed in a shaker for 30 minutes, followed by five minutes in a centrifuge at 6000 rpm. The supernatant liquid was extracted and placed in a separate clean tube. The second extraction was done with 10 mL of acidified methanol and the rest of the steps were repeated the same as detailed above. Both supernatants were combined and dried in a rotary evaporator and reconstituted with 2 mL of methanol before analysis in ^{19}F NMR. The solid samples of the fiber plate were sent for PIGE analysis as previously described.

4.3.2 Results and Discussion:

There were no PFAS detected in any of the compost extracts from reactors R_{45} and R_{60} from the bench-scale experiments I and II. Figure 4.4 illustrates that the fluorine content on the fiber plate increased during the 24-day composting period. It is important to note that these experiments were performed using only cow manure as the inoculant and only evaluated the fiber plate (containing no plastic). The change in mass observed in the FSP could indicate that the microbial communities present in cow manure degraded other components of the FSP such as the bamboo and unbleached plant fiber in the fiber plate. Further microbial community data analysis will allow us to better understand the biological systems that are associated with the FSP biodegradation during bench-scale composting. Microbial community testing will reveal fractions of specific bacteria and fungi present in cow manure that can be correlated with the degree of composting. Bench-scale composting experiments with another inoculant such as old compost for example could provide results that would allow us to correlate microbial community with PFAS and FSP biodegradation.

Table 4.2: Summary of PFAS from Bench-Scale Composting

Reactor Name	Moisture Content (%)	PFAS in Compost (Y/N)	PFAS in FSP (Y/N)
R_{45} (triplicates)	53.4 ± 11.8	N	Y
R_{60} (triplicates)	60.3 ± 9.04	N	Y

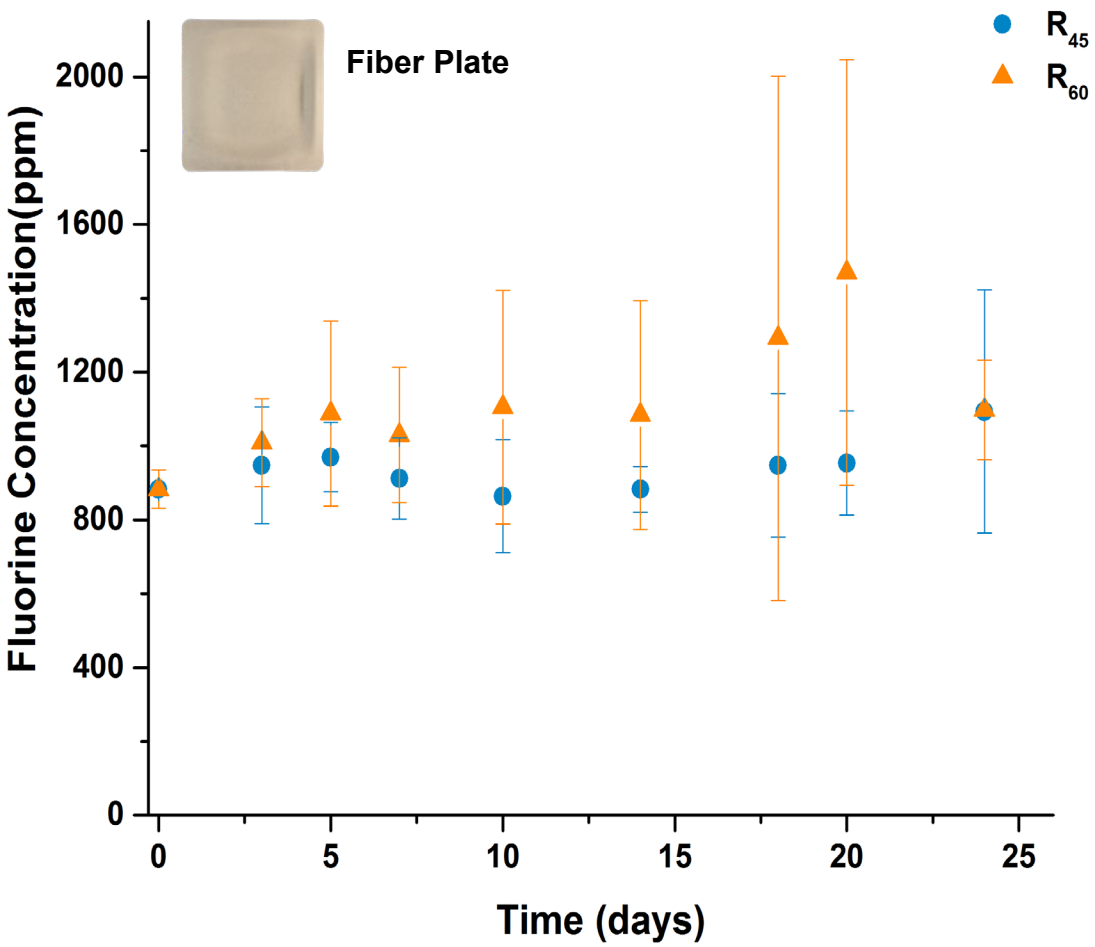

Figure 4.4: Fluorine Concentration in ppm on Fiber Plate During Bench-Scale Composting

4.4: Evaluate the Fate of PFAS During Commercial-Scale Composting

4.4.1 Approach:

PFAS were extracted from the solid compost obtained from the Commercial-scale experiments for T=0 to T=24 days in the following way. Two extractions were done on five grams of solid compost in a 50 mL centrifuge tube to ensure efficiency. In the first extraction, 13 mL of acidified methanol was added to the solid waste and vortexed for 30 seconds and sonicated for one hour in warm water. Then the tube was placed in a shaker for 30 minutes followed by five minutes in a centrifuge at 6000 rpm. The supernatant liquid was extracted and placed in a separate clean tube. The second extraction was done with 10 mL of acidified methanol and the rest of the steps are repeated the same as detailed above. Both supernatants are combined and dried in a rotary evaporator and reconstituted with 2 mL of methanol before analysis.

To detect the presence of PFAS on the solid FSP, the samples were sent for PIGE analysis. A 1x1 inch piece of each FSP, from the experiments detailed earlier in this report, were placed under gamma rays to detect fluorine and its concentration in parts per million. This procedure is identical to the procedure mentioned in Section 4.1.1.

4.4.2 Results and Discussion:

No PFAS were detected in any of the compost extracts from commercial-scale experiments. The PIGE data suggest that the PFAS remained on the fiber plate and PLA lined bagasse clamshell throughout the composting experiment as seen in Figure 4.5. The change in fluorine concentration on the fiber plate is slightly higher in food waste containing piles. For PLA lined bagasse clamshell, it appears that both piles affect the fluorine concentration similarly. The large error bars associated with food waste piles in the PIGE data are due to the increased thickness of the plastic product tested from those piles. The food waste stuck to the FSP obstructs the rays from the PIGE instrument, resulting in decreased fluorine detection accuracy. This is more visible after day 18 in the pile.

Compost piles are complex mixtures that can create challenges for accurate concentration measurements. To mitigate inaccurate measurements, the compost from each pile was also analyzed for PFAS concentration, but no PFAS were detected. The change in mass observed in the FSP could mean that the microbial communities in food waste and old compost degraded other components of the FSP, such as the bamboo and unbleached plant fiber in the fiber plate, and sugar cane bagasse and PLA in the PLA lined bagasse clamshell. Since the carbon-fluorine bonds in PFAS are strong and difficult to breakdown, it is possible that the head groups consisting of carbon-oxygen bonds are being transformed to other groups. Therefore, PFAS are being converted from one group to another rather than degraded. Further microbial community data analysis will provide a better understanding of the biological systems that are allowing the components of FSP to degrade but not the PFAS. It is also important to note that the commercial-scale experiments were performed without inoculants whereas the bench-scale composting experiments were done using cow manure as the inoculant. Thus, PIGE data and microbial community information from bench-scale composting will further expand knowledge on the relationship between inoculant and PFAS degradation on FSP. Details on specific populations of bacteria and fungi in the microbial community can be correlated with biodegradation of PFAS and FSP. Analysis of microbial community from the FSP could be correlated with microbial community in the compost to see which communities bind to FSP with PFAS and which bind to FSP without PFAS.

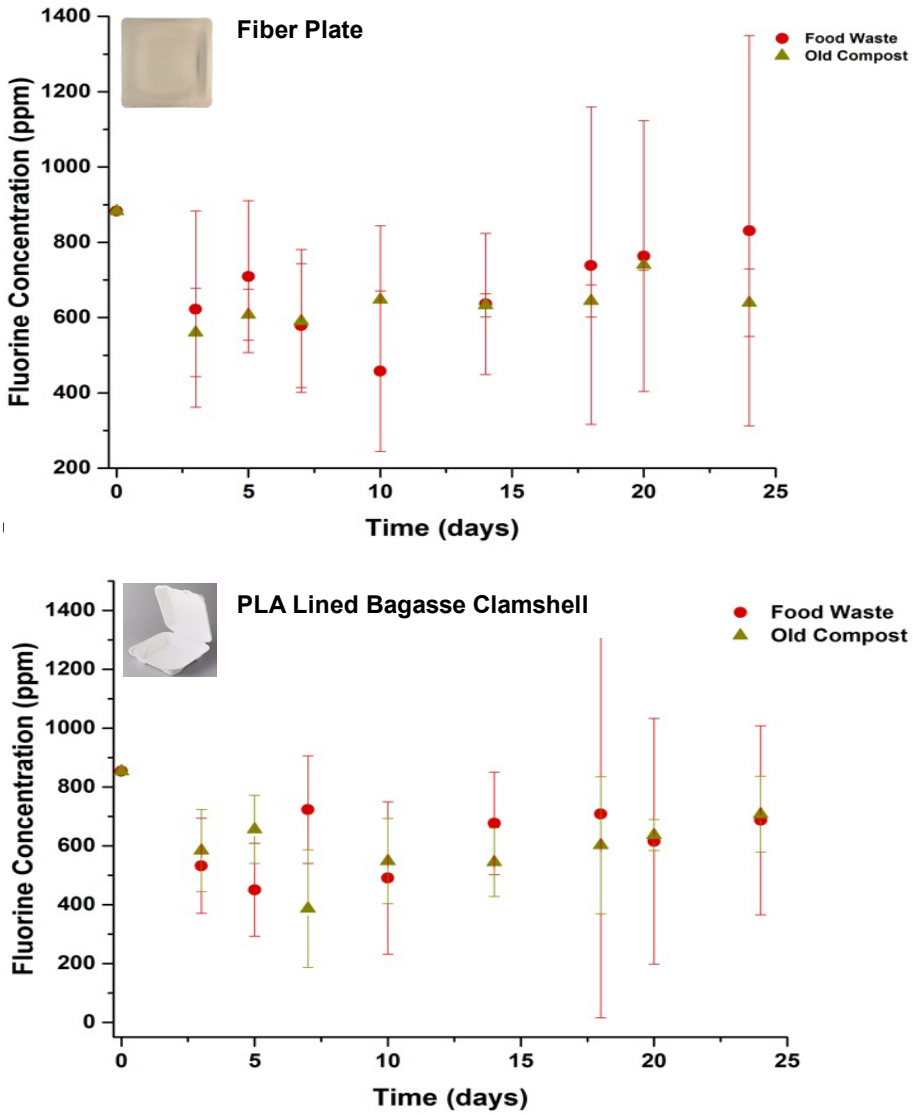

Figure 4.5: Fluorine Concentration in ppm During Commerical-Scale for Fiber Plate (top), and PLA Lined Bagasse Clamshell (bottom)

Table 4.3: Summary of PFAS Present in FSP During Commercial-Scale Experiments

Moisture Content (%)	Pile Feedstock	PFAS in Leachate (Y/N)	PFAS in FSP (Y/N)
60.9 ± 6.82	Food Waste	N	Y
58.4 ± 5.16	Old Compost	N	Y

Part V. Synthesis of Mesoporous Hafnium Oxide for PFAS Adsorption

5.1: Synthesis of Mesoporous Hafnium Oxide

5.1.1 Approach:

These experiments were performed in the lab of Dr. Jesús M. Velázquez in the Department of chemistry at UC Davis. Fatima Hussain performed these experiments as part of her Ph.D. dissertation research. Mesoporous hafnium oxide (MHO) ceramic monoliths were synthesized using the sol–gel method (Ferrer-Lassala, 2013). Glass vials were treated with 0.1 M sodium hydroxide for one hour, 0.1 M hydrochloric acid for one hour, and Rain-x overnight. After removing the Rain-x, vials were rinsed with methanol and dried in an oven. Hafnium (IV) chloride was dissolved in ultrapure water (resistivity >18.2 MΩ). Then, *N*-Methylformamide (NMF) was added to increase the pH of the solution and induce phase separation. Polyethylene oxide was added to strengthen the pore network. In addition, propylene oxide was added to induce polymerization, turning the clear liquid to a white gel. The gel was then aged at 50°C for three days. The monolith was washed with ultrapure water, methanol, acetone, hexanes, and pentane to remove any excess reagents, and to prevent cracks during heating. Finally, the sample underwent heat treatment in a furnace in air to 700°C, which yields a crystalline white monolithic ceramic (Hussain, Zamora, Ferrer, Kinyua, & Velázquez, 2020).

After the synthesis, the crystalline structure of the material was determined by powder X-ray diffraction (XRD) using an X-ray diffractometer. Experimentally obtained diffraction patterns were then compared to patterns from the Inorganic Crystal Structure Database to confirm the structure. The pore structure and network of the material was determined by a Thermofisher Quattro Environmental scanning electron microscope. The sample was placed on double sided copper tape and operated at an accelerating voltage of 10 keV under low vacuum. The surface of the MHO ceramic was analyzed using Fourier transform infrared (FTIR) spectroscopy. The FTIR was equipped with an attenuated total reflectance (ATR) pike accessory. The experiment was performed using 32 scans, a resolution of two cm^{-1}, and a spectral range of 400–4000 cm^{-1}. The surface area was measured by Brunauer-Emmet-Teller (BET) method with nitrogen adsorption using a surface area analyzer. The pH_{PZC} (point of zero charge) is the pH when the charge on the surface of the adsorbent is neutral. The pH_{PZC} of MHO was analyzed using the pH drift method (Xie et al., 2016).

5.1.2 Results and Discussion:

The MHO ceramic monolith obtained after synthesis has a diameter of 0.8 cm as shown in Figure 5.1a. The size and shape depend on the gelation vessel, which in this case was a 10 mL scintillation glass vial. Figure 5.1b depicts the MHO ceramic bimodal distribution comprised of a network of macropores and mesopores. The macropores are interconnected and appear to be approximately one μm in diameter based on the SEM. The three tunable sites on the surface of MHO are shown in Figure 5.2; Lewis acid sites

originating from unoccupied hafnium d orbitals, Brönsted acid sites which donate a proton in basic media, and Brönsted base sites which accept a proton in acidic media (Nawrocki, Rigney, McCormick, & Carr, 1993). These sites are activated at a specific pH to create a favorable interaction between the PFAS and the MHO. The monoclinic crystalline structure was confirmed by XRD and compared to literature values as shown in Figure 5.3. The BET surface area of MHO was calculated to be 10.5 ± 0.60 m^2/g. The FTIR illustrating the various functional groups on the surface of MHO is shown in Figure 5.4. The peaks present between 400–800 cm^{-1} represent the monoclinic hafnium oxide stretches of Hf–O and Hf–O_2. Peaks in the range of 1200–1600 cm^{-1} correspond to symmetric and antisymmetric formato (COO^-) ligand vibrations originating from the hydrolysis of N-methyl formamide during the sol-gel synthesis. The peak at 2390 cm^{-1} is identified as CO_2 that is alpha-coordinated to the Lewis acid sites on the surface. The peak at 3400 cm^{-1} corresponds to OH due to the moisture on the surface, since MHO is hydrophilic. The pH at which the surface of MHO is neutral (pH_{PZC}) was determined to be 4.7.

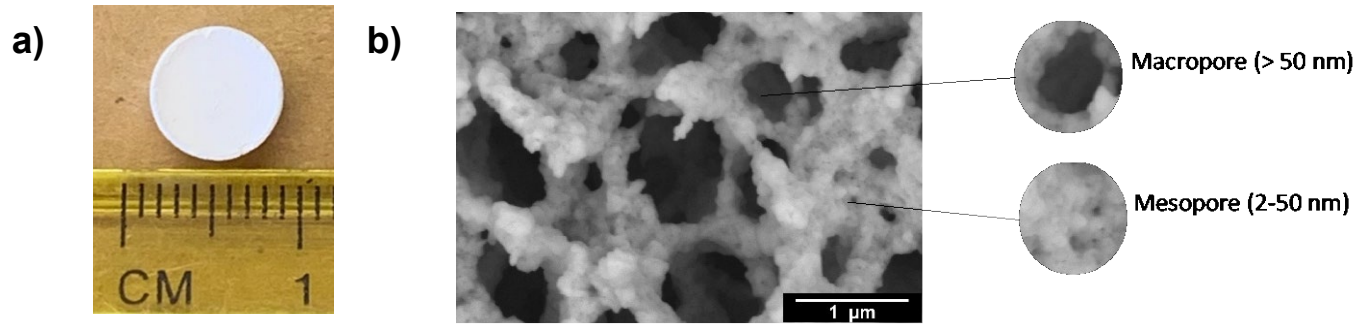

Figure 5.1: a) Free Standing MHO Ceramic with a Diameter of 0.8 cm, b) SEM Image of MHO Ceramic Illustrating Network of Macropores and Mesopores

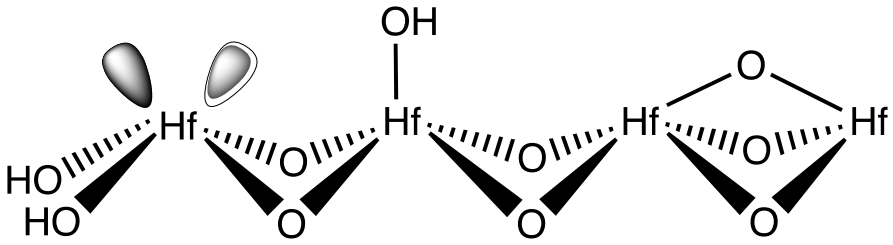

Figure 5.2: Active Sites on the Surface of Mesoporous Hafnium Oxide: Lewis Acid Site (left), Brönsted Acid Site (middle), and Brönsted Base Site (right)

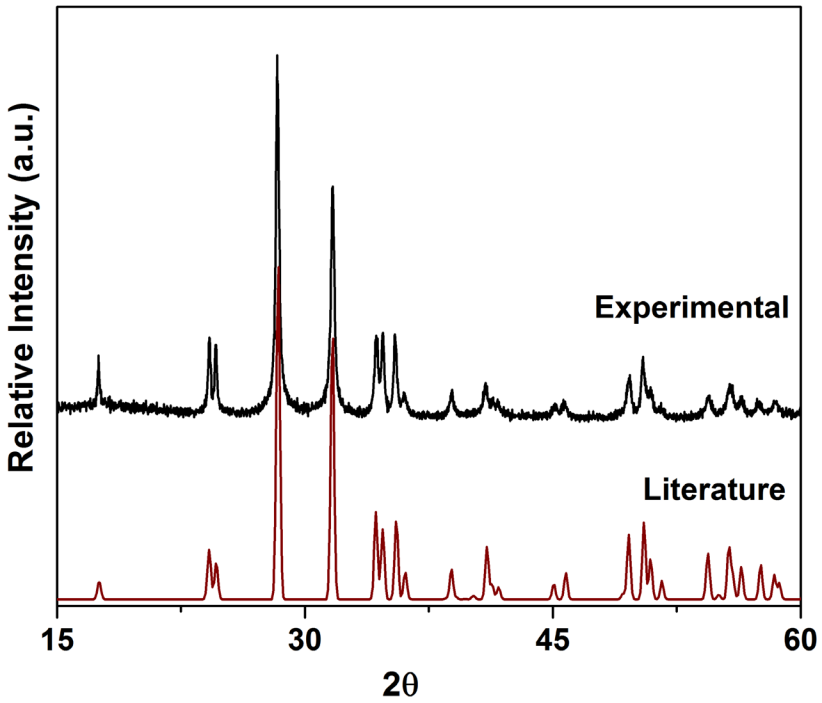

Figure 5.3: XRD Patter of Monoclinic MHO Ceramic (top) Overlaid with the Published Spectrum for Monoclinic MHO with Heat Treatment at 700℃ (bottom, ICSD 57385)

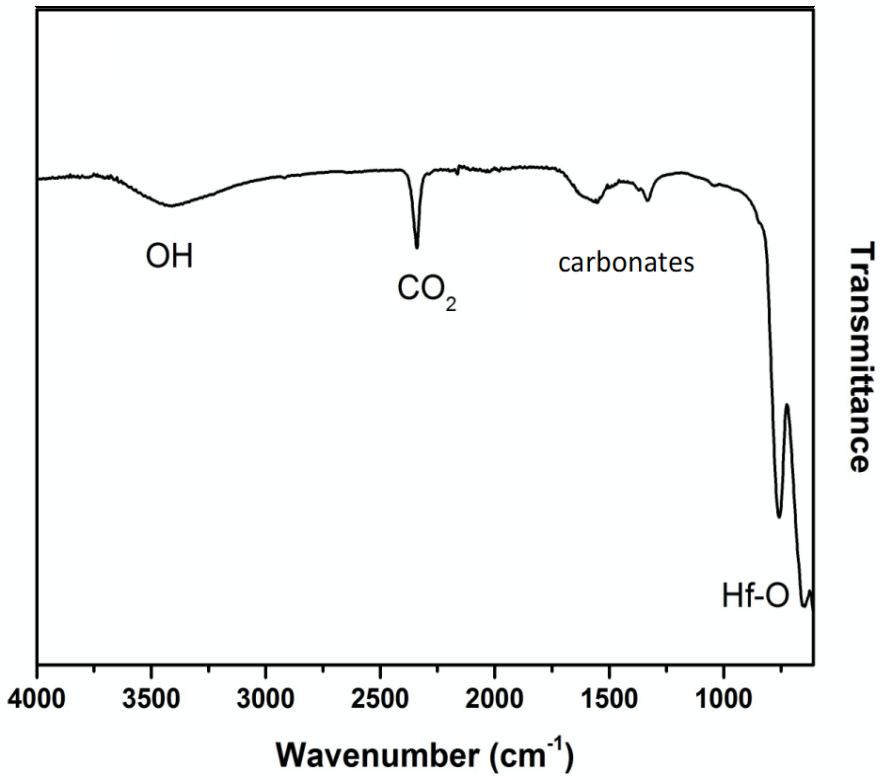

Figure 5.4: FTIR Spectrum of MHO Ceramic After Synthesis at 700℃

5.2: Filtration Experiments Results Using Mesoporous Hafnium Oxide

5.2.1 Approach:

A vacuum filtration experiment was set up as shown in Figure 5.5b below. For each filtration a monolith of mesoporous hafnium oxide (MHO) of 0.2 grams was attached to the stem of the funnel using a halogen free shrinking tube (Figure 5.5a). The PFAS that were used were perfluorobutanoic acid (PFBA), perfluorohexanoic acid (PFHxA), and perfluorooctanoic acid (PFOA). The PFAS concentration in the liquid before and after filtration was quantitatively determined using ^{19}F NMR spectroscopy.

The percentage of PFAS adsorbed after filtration is calculated using equation (4):

Equation (4):

$$\%\ \text{PFAS Adsorbed} = \frac{(C_0 - C)}{C_0} \times 100\%$$

Where C_0 is the initial concentration of PFAS in ppm before filtration, and C is the concentration of PFAS after filtration in ppm.

PFOA adsorption experiments were performed using a Benchmark tabletop shaker. The white MHO was crushed and sieved to be 0.6 mm to 2 mm in size. Each 50 mL Falcon tube contained 1.25 g of MHO, 50 mL of 1000 ppm PFOA. The concentration of PFOA used in the experiments was higher than the concentrations found typically in wastewater streams for ease of sample handling and analysis. The pH was adjusted for some experiments using 0.1M sodium hydroxide and 0.1M sulfuric acid. The tubes were shaken for twelve hours, and a one mL aliquot of liquid was extracted every two hours for analysis. The quantity of PFAS adsorbed at each time interval during adsorption and after filtration is calculated using equation (5):

Equation (5):

$$q_t = \frac{(C_0 - C_t) \times V}{m}$$

Where q_t is the quantity of PFOA adsorbed in mg per gram of MHO, C_0 is the initial concentration of PFOA in ppm, C_t is the concentration of PFOA at a time t, V is the total volume of solution used in the experiment in mL, and m is mass of the MHO adsorbent in grams.

All experiments were performed in triplicates and the error bars have been included in the figures to report one standard deviation. The PFAS concentration in the liquid aliquots was determined using ^{19}F NMR spectroscopy on a Bruker 400 MHz spectrometer. 200 µL of liquid sample is added to 400 µL of deuterium oxide spiked with Trifluoroacetic acid in a Wilmad NMR tube. The solids are analyzed using ATR-FTIR spectroscopy as described earlier.

5.2.2 Results and Discussion:

Results from Table 5.1 show that as the chain length increases from four carbons to eight carbons, the percent removal of PFAS increases as there is an increased number of fluorinated substituents to bind to the surface of MHO. This phenomenon has been reported previously in literature by Vu, 2020. The quantity of PFAS adsorbed per mass of MHO (qt) was calculated after each filtration as shown in Table 5.2. The higher concentration showed higher qt values as expected. The qt was higher for longer chain PFAS as compared to shorter chain PFAS. These results suggest that the more common longer chain PFAS can be removed from water at a higher efficiency than the shorter chain PFAS using MHO synthesized in the lab. This means that higher mass of MHO would be needed to remove the shorter chain PFAS molecules.

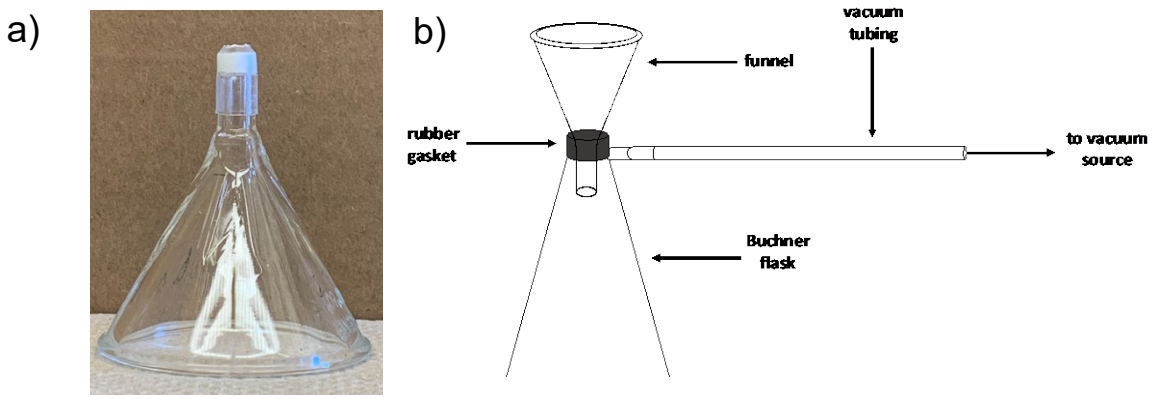

Figure 5.5: a) Funnel with MHO Ceramic Attached Using Shrinking Tube, b) Vacuum Filtration Setup for PFAS Removal

Table 5.1: Percent of PFAS Adsorbed by MHO

Initial Concentration (ppm)	% of PFBA Adsorbed (C4)	% of PFHxA Adsorbed (C6)	% of PFOA Adsorbed (C8)
2000	2.16 ± 0.3	30 ± 6	48.7 ± 10
100	31.1 ± 7	45.6 ± 12	50.2 ± 10
25	39.9 ± 3	35 ± 4	46.6 ± 11

Table 5.2: Quantity of PFAS Adsorbed per Mass of MHO

Initial Concentration (ppm)	mg of PFBA (C4) adsorbed/g of MHO	mg of PFHxA (C6) adsorbed/g of MHO	mg of PFOA (C8) adsorbed/g of MHO
2000	1.08 ± 0.2	14.9 ± 3	24.3 ± 5
100	0.78 ± 0.2	1.14 ± 0.3	1.31 ± 0.8
25	0.20 ± 0.2	0.22 ± 0.03	0.29 ± 0.07

5.2.2.1 Effect of pH on Adsorption of PFOA by MHO

pH is an important factor in adsorption processes due to the reactivity of H+ and OH- ions in solution (Wang & Shih, 2011). The adsorption of PFOA on MHO was evaluated at three different pH values: pH 2.3, pH 4.3, and pH 6.3. Figure 5.6 shows that at pH 2.3 the adsorption capacity of PFOA on MHO was the highest at 20.9 ± 0.4 mg/g. However, as the pH increased, the adsorption capacity decreased to 13.0 ± 0.3 mg/g and 9.12 ± 0.5 mg/g at pH 4.3 and pH 6.3, respectively. This is due to a change in pH affects the surface charge of MHO and the charge of the PFOA molecule. The pKa of PFOA is reported to be in the range of 0.5-3.8 (Burns, Ellis, Li, McMurdo, & Webster, 2008) and the PZC of MHO was measured to be 4.7. At pH 2.3 the surface of the MHO is positively charged because the pH<PZC. The PFOA is in equilibrium with the negatively charged PFOA anion since the pH is almost the same value as the to pKa. This leads to electrostatic attraction between the positively charged surface of MHO and the negatively charged PFOA anion. There will also be some interaction between the hydrophobic tail of the PFOA molecule and the hydrophilic surface of MHO. As the pH of the solution increases the surface of MHO becomes more negative and the amount of PFOA anion in solution also increases. This leads to increased electrostatic repulsion between the PFOA anion and MHO, and decreased electrostatic attraction, therefore decreasing PFOA adsorption.

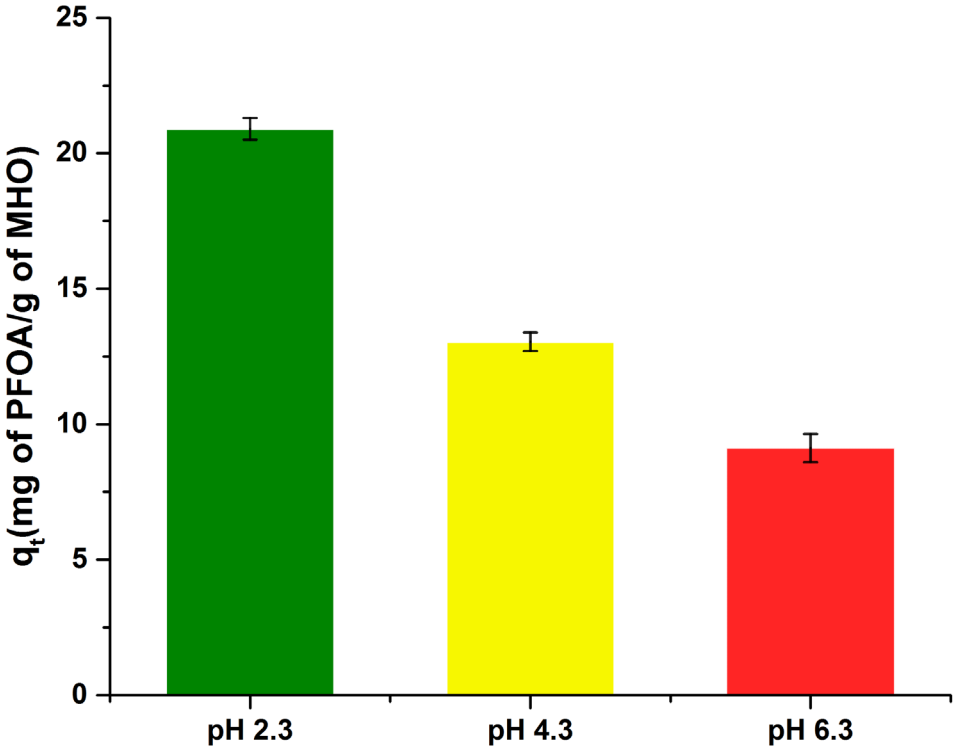

Figure 5.6: Rate of PFOA Adsorption on MHO at pH 2.3, 4.3, and 6.3 using 1.25 g of MHO and 50 mL of 1000 ppm of PFOA

5.2.2.2 Comparing MHO with Other PFOA Adsorbents

The rate of adsorption of PFOA on MHO was compared to other porous materials used for PFOA adsorption and summarized in Table 5.3. PFOA adsorption on MHO is rapid in comparison to GAC (Yao, Volchek, Brown, Robinson, & Obal, 2014), which required 24 hours to reach equilibrium, and had an adsorption capacity of 22.7 mg/g. Commercially available multi-walled carbon nanotubes had a shorter equilibrium time (4 hours), however, the adsorption capacity was also significantly lower at 12.4 mg/g (Yao et al., 2014). MHO was also compared to another metal oxide, silica, which had an equilibrium time of 14 hours and adsorption capacity of 21.2 mg/g (Stebel et al., 2019). Despite MHO having a significantly lower BET surface area as compared to the adsorbents, the adsorption capacity of PFOA is still comparable. That is due to the fact that mesoporous particles have larger external surface area and therefore more functional groups are available for PFOA adsorption (Kuvayskaya, Lotsi, Mohseni, & Vasiliev, 2020).

Table 5.3: Comparison of This Work on PFOA Adsorption by MHO with Other Mesoporous Adsorbents

Material	BET Surface Area (m^2/g)	qt (mg of PFOA/g of adsorbent)	Equilibrium Time (Hours)	Reference
Granular activated carbon	1100	22.7	24	Yao et al
Silica	650	21.2	14	Stebel et al
Multi-walled carbon nanotube	350	12.4	4	Yao et al
Mesoporous hafnium oxide	10.5 ± 0.60	20.9 ± 0.40	10	This Work

5.2.2.3 Analysis of Solid MHO Powders After PFOA Adsorption

In Figures 5.7a-c the pink line at the top corresponds to the spectrum of MHO before filtration. It has all the peaks the MHO is expected to have such as the monoclinic hafnium oxide peaks between 400-800 cm^{-1}, the formato ligand binding on the hafnium shown by the peaks between 1200-1600 cm^{-1}, and the carbon dioxide and water peaks at 2390 cm^{-1} and 2900 cm^{-1} repectively. The blue line in Figure 5.7a corresponds to PFBA the shortest PFAS tested with only four carbons in the chain. It has peaks between 1000-1450 cm^{-1}, which correspond to the symmetric and asymmetric stretching of CF_2 and CF_3 stretching modes. The peak at 1750 cm^{-1} corresponds to the carboxylate group present in all the PFAS that were used in these filtration experiments (Gao & Chorover, 2012). Similar peaks were observed in Figure 5.7b and 5.7c corresponding to PFHxA and PFOA,

respectively. The black lines in Figure 5.7a and Figure 5.7b show the spectrum of MHO after filtration with PFBA and PFHxA, respectively. Both of these spectra show peaks between 1000-1450 cm^{-1}, which correspond to the symmetric and asymmetric stretching of CF_2 and CF_3 stretching modes, and the peak at 1750 cm^{-1} corresponds to the carboxylate group. This confirms PFAS removal from water and onto the MHO surface. The black line in Figure 5.7c corresponds to MHO after filtration with PFOA. The peak at 1750 cm^{-1}, which corresponds to the carboxylate group is more intense than the PFAS corresponding to symmetric and asymmetric stretching of CF_2 and CF_3 modes. This leads us to believe that the driving force for adsorption of PFOA on MHO is dominated by the electrostatic interaction between the negative carboxylate group of PFOA in solution and the positive surface groups on MHO.

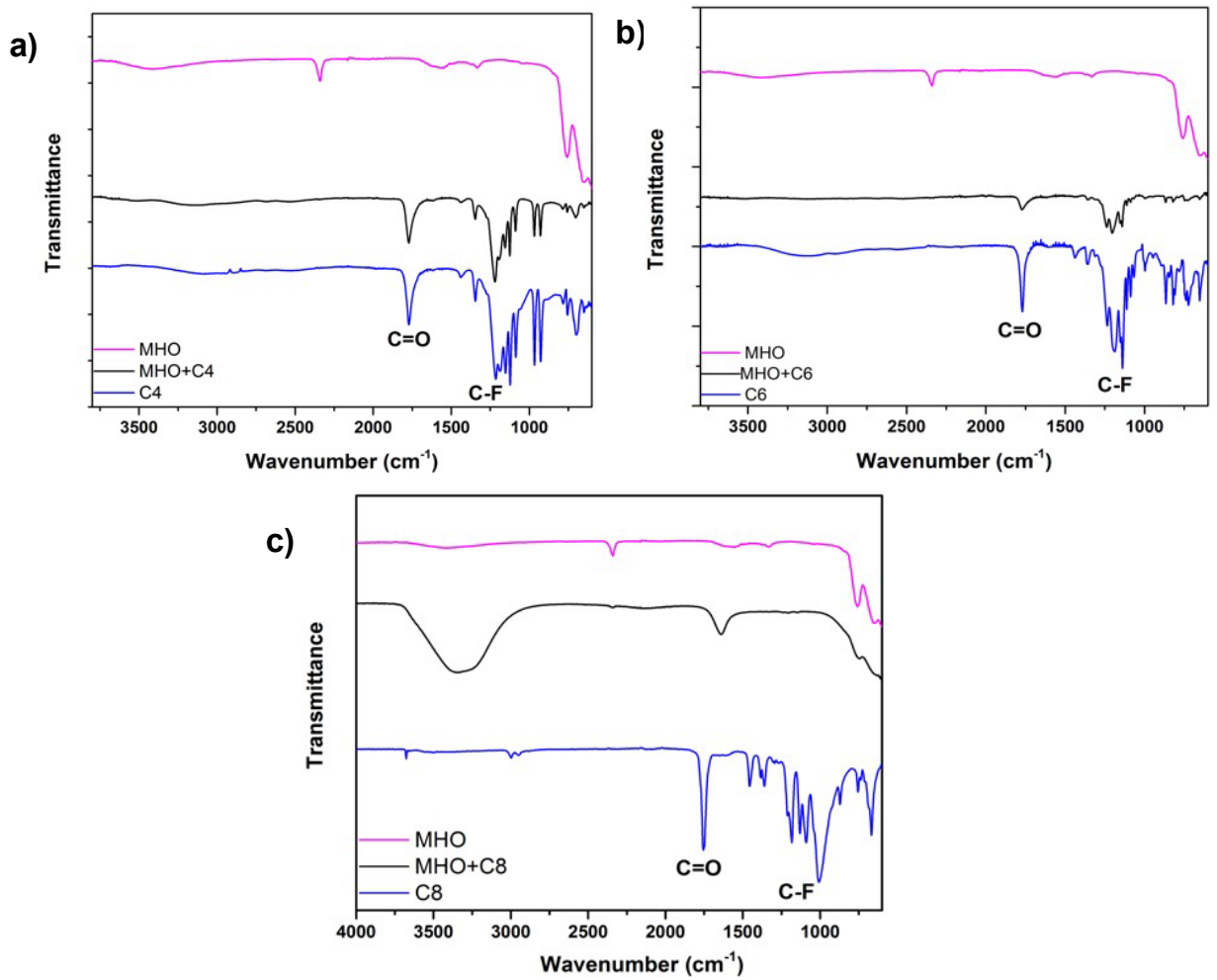

Figure 5.7: FTIR Spectra of MHO Before Filtration (in pink, top), After Filtration of PFAS (black, center), and of the PFAS Molecule (in blue, bottom) for a) PFBA, b) PFHxA, and c) PFOA

Part VI. Conclusion

This research aimed to assess the optimal conditions that facilitate disintegration and biodegradation of compostable FSP and to evaluate inoculants to improve composting. The research also examined the concentration of PFAS contained in the FSP test specimens. This included chemical sampling to detect the presence of fluorinated compounds (a proxy for determining the presence PFAS) in FSP and samples of finished compost. The removal of short and long chain PFAS molecules from water as a simulation of compost leachate was also assessed using porous materials via adsorption and filtration. Based on the data gathered through bench-scale and commercial-scale composting of compostable FSP containing PFAS (fiber plate and PLA lined bagasse clamshell) and FSP without PFAS (PLA clamshell and synthetic/starch blended bag), the following conclusions were drawn:

1. The most effective inoculant used at bench scale, cow manure, resulted in the highest degree of biodegradation of the FSP when the moisture content was at the highest level tested in reactors (60 percent). While the cow manure inoculant initiated the highest degree of biodegradation in the tested FSP products at bench scale, it proved not to be viable for use as an inoculant at a commercial scale testing facility. The main limitation associated with using cow manure as the inoculant at a commercial scale compost facility is its unavailability in large quantities.
2. Cow manure was the only inoculant used in the bench-scale reactors. For this reason, further evaluation of composting inoculants (e.g., matured compost, mixed liquor, or landfill sludge) at bench-scale is required to identify other potentially beneficial substances that may contribute to higher biodegradation rates.
3. The commercial-scale composting pile containing additional food waste feedstock had a higher rate of biodegradation than the old compost containing pile. Thus, food waste induced feedstock can be a more viable option to degrade FSP at commercial compost facilities.
4. There was no observable PFAS degradation in FSP using PIGE analysis of compost extracts. The absence of PFAS detected in compost extractions suggests PFAS are retained on or in the FSP rather than released into the compost. Although PFAS were not detected in solid compost samples, leachate from commercial-scale piles was not assessed as part of this study and may have contained measurable amounts of PFAS.
5. Further research evaluating PFAS concentration in liquid leachate is necessary to better understand the fate and migration of PFAS from FSP. Liquid analysis would determine if PFAS were converted from one form to another during composting.
6. The solid MHO remediation technique generally removed longer chain PFAS molecules at a higher rate than shorter chain PFAS molecules. While this technique shows promise for removing certain types of PFAS from water, it is not known if MHO would prove to be equally effective if used to extract PFAS from compost leachate.

Bibliography

Adhikari, B. K., Barrington, S., Martinez, J., & King, S. (2009). Effectiveness of three bulking agents for food waste composting. Waste Management, 29(1), 197–203. https://www.sciencedirect.com/science/article/abs/pii/S0956053X08001190?via%3Dihub

Ahmad, M., Rajapaksha, A. U., Lim, J. E., Zhang, M., Bolan, N., Mohan, D., … Ok, Y. S.

(2014). Biochar as a sorbent for contaminant management in soil and water: A review. Chemosphere, 99, 19–33. https://www.sciencedirect.com/science/article/abs/pii/S0045653513015051?via%3Dihub

Ahmed, T., Shahid, M., Azeem, F., Rasul, I., Shah, A., Noman, M. (2018). Utilization of agricultural and forest industry waste and residues in natural fiber-polymer composites: A review. Environ. Sci. Poll. Res., 25, 7287-7298. https://www.sciencedirect.com/science/article/abs/pii/S0956053X16302355

Allen, Hill, Bloom, Friedman, & Stern. (2021). SB-1335 Solid waste: food service packaging: state agencies, facilities, and property. Retrieved from: https://leginfo.legislature.ca.gov/faces/billTextClient.xhtml?bill_id=201720180SB1335

Amass, W., Amass, A., Tighe, B. (1998). A Review of Biodegradable Polymers: Uses, Current Developments in the Synthesis and Characterization of Biodegradable Polyesters, Blends of Biodegradable Polymers and Recent Advances in Biodegradation Studies. Poly. Int. 47, 89-144. https://onlinelibrary.wiley.com/doi/abs/10.1002/(SICI)1097-0126(1998100)47:2%3C89::AID-PI86%3E3.0.CO;2-F

ASTM D6400. (2012.2). ASTM D6400 - Standard Specification for Labeling of Plastics Designed to be Aerobically Composted in Municipal or Industrial Facilities | Engineering360. *Astm*, 3. https://doi.org/10.1520/D6400-12.2

ASTM Standard D5988. (2012). Standard Test Method for Determining Aerobic Biodegradation of Plastic Materials in. *ASTM International*, 1–6. https://doi.org/10.1520/D5338-15.2

ASTM-D-2216-98. (1998). Standard Test Method for Laboratory Determination of Water (Moisture) Content of Soil and Rock by Mass. *ASTM International*, (January), 1–5. https://doi.org/10.1520/D2216-19

Aura, R., Harte, B., Selke, S. (2004). An overview of polylactides as packaging materials. Macromolecular Bioscience, 4, 835-864 https://pubmed.ncbi.nlm.nih.gov/15468294/

Awasthi, M. K., Pandey, A. K., Khan, J., Bundela, P. S., Wong, J. W. C., & Selvam, A. (2014). Evaluation of thermophilic fungal consortium for organic municipal solid

waste composting. *Bioresource Technology*, *168*, 214–221. https://doi.org/10.1016/j.biortech.2014.01.048

Bandini, F., Misci, C., Taskin, E., Cocconcelli, P. S., & Puglisi, E. (2020). Biopolymers modulate microbial communities in municipal organic waste digestion. *FEMS Microbiology Ecology*, *96*(10), 1–13. https://doi.org/10.1093/femsec/fiaa183

Bernal, M. P., Alburquerque, J. A., & Moral, R. (2009). Composting of animal manures and chemical criteria for compost maturity assessment. A review. *Bioresource Technology*, *100*(22), 5444–5453. https://doi.org/10.1016/j.biortech.2008.11.027

Berthet, M., Angellier-Coussy, H., Guillard V., Gontard, J. (2015). Vegetal fiber-based biocomposites: Which stakes for food packaging applications? Appl. Polym. Sci. DOI: 10.1002/app.42528 https://onlinelibrary.wiley.com/doi/full/10.1002/app.42528

Bewick, M. (1980). Handbook of Organic Waste Conversion. New York: Van Nostrand Reinhold Company.

Bogoeva-Gaceva, G., Avella, M., Malinconico, M., Buzarovska, A., Grozdanob, A., Gentile, G., Errico, M. (2007). Natural fiber eco-composites. Polymer composites, 28(1), 98-107. https://onlinelibrary.wiley.com/doi/abs/10.1002/pc.20270?casa_token=BgAjR7Kv9W4AAAAA:HaNcho8GjViLs_SQkOWi9hJcUbZ0k5Ya_C6gbPnq5OUoWbN0FDlusrACFypTC0cnr4d2Uc3wgiVf7lM

Bolyen, E., Rideout, J. R., Dillon, M. R., Bokulich, N. A., Abnet, C. C., Al-Ghalith, G. A., … Caporaso, J. G. (2019). Reproducible, interactive, scalable and extensible microbiome data science using QIIME 2. *Nature Biotechnology*, *37*(8), 852–857. https://doi.org/10.1038/s41587-019-0209-9

Brown, S., & Leonard, P. (2004). Biosolids and global warming: Evaluating the management impacts. BioCycle, 45(8), 54–61. https://www.biocycle.net/biosolids-and-global-warming-evaluating-the-management-impacts/

Burns, D. C., Ellis, D. A., Li, H., McMurdo, C. J., & Webster, E. (2008). Experimental p K a Determination for Perfluorooctanoic Acid (PFOA) and the Potential Impact of p K a Concentration Dependence on Laboratory-Measured Partitioning Phenomena and Environmental Modeling. Environmental Science & Technology, 42(24), 9283–9288. https://doi.org/10.1021/es802047v

Buzby, J. C., Hyman, J., Stewart, H., & Wells, H. F. (2011). The Value of Retail- and Consumer-Level Fruit and Vegetable Losses in the United States. Journal of Consumer Affairs, 45(3), 492–515. https://onlinelibrary.wiley.com/doi/10.1111/j.1745-6606.2011.01214.x

C8 Science Panel. (2012). C8 Probable Link Reports. http://www.c8sciencepanel.org/prob_link.html

Callahan, B. J., McMurdie, P. J., & Holmes, S. P. (2017). Exact sequence variants should replace operational taxonomic units in marker-gene data analysis. *ISME Journal*,

11(12), 2639–2643. https://doi.org/10.1038/ismej.2017.119

Callahan, B. J., McMurdie, P. J., Rosen, M. J., Han, A. W., Johnson, A. J. A., & Holmes, S. P. (2016). DADA2: High-resolution sample inference from Illumina amplicon data. *Nature Methods*, *13*(7), 581–583. https://doi.org/10.1038/nmeth.3869

CalRecycle. (2015). State of disposal in California. Retrieved from www.calrecycle.ca.gov/Publications/ on September 26, 2018. https://www2.calrecycle.ca.gov/Publications/Details/1643

CalRecycle. (2018). Benefits of Compost.

Campos-Pereira, H., Kleja, D. B., Sjöstedt, C., Ahrens, L., Klysubun, W., & Gustafsson, J. P. (2020). The Adsorption of Per- and Polyfluoroalkyl Substances (PFASs) onto Ferrihydrite Is Governed by Surface Charge. Environmental Science & Technology, 54(24), 15722–15730. https://doi.org/10.1021/acs.est.0c01646

Cekmecelioglu, D., Demirci, A., Graves, R. E., & Davitt, N. H. (2005). Applicability of Optimised In-vessel Food Waste Composting for Windrow Systems. Biosystems Engineering, 91(4), 479–486. https://www.sciencedirect.com/science/article/abs/pii/S1537511005000796?via%3Dihub

Cerda, A., Artola, A., Font, X., Barrena, R., Gea, T., & Sánchez, A. (2018). Composting of food wastes: Status and challenges. Bioresource Technology, 248, 57–67. https://www.sciencedirect.com/science/article/abs/pii/S0960852417310374?via%3Dihub

Cerda, A., Artola, A., Font, X., Barrena, R., Gea, T., & Sánchez, A. (2018). Composting of food wastes: Status and challenges. *Bioresource Technology*, *248*, 57–67. https://doi.org/10.1016/j.biortech.2017.06.133

Chan, M. T., Selvam, A., & Wong, J. W. C. (2016). Reducing nitrogen loss and salinity during “struvite” food waste composting by zeolite amendment. *Bioresource Technology*, *200*, 838–844. https://doi.org/10.1016/j.biortech.2015.10.093

Chandra, R.; Rustgi, R. (1998). Biodegradable polymers. Prog. Polym. Sci. 1998, 23, 1273–1335. https://www.scirp.org/(S(351jmbntvnsjt1aadkozje))/journal/paperinformation.aspx?paperid=50669

Chang, J. I., & Chen, Y. J. (2010). Effects of bulking agents on food waste composting. Bioresource Technology, 101(15), 5917–5924. https://www.sciencedirect.com/science/article/abs/pii/S0960852410003159?via%3Dihub

Chang, J. I., & Hsu, T.-E. (2008). Effects of compositions on food waste composting. Bioresource Technology, 99(17), 8068–8074. https://www.sciencedirect.com/science/article/abs/pii/S0960852408002654?via%3Dihub

Chang, J. I., Tsai, J. J., & Wu, K. H. (2005). Mathematical model for carbon dioxide evolution from the thermophilic composting of synthetic food wastes made of dog food. Waste Management, 25(10), 1037–1045. https://www.sciencedirect.com/science/article/abs/pii/S0956053X05000498?via%3Dihub

Chiellini, E., Corti, A. (2003). A simple method suitable to test the ultimate biodegradability of environmentally degradable polymers. Macromol. Symp. 197, 381-395. https://onlinelibrary.wiley.com/doi/abs/10.1002/masy.200350733

Chikae, M., Ikeda, R., Kerman, K., Morita, Y., & Tamiya, E. (2006). Estimation of maturity of compost from food wastes and agro-residues by multiple regression analysis. Bioresource Technology, 97(16), 1979–1985. https://www.sciencedirect.com/science/article/abs/pii/S096085240500468 2?via%3Dihub

Contea, L., Fallettia, L., Zaggiaa, A., & Milan, M. (2015). Polyfluorinated organic micropollutants removal from water by ion exchange and adsorption. Chemical Engineering Transactions, 43, 2257–2262. https://www.aidic.it/cet/15/43/377.pdf

Cooperband, L. (2002). The Art and The Art and Science of Composting Science of Composting: A resource for farmers and compost producers. https://www.iowadnr.gov/Portals/idnr/uploads/waste/artandscienceofcomposting.pdf

Das, K., & Keener, H. M. (1994). Numerical model for the dynamic simulation of a large scale composting system. Transactions of the ASAE, 40(4), 1179–1189. https://elibrary.asabe.org/abstract.asp?aid=21339

De Silva, A. O., Allard, C. N., Spencer, C., Webster, G. M., & Shoeib, M. (2012). Phosphorus-Containing Fluorinated Organics: Polyfluoroalkyl Phosphoric Acid Diesters (diPAPs), Perfluorophosphonates (PFPAs), and Perfluorophosphinates (PFPIAs) in Residential Indoor Dust. Environmental Science & Technology, 46(22), 12575–12582. https://pubs.acs.org/doi/10.1021/es303172p

Eklind, Y., Sundberg, C., Smårs, S., Steger, K., Sundh, I., Kirchmann, H., & Jönsson, H. (2007). Carbon Turnover and Ammonia Emissions during Composting of Biowaste at Different Temperatures. Journal of Environment Quality, 36(5), 1512. https://acsess.onlinelibrary.wiley.com/doi/full/10.2134/jeq2006.0253

Emadian, S. M., Onay, T. T., & Demirel, B. (2017). Biodegradation of bioplastics in natural environments. *Waste Management*, *59*, 526–536. https://doi.org/10.1016/j.wasman.2016.10.006

EPA. (2014). Municipal Solid Waste Generation, Recycling, and Disposal in the United States: Facts and Figures for 2012. Retrieved from https://www.epa.gov/sites/default/files/2015-09/documents/2012_msw_fs.pdf

EPA. (2018a). Basic Information about Landfill Gases. Retrieved from https://www.epa.gov/lmop/basic-information-about-landfill-gas

EPA. (2018b). Overview of Greenhouse Gases. Retrieved from https://www.epa.gov/ghgemissions/overview-greenhouse-gases

Ferrer-Lassala, I. M. (2013). Metal Oxide Electrokinetic Micropumps & Capillary Electrophoresis of Biomolecules and Carbon based nanomaterials. SUNY Buffalo.

Finstein, M., & Morris, M. (1975). Microbiology of municipal solid waste composting. In P. D (Ed.), Advances in Applied Microbiology (pp. 113–151). New York: Academic Press. https://www.sciencedirect.com/science/article/abs/pii/S0065216408704271

Gajalakshmi, S., & Abbasi, S. (2008). Solid Waste Management by Composting: State of the Art. Environmental Science and Technology38, 38(5), 311–400. https://www.tandfonline.com/doi/abs/10.1080/10643380701413633

Gallardo-Altamirano, M. J., Maza-Márquez, P., Montemurro, N., Pérez, S., Rodelas, B., Osorio, F., & Pozo, C. (2021). Insights into the removal of pharmaceutically active compounds from sewage sludge by two-stage mesophilic anaerobic digestion. *Science of the Total Environment*, *789*. https://doi.org/10.1016/j.scitotenv.2021.147869

Gao, X., & Chorover, J. (2012). Adsorption of perfluorooctanoic acid and perfluorooctanesulfonic acid to iron oxide surfaces as studied by flow-through ATR-FTIR spectroscopy. Environmental Chemistry, 9(2), 148. https://doi.org/10.1071/EN11119

Gea, T., Barrena, R., Artola, A., & Sánchez, A. (2007). Optimal bulking agent particle size and usage for heat retention and disinfection in domestic wastewater sludge composting. Waste Management, 27(9), 1108–1116. https://www.sciencedirect.com/science/article/abs/pii/S0956053X06002182?via%3Dihub

George, M., Chae, M., Bressler, D. (2016). Composite materials with bast fibers: structural, technical and environmental properties. Prog. Mat. Sci. 83, 1-23. https://www.sciencedirect.com/science/article/abs/pii/S007964251630007X

Goldstein, N. (2017). The State Of Organics Recycling In The U.S. Retrieved from https://www.biocycle.net/state-organics-recycling-u-s/

Gopferich, A. (1996). Mechanisms of polymer degradation and erosion. Biomaterials, 17, 103-114. https://www.sciencedirect.com/science/article/abs/pii/0142961296857553

Grandjean, P., Heilmann, C., Weihe, P., Nielsen, F., Mogensen, U. B., Timmermann, A., & Budtz-Jørgensen, E. (2017). Estimated exposures to perfluorinated compounds in infancy predict attenuated vaccine antibody concentrations at age 5-years. Journal of Immunotoxicology, 14(1), 188–195. https://www.tandfonline.com/doi/full/10.1080/1547691X.2017.1360968

Graspeuntner, S., Loeper, N., Künzel, S., Baines, J. F., & Rupp, J. (2018). Selection of validated hypervariable regions is crucial in 16S-based microbiota studies of the female genital tract. *Scientific Reports*, *8*(1), 4–10. https://doi.org/10.1038/s41598-018-27757-8

Guo, R., Li, G., Jiang, T., Schuchardt, F., Chen, T., Zhao, Y., & Shen, Y. (2012). Effect of aeration rate, C/N ratio and moisture content on the stability and maturity of compost. Bioresource Technology, 112, 171–178. https://www.sciencedirect.com/science/article/abs/pii/S0960852412003501?via%3Dihub

Guo, R., Li, G., Jiang, T., Schuchardt, F., Chen, T., Zhao, Y., & Shen, Y. (2012). Effect of aeration rate, C/N ratio and moisture content on the stability and maturity of compost. *Bioresource Technology*, *112*, 171–178. https://doi.org/10.1016/j.biortech.2012.02.099

Hachicha, S., Sellami, F., Cegarra, J., Hachicha, R., Drira, N., Medhioub, K., & Ammar, E. (2009). Biological activity during co-composting of sludge issued from the OMW evaporation ponds with poultry manure-Physico-chemical characterization of the processed organic matter. *Journal of Hazardous Materials*, *162*(1), 402–409. https://doi.org/10.1016/j.jhazmat.2008.05.053

Hale, J. R. (2016). Distribution of PFOS in Groundwater from AFFF Storage, Handling, and Use. In NGWA Groundwater Solutions: Innovating to Address Emerging Issues in Groundwater Resources Symposium. https://ngwa.confex.com/ngwa/gs2017/webprogram/Paper11334.html

Hamid, H., & Li, L. (2016). Role of wastewater treatment plant (WWTP) in environmental cycling of poly- and perfluoroalkyl (PFAS) compounds. Ecocycles, 2(2). https://www.ecocycles.net/ojs/index.php/ecocycles/article/view/62

Henton, D.E.; Gruber, P.; Lunt, J.; Randall, J. (2005). Polylactic acid technology. In Natural Fibres, Biopolymers and Biocomposites; Mohanty, A.K.; Misra, M.; Drzal, L.T., Eds.; CRC Press: Boca Raton, FL, pp. 527–577 https://citeseerx.ist.psu.edu/viewdoc/download?doi=10.1.1.476.9328&rep=rep1&type=pdf

Herbert, N. (2010). Composting. In Environmental Engineering National Engineering Handbook. United States Department of Agriculture.

Ho, K., Pometto, A., Gadea-Rivas, A., Briceno, J., Rojas, A. (1999). Degradation of Polylactic Acid (PLA) Plastic in Costa Rican Soil and Iowa State University Compost Rows. J. Env. Poly. Degrad. 7(4), 173-177. https://link.springer.com/article/10.1023/A:1022874530586

Hu, X. C., Andrews, D. Q., Lindstrom, A. B., Bruton, T. A., Schaider, L. A., Grandjean, P., … Sunderland, E. M. (2016). Detection of Poly- and Perfluoroalkyl Substances (PFASs) in U.S. Drinking Water Linked to Industrial Sites, Military Fire Training

Areas, and Wastewater Treatment Plants. Environmental Science & Technology Letters, 3(10), 344–350. https://pubs.acs.org/doi/10.1021/acs.estlett.6b00260

Huang, G. F., Wong, J. W. C., Wu, Q. T., & Nagar, B. B. (2004). Effect of C/N on composting of pig manure with sawdust. *Waste Management*, *24*(8), 805–813. https://doi.org/10.1016/j.wasman.2004.03.011

Hussain, F. A., Zamora, J., Ferrer, I. M., Kinyua, M., & Velázquez, J. M. (2020). Adsorption of crude oil from crude oil–water emulsion by mesoporous hafnium oxide ceramics. Environmental Science: Water Research & Technology. https://doi.org/10.1039/D0EW00451K

Iqbal, M. K., Shafiq, T., & Ahmed, K. (2010). Characterization of bulking agents and its effects on physical properties of compost. Bioresource Technology, 101(6), 1913–1919. https://www.sciencedirect.com/science/article/abs/pii/S0960852409014060?via%3Dihub

Iqbal, M. K., Shafiq, T., & Ahmed, K. (2010). Characterization of bulking agents and its effects on physical properties of compost. *Bioresource Technology*, *101*(6), 1913–1919. https://doi.org/10.1016/j.biortech.2009.10.030

Juárez, M., Prähauser, B., Walter, A., Insam, H., & Franke-Whittle, H. (2015). Co-composting of biowaste and wood ash, influence on a microbially driven-process. Waste Management, 46, 155–164. https://pubmed.ncbi.nlm.nih.gov/26394680/

Kale, G., Kijchavengkul,T., Auras, R., Rubino, M., Selke, S., Singh, S. (2007). Compostability of bioplastic packaging materials: an overview. Macromolecular Bioscience, 7, 255-277. https://pubmed.ncbi.nlm.nih.gov/17370278/

Kim, K.-Y., Kim, H.-W., Han, S.-K., Hwang, E.-J., Lee, C.-Y., & Shin, H.-S. (2008). Effect of granular porous media on the composting of swine manure. Waste Management, 28(11), 2336–2343. https://www.sciencedirect.com/science/article/abs/pii/S0956053X07003911?via%3Dihub

Kissa, E. (2001). Fluorinated surfactants and repellents. (A. T. Hubbard, Ed.) (2nd ed., r). New York: Marcel Dekker Inc. https://pubs.acs.org/doi/10.1021/ja015260a

Kõljalg, U., Nilsson, H. R., Schigel, D., Tedersoo, L., Larsson, K. H., May, T. W., … Abarenkov, K. (2020). The taxon hypothesis paradigm—On the unambiguous detection and communication of taxa. *Microorganisms*, *8*(12), 1–24. https://doi.org/10.3390/microorganisms8121910

Kowalczyk, J., Ehlers, S., Fürst, P., Schafft, H., & Lahrssen-Wiederholt, M. (2012). Transfer of Perfluorooctanoic Acid (PFOA) and Perfluorooctane Sulfonate (PFOS) From Contaminated Feed Into Milk and Meat of Sheep: Pilot Study. Arch Environ Contam Toxicol, 63, 288–298. https://link.springer.com/article/10.1007/s00244-012-9759-2#citeas

Kumar, M., Ou, Y.-L., & Lin, J.-G. (2010). Co-composting of green waste and food waste at low C/N ratio. Waste Management, 30(4), 602–609. https://www.sciencedirect.com/science/article/abs/pii/S0956053X0900525X?via%3Dihub

Kuvayskaya, A., Lotsi, B., Mohseni, R., & Vasiliev, A. (2020). Mesoporous adsorbents for perfluorinated compounds. Microporous and Mesoporous Materials, 305, 110374. https://doi.org/10.1016/j.micromeso.2020.110374

Lei, F., & VanderGheynst, J. . (2000). The effect of microbial inoculation and pH on microbial community structure changes during composting. Process Biochemistry, 35(9), 923–929. https://www.sciencedirect.com/science/article/abs/pii/S0032959299001557?via%3Dihub

Li, Z., Lu, H., Ren, L., & He, L. (2013). Experimental and modeling approaches for food waste composting: A review. Chemosphere, 93(7), 1247–1257. https://www.sciencedirect.com/science/article/abs/pii/S0045653513009211?via%3Dihub

Lin, L., Xu, F., Ge, X., & Li, Y. (2018). Improving the sustainability of organic waste management practices in the food-energy-water nexus: A comparative review of anaerobic digestion and composting. Renewable and Sustainable Energy Reviews, 89, 151–167. https://www.sciencedirect.com/science/article/abs/pii/S1364032118301023?via%3Dihub

Lindstrom, A. B. (2017). Introduction to Per- and Polyfluoroalkyl Substances (PFAS) In Food Service Ware. Retrieved October 10, 2018, from http://www.responsiblepurchasing.org/webinars/toxics_food_service_ware_webinar_slides_111617.pdf

Lou, X. F., & Nair, J. (2009). The impact of landfilling and composting on greenhouse gas emissions – A review. Bioresource Technology, 100(16), 3792–3798. https://www.sciencedirect.com/science/article/abs/pii/S0960852408010572?via%3Dihub

Makino, K., Arakawa, M., Kondo, T. (1985). Preparation and in vitro Degradation Properties of Polylactide Microcapsules. Membranes and Membrane Processes. 371-377 https://www.jstage.jst.go.jp/article/cpb1958/33/3/33_3_1195/_article

Mänttäri, M., Van der Bruggen, B., & Nyström, M. (2013). Nanofiltration. In S. Ramaswamy, H.-J. Huang, & B. V. Ramarao (Eds.), Separation and Purification Technologies in Biorefineries (pp. 233–258). London: Wiley. https://doi.org/10.1002/9781118493441

McIlroy, S. J., Saunders, A. M., Albertsen, M., Nierychlo, M., McIlroy, B., Hansen, A. A., … Nielsen, P. H. (2015). MiDAS: the field guide to the microbes of activated sludge. *Database*, *2015*(2), bav062. https://doi.org/10.1093/database/bav062

McNamara, J., Westreich, P., & Brewer, J. (2017). CleanUp Conference. In GRANULAR ACTIVATED CARBON: A PROVEN SOLUTION FOR PFAS TREATMENT (pp. 462–463). Melbourne. Retrieved from https://www.cleanupconference.com/wp-content/uploads/2017/09/CleanUp_2017_Proceedings_Low-Res.pdf

Morterra, C., Cerrato, G., Bolis, V., & Fubini, B. (1993). A characterization of the surface acidity of HfO2by FTIR spectroscopy of adsorbed species, electron microscopy and adsorption microcalorimetry. Spectrochimica Acta Part A: Molecular Spectroscopy, 49(9), 1269–1288. https://doi.org/https://doi.org/10.1016/0584-8539(93)80035-9

Nawrocki, J., Rigney, M., McCormick, A., & Carr, P. (1993). Chemistry of zirconia and its use in chromatography. Journal of Chromatography A, 657(2), 229–282. https://pubmed.ncbi.nlm.nih.gov/8130879/

OEHHA. (2021). Proposed Public Health Goals for PFOA and PFOS in Drinking Water. Retrieved from: https://oehha.ca.gov/media/downloads/crnr/pfoapfosphgdraft061021.pdf

Onwosi, C. O., Igbokwe, V. C., Odimba, J. N., Eke, I. E., Nwankwoala, M. O., Iroh, I. N., & Ezeogu, L. I. (2017). Composting technology in waste stabilization: On the methods, challenges and future prospects. Journal of Environmental Management, 190, 140–157. https://www.sciencedirect.com/science/article/pii/S0301479716310349?via%3Dihub

Östlund, A. (2015). Removal Efficiency of Perfluoroalkyl Substances (PFASs) in Drinking Water. Swedish University of Agricultural Sciences. Retrieved from https://stud.epsilon.slu.se/8158/13/ostlund_a_150709.pdf

Palaniveloo, K., Amran, M. A., Norhashim, N. A., Mohamad-Fauzi, N., Peng-Hui, F., Hui-Wen, L., … Razak, S. A. (2020). Food waste composting and microbial community structure profiling. *Processes*, *8*(6), 1–30. https://doi.org/10.3390/pr8060723

Pandey, J., Ahn, S., Lee, C., Mohanty, A., Misra, M. (2010). Recent Advances in the Application of Natural Fiber Based Composites. Macromol. Mat. Eng. 295(11), 975-989. https://onlinelibrary.wiley.com/doi/10.1002/mame.201000095

Priyanka N, Archana T. (2012). Biodegradability of polythene and plastic by the help of microorganism: a way for brighter future. J Environ. Anal. Toxicol. 1:12–15 https://www.hilarispublisher.com/open-access/biodegradability-of-polythene-and-plastic-by-the-help-of-microorganism-a-way-for-brighter-future-2161-0525.1000111.pdf

Raghab, S. M., Abd El Meguid, A. M., & Hegazi, H. A. (2013). Treatment of leachate from municipal solid waste landfill. HBRC Journal, 9(2), 187–192. https://www.tandfonline.com/doi/full/10.1016/j.hbrcj.2013.05.007

Rahman, M. F. (2014). Removal of Perfluorinated Compounds from Ultrapure and Surface Waters by Adsorption and Ion Exchange. University of Waterloo. Retrieved from https://uwspace.uwaterloo.ca/bitstream/handle/10012/9161/Rahman_Mohammad_Feisal.pdf;sequence=3

Rao, N. S., & Baker, B. E. (1994). Textile Finishes and Fluorosurfactants. In R. E. Banks, B. E. Smart, & J. C. Tatlow (Eds.), Organofluorine Chemistry Principles and Commercial Applications. New York: Plenum Press. https://link.springer.com/book/10.1007%2F978-1-4899-1202-2

Rasapoor, M., Adl, M., & Pourazizi, B. (2016). Comparative evaluation of aeration methods for municipal solid waste composting from the perspective of resource management: A practical case study in Tehran, Iran. Journal of Environmental Management, 184, 528–534. https://www.sciencedirect.com/science/article/pii/S0301479716308118?via%3Dihub

Rastogi, M., Nandal, M., Khosla, B., Vendries, J., Sauer, B., Hawkins, T. R., … Paul, E. (2009). Comparison of organic matter degradation and microbial community during thermophilic composting of two different types of anaerobic sludge [Research-article]. *Waste Management*, *28*(1), 1–13. https://doi.org/10.1016/j.rser.2020.110637

Ritter, E. E., Dickinson, M. E., Harron, J. P., Lunderberg, D. M., DeYoung, P. A., Robel, A. E., … Peaslee, G. F. (2017). PIGE as a screening tool for Per- and polyfluorinated substances in papers and textiles. Nuclear Instruments and Methods in Physics Research Section B: Beam Interactions with Materials and Atoms, 407, 47–54. https://www.sciencedirect.com/science/article/abs/pii/S0168583X1730633X?via%3Dihub

Ross, I., McDonough, J., Miles, J., Storch, P., Thelakkat Kochunarayanan, P., Kalve, E., … Burdick, J. (2018). A review of emerging technologies for remediation of PFASs. Remediation Journal, 28(2), 101–126. https://onlinelibrary.wiley.com/doi/10.1002/rem.21553

Sahu, S. P., Qanbarzadeh, M., Ateia, M., Torkzadeh, H., Maroli, A. S., & Cates, E. L. (2018). Rapid Degradation and Mineralization of Perfluorooctanoic Acid by a New Petitjeanite Bi 3 O(OH)(PO 4) 2 Microparticle Ultraviolet Photocatalyst. Environmental Science & Technology Letters, 5(8), 533–538. https://pubs.acs.org/doi/10.1021/acs.estlett.8b00395

Sánchez-Monedero, M. A., Roig, A., Paredes, C., & Bernal, M. P. (2001). Nitrogen transformation during organic waste composting by the Rutgers system and its effects on pH, EC and maturity of the composting mixtures. *Bioresource Technology*, *78*(3), 301–308. https://doi.org/10.1016/S0960-8524(01)00031-1

Schultz, M. M., Higgins, C. P., Huset, C. A., Luthy, R. G., Barofsky, D. F., & Field, J. A. (2006). Fluorochemical Mass Flows in a Municipal Wastewater Treatment Facility †. Environmental Science & Technology, 40(23), 7350–7357. https://pubs.acs.org/doi/10.1021/es061025m

Seo, J. Y., Heo, J. S., Kim, T. H., Joo, W. H., & Crohn, D. M. (2004). Effect of vermiculite addition on compost produced from Korean food wastes. Waste Management, 24(10), 981–987. https://www.sciencedirect.com/science/article/abs/pii/S0956053X04001357?via%3Dihub

Singh, B., Sharma, N. (2008). Mechanistic implication of plastic degradation. Poly. Deg. Stab. 93, 561-584 https://www.sciencedirect.com/science/article/pii/S0141391007003539

Siracusa, V. (2019). Microbial degradation of synthetic biopolymers waste. *Polymers*, *11*(6). https://doi.org/10.3390/polym11061066

Siracusa, V., Rocculi, P., Romani, S., Rosa, M. (2008). Biodegradable polymers for food packaging: a review. Trends in food science and technology, 19, 634-643 https://www.sciencedirect.com/science/article/abs/pii/S0924224408002185

Solomon, E. B., Yaron, S., & Matthews, K. R. (2002). Transmission of Escherichia coli O157:H7 from contaminated manure and irrigation water to lettuce plant tissue and its subsequent internalization. Applied and Environmental Microbiology, 68(1), 397–400. https://pubmed.ncbi.nlm.nih.gov/11772650/

Stebel, E. K., Pike, K. A., Nguyen, H., Hartmann, H. A., Klonowski, M. J., Lawrence, M. G., … Edmiston, P. L. (2019). Absorption of short-chain to long-chain perfluoroalkyl substances using swellable organically modified silica. Environmental Science: Water Research & Technology, 5(11), 1854–1866. https://doi.org/10.1039/C9EW00364A

Steinle-Darling, E., & Reinhard, M. (2008). Nanofiltration for Trace Organic Contaminant Removal: Structure, Solution, and Membrane Fouling Effects on the Rejection of Perfluorochemicals. Environmental Science & Technology, 42(14), 5292–5297. https://pubs.acs.org/doi/10.1021/es703207s

Stentiford, E. (1996). Composting control: principles and practice.

Sun, W., Huang, G. H., Zeng, G., Qin, X., & Sun, X. (2009). A stepwise-cluster microbial biomass inference model in food waste composting. Waste Management, 29(12), 2956–2968. https://www.sciencedirect.com/science/article/abs/pii/S0956053X09002384?via%3Dihub

Sundberg, C., Yu, D., Franke-Whittle, I., Kauppi, S., Smårs, S., Insam, H., … Jönssona, H. (2013). Effects of pH and microbial composition on odour in food waste

composting. Waste Management, 33(1), 204–211. https://www.sciencedirect.com/science/article/pii/S0956053X12004564

Tang, C. Y., Fu, Q. S., Criddle, C. S., & Leckie, J. O. (2007). Effect of Flux (Transmembrane Pressure) and Membrane Properties on Fouling and Rejection of Reverse Osmosis and Nanofiltration Membranes Treating Perfluorooctane Sulfonate Containing Wastewater. Environmental Science & Technology, 41(6), 2008–2014. https://pubs.acs.org/doi/10.1021/es062052f

Ting, A., & Friedman, A. (2021). AB-1200 Plant-based food packaging: cookware: hazardous chemicals. Retrieved from: https://leginfo.legislature.ca.gov/faces/billTextClient.xhtml?bill_id=202120220AB1200

Ting, Friedman, Gonzalez, & Mathis. (2021). AB-1201 Solid waste: products: labeling: compostability and biodegradability. Retrieved from: https://leginfo.legislature.ca.gov/faces/billTextClient.xhtml?bill_id=202120220AB1201

Tokiwa, T., Calabia, B. (2007). Biodegradability and biodegradation of polyesters. J Polym Environ, 15, 259-267. https://link.springer.com/article/10.1007/s10924-007-0066-3

Tokiwa, Y., Calabia, B., Ugwu, C., Aiba, S. (2009). Biodegradability of plastics. Int. J. Mol. Sci. 2009, 10, 3722-3742; https://www.mdpi.com/1422-0067/10/9/3722

Tsuji, H., Ikada, Y. (1998). Properties and morphology of poly(L-lactide). II. Hydrolysis in alkaline solution. Polym. Chem. 36(1), 59-66. https://onlinelibrary.wiley.com/doi/abs/10.1002/%28SICI%291099-0518%2819980115%2936%3A1%3C59%3A%3AAID-POLA9%3E3.0.CO%3B2-X

Tsuji, H., Nakahara, K., Ikarashi, K. (2001). Poly(L-Lactide), 8. High-Temperature Hydrolysis of Poly(L-Lactide) Films with Different Crystallinities and Crystalline Thicknesses in Phosphate-Buffered Solution. Macromol. Mat. Eng. 286(7), 398-406. https://onlinelibrary.wiley.com/doi/abs/10.1002/1439-2054%2820010701%29286%3A7%3C398%3A%3AAID-MAME398%3E3.0.CO%3B2-G

US EPA. (2016). FACT SHEET PFOA & PFOS Drinking Water Health Advisories. Retrieved October 28, 2018, from https://www.epa.gov/sites/default/files/2016-06/documents/drinkingwaterhealthadvisories_pfoa_pfos_updated_5.31.16.pdf

US EPA. (2018). Fact Sheet: 2010/2015 PFOA Stewardship Program. Retrieved October 24, 2018, from https://www.epa.gov/assessing-and-managing-chemicals-under-tsca/fact-sheet-20102015-pfoa-stewardship-program

Vaisanen, T., Haapala, A., Lappalainen, R., Tomppo, L. (2016). Utilization of agricultural and forest industry waste and residues in natural fiber-polymer composites: A

review. Waste Management, 54, 62-73. https://www.sciencedirect.com/science/article/abs/pii/S0956053X16302355

Van der Bruggen, B., & Geens, J. (2008). Nanofiltration. In N. N. Li, A. G. Fane, W. S. W. Ho, & T. Matsuura (Eds.), Advanced Membrane Technology and Applications (pp. 271–295). Hoboken, NJ, USA: John Wiley & Sons, Inc. https://onlinelibrary.wiley.com/doi/10.1002/9780470276280.ch11

Vecitis, C. D., Park, H., Cheng, J., Mader, B. T., & Hoffmann, M. R. (2008). Kinetics and Mechanism of the Sonolytic Conversion of the Aqueous Perfluorinated Surfactants, Perfluorooctanoate (PFOA), and Perfluorooctane Sulfonate (PFOS) into Inorganic Products. The Journal of Physical Chemistry A, 112(18), 4261–4270. https://pubs.acs.org/doi/10.1021/jp801081y

Vu, C., Wu, T. (2020). Adsorption of short-chain perfluoroalkyl acids (PFAAs) from water/wastewater. *Environ. Sci.: Water Res. Technol.*, 2020,6, 2958-2972 https://pubs.rsc.org/en/content/articlelanding/2020/ew/d0ew00468e

Wang, F., & Shih, K. (2011). Adsorption of perfluorooctanesulfonate (PFOS) and perfluorooctanoate (PFOA) on alumina: Influence of solution pH and cations. Water Research, 45(9), 2925–2930. https://doi.org/10.1016/j.watres.2011.03.007

Wei, Y., Li, J., Shi, D., Liu, G., Zhao, Y., & Shimaoka, T. (2017). Environmental challenges impeding the composting of biodegradable municipal solid waste: A critical review. Resources, Conservation and Recycling, 122, 51–65. https://www.sciencedirect.com/science/article/abs/pii/S0921344917300332?via%3Dihub

Wilkinson, J. T., McGuinness, S. R., & Peaslee, G. F. (2020). External beam normalization measurements using atmospheric argon gamma rays. Nuclear Instruments and Methods in Physics Research Section B: Beam Interactions with Materials and Atoms, 484, 1–4. https://doi.org/10.1016/j.nimb.2020.10.007

Xiao, X., Ulrich, B. A., Chen, B., & Higgins, C. P. (2017). Sorption of Poly- and Perfluoroalkyl Substances (PFASs) Relevant to Aqueous Film-Forming Foam (AFFF)-Impacted Groundwater by Biochars and Activated Carbon. Environmental Science & Technology, 51(11), 6342–6351. https://pubs.acs.org/doi/10.1021/acs.est.7b00970

Xie, A., Dai, J., Chen, X., He, J., Chang, Z., Yan, Y., & Li, C. (2016). Hierarchical porous carbon materials derived from a waste paper towel with ultrafast and ultrahigh performance for adsorption of tetracycline. RSC Advances, 6(77), 72985–72998. https://doi.org/10.1039/C6RA17286E

Xu, Y., Noonan, G.O., & Begley, T.H. (2013) Migration of perfluoroalkyl acids from food packaging to food simulants. Food Additives & Contaminants: Part A, 30 (5), 899-908. https://www.tandfonline.com/doi/full/10.1080/19440049.2013.789556?scroll=top&needAccess=true

Yang, F., Li, G., Shi, H., & Wang, Y. (2015). Effects of phosphogypsum and superphosphate on compost maturity and gaseous emissions during kitchen waste composting. *Waste Management*, *36*, 70–76. https://doi.org/10.1016/j.wasman.2014.11.012

Yao, Y., Volchek, K., Brown, C. E., Robinson, A., & Obal, T. (2014). Comparative study on adsorption of perfluorooctane sulfonate (PFOS) and perfluorooctanoate (PFOA) by different adsorbents in water. Water Science and Technology, 70(12), 1983–1991. https://doi.org/10.2166/wst.2014.445

Yu, H., & Huang, G. H. (2009). Effects of sodium acetate as a pH control amendment on the composting of food waste. Bioresource Technology, 100(6), 2005–2011. https://www.sciencedirect.com/science/article/abs/pii/S0960852408008602?via%3Dihub

Zhang, K., Huang, J., Yu, G., Zhang, Q., Deng, S., & Wang, B. (2013). Destruction of Perfluorooctane Sulfonate (PFOS) and Perfluorooctanoic Acid (PFOA) by Ball Milling. Environmental Science & Technology, 47(12), 6471–6477. https://pubs.acs.org/doi/10.1021/es400346n

Zhang, L., & Sun, X. (2016). Improving green waste composting by addition of sugarcane bagasse and exhausted grape marc. *Bioresource Technology*, *218*, 335–343. https://doi.org/10.1016/j.biortech.2016.06.097

Zhang, R., El-Mashad, H. M., Hartman, K., Wang, F., Liu, G., Choate, C., & Gamble, P. (2007). Characterization of food waste as feedstock for anaerobic digestion. *Bioresource Technology*, *98*(4), 929–935. https://doi.org/10.1016/j.biortech.2006.02.039

Zhao, P., Xia, X., Dong, J., Xia, N., Jiang, X., Li, Y., Zhu,Y. (2016). Short- and long-chain perfluoroalkyl substances in the water, suspended particulate matter, and surface sediment of a turbid river. Science of The Total Environment, 568, 57–65. https://doi.org/10.1016/j.scitotenv.2016.05.221

Zhu, R., Chen, Q., Zhou, Q., Xi, Y., Zhu, J., & He, H. (2016). Adsorbents based on montmorillonite for contaminant removal from water: A review. Applied Clay Science, 123, 239–258. https://www.sciencedirect.com/science/article/abs/pii/S0169131715302155?via%3Dihub